CHEMICAL REVIEWS

Review

pubs.acs.org/CR

From Chemical Gardens to Chemobrionics

Laura M. Barge,[†] Silvana S. S. Cardoso,[‡] Julyan H. E. Cartwright,[*,§] Geoffrey J. T. Cooper,[∥] Leroy Cronin,[∥] Anne De Wit,[⊥] Ivria J. Doloboff,[†] Bruno Escribano,[▽] Raymond E. Goldstein,[#] Florence Haudin,[⊥] David E. H. Jones,[^] Alan L. Mackay,[△] Jerzy Maselko,[&] Jason J. Pagano,[○] J. Pantaleone,[□] Michael J. Russell,[†] C. Ignacio Sainz-Díaz,[§] Oliver Steinbock,[*,▲] David A. Stone,[●] Yoshifumi Tanimoto,[■] and Noreen L. Thomas[◆]

[†]Jet Propulsion Laboratory, California Institute of Technology, Pasadena, California 91109, United States
[‡]Department of Chemical Engineering and Biotechnology, University of Cambridge, Cambridge CB2 3RA, United Kingdom
[§]Instituto Andaluz de Ciencias de la Tierra, CSIC−Universidad de Granada, E-18100 Armilla, Granada, Spain
[∥]WestCHEM School of Chemistry, University of Glasgow, Glasgow G12 8QQ, United Kingdom
[⊥]Nonlinear Physical Chemistry Unit, CP231, Université libre de Bruxelles (ULB), B-1050 Brussels, Belgium
[▽]Basque Center for Applied Mathematics, E-48009 Bilbao, Spain
[#]Department of Applied Mathematics and Theoretical Physics, University of Cambridge, Cambridge CB3 0WA, United Kingdom
[^]Department of Chemistry, University of Newcastle upon Tyne, Newcastle upon Tyne NE1 7RU, United Kingdom
[△]Birkbeck College, University of London, Malet Street, London WC1E 7HX, United Kingdom
[&]Department of Chemistry, University of Alaska, Anchorage, Alaska 99508, United States
[○]Department of Chemistry, Saginaw Valley State University, University Center, Michigan 48710-0001, United States
[□]Department of Physics, University of Alaska, Anchorage, Alaska 99508, United States
[▲]Department of Chemistry and Biochemistry, Florida State University, Tallahassee, Florida 32306-4390, United States
[●]Iron Shell LLC, Tucson, Arizona 85717, United States
[■]Faculty of Pharmacy, Osaka Ohtani University, Tondabayashi 548-8540, Japan
[◆]Department of Materials, Loughborough University, Loughborough LE11 3TU, United Kingdom

CONTENTS

Received: January 7, 2015

DOI: 10.1021/acs.chemrev.5b00014
Chem. Rev. XXXX, XXX, XXX−XXX

1. INTRODUCTION

Chemical gardens are perhaps the best example in chemistry of a self-organizing nonequilibrium process that creates complex structures. Many different chemical systems and materials can form these self-assembling structures, which span at least 8 orders of magnitude in size, from nanometers to meters. Key to this marvel is the self-propagation under fluid advection of reaction zones forming semipermeable precipitation membranes that maintain steep concentration gradients, with osmosis and buoyancy as the driving forces for fluid flow. Chemical gardens have been studied from the alchemists onward, but now in the 21st century we are beginning to understand how they can lead us to a new domain of self-organized structures of semipermeable membranes and amorphous as well as polycrystalline solids produced at the interface of chemistry, fluid dynamics, and materials science. We propose to call this emerging field chemobrionics.

For the past four centuries, the amazing precipitation structures known as chemical (or silica, silicate, and crystal) gardens have been the subject of fascination, as well as the basis of different philosophical and scientific theories, an inspiration for literature, and the motivation for many experiments. There is an obvious visual similarity between precipitated chemical-garden structures (Figure 1) and a variety of biological forms including

Figure 1. Classical chemical garden formed by the addition of cobalt, copper, iron, nickel, and zinc salts to a sodium silicate solution. The image corresponds to 5.5 × 3.7 cm. Image courtesy of Bruno Batista.

those of plants, fungi, and insects, and in some ways, the process of formation of chemical gardens from an inorganic "seed" in a reactive solution is reminiscent of plant growth from a seed in water or soil. These biomimetic structures and processes have from the very beginning caused researchers to wonder: Do chemical gardens and biological structures share any similar processes of formation; can these inorganic structures teach us about biological morphogenesis, or is the similarity only accidental? Are they related to the origin of life? And, if their precipitation is affected by chemical and environmental parameters, can the process be controlled to build complex structures as biology does, to produce self-organized precipitates as useful materials?

Classical chemical gardens are the hollow precipitation structures that form when a metal-salt seed is dropped into an aqueous solution containing anions such as silicate, phosphate, carbonate, oxalate, or sulfide. The dissolving seed releases metal ions that precipitate with the anions in the outer solution, forming a gelatinous colloidal membrane enclosing the seed. There are many other reaction systems that can form analogous chemical gardens, and many details of their formation process are specific to the particular system, but the key universal aspect is the formation of a semipermeable precipitation membrane of some sort, across which steep concentration gradients may be formed and maintained, leading to osmotic and buoyancy forces. Of course chemical gardens are by no means the only pattern-forming system in chemistry; Liesegang rings, for example, are another long-studied pattern-forming system involving chemical precipitation. However, Liesegang rings do not involve semipermeable membranes and are as such a quite different phenomenon. Thus, in this review we shall restrict ourselves to chemical gardens and related systems. We shall describe chemical gardens in laboratory chemistries ranging from silicates to polyoxometalates, in applications ranging from corrosion products to the hydration of Portland cement, and in natural settings ranging from hydrothermal vents in the ocean depths to brinicles beneath sea ice.

The structures formed in chemical-garden experiments can be very complex. Experimental and theoretical studies of chemical-garden systems have accelerated from the end of the 20th century with the development of nonlinear dynamics, the study of

DOI: 10.1021/acs.chemrev.5b00014
Chem. Rev. XXXX, XXX, XXX−XXX

complex systems, the understanding of pattern formation in chemical and physical systems, and the development of more advanced experimental and analytical techniques. Many aspects of the chemical-garden system, such as electrochemical and magnetic properties, have recently been and are being characterized, and it has been observed that, in certain systems, self-assembling chemical engines, or motors, can spontaneously emerge. The increased understanding of the chemical-garden formation process in the past several decades has also enabled researchers to begin to control it, to produce intentional structures via sophisticated precipitation techniques that have many potential uses for materials science and technology, especially on the nanoscale.

Chemical gardens on one hand show us that complex structures do not have to be biotic in origin, and thus highlight the dangers of using morphology as a sign of biological origin, and on the other hand point to a possible way to arrive at a proto-cell from an abiotic beginning. We now know that biomimetic forms are not a direct indication of the existence of life, because they can be produced by organic matter, as in living organisms, or by abiotic phenomena, as in chemical gardens. However, as we shall discuss, modern research shows that chemical gardens at hydrothermal vents in the ocean floor are a plausible pathway toward the emergence of life on Earth.

In this review we recount the history of chemical-garden studies, we survey the state of knowledge in this field, and we give overviews of the new fundamental understanding and of the technological applications that these self-assembling precipitation-membrane systems are providing. The scientific and technological importance of chemical-garden systems today reaches far beyond the early experiments that noted their visual similarity to plant growth. Chemical-garden-type systems now encompass a multitude of self-organizing processes involving the formation of a semipermeable membrane that create persistent, macroscopic structures from the interplay of precipitation reactions and solidification processes with diffusion and fluid motion. We therefore suggest a new overall name for this emerging field that intersects with chemistry, physics, biology, and materials science: Chemobrionics.

2. HISTORY

> *"Though this process in Physick may be of no great use: yet in regard that to a Chymical Physitian it gives good information of the condition of natural things, and their change."*

Johann Glauber, *Furni Novi Philosophici*

2.1. 17th−18th Centuries

In 1646 Johann Glauber published *Furni Novi Philosophici* (New Philosophical Furnaces), a textbook of the new science of chemistry.[1] In it, among many other experimental techniques, he discussed

> *"A water [solution] into which when any metal is put, it begins to grow within twenty four hours time in the form of plants and trees, each metal according to its inmost colour and property, which metalline vegetations are called philosophical trees, both pleasant to the eye and of good use."*

He provides this first detailed description of how to produce what we now term a chemical garden:

> *"To demonstrate this further, that the growth of all things proceeds from the strife of two contraries, take this instance: Dissolve some iron or copper in spirit of salt [hydrochloric acid] or oyl of vitriol [sulfuric acid], draw off the flegm, in which distillation none of the acid spirit will come over; because it is joyn'd and concentred with the metal, animating and disposing it to shoot up and to grow swiftly, so as the eye may perceive it grow, like a tree with a body, boughs, branches, and twigs. Take this spirit of salt or vitriol concentred by the iron, as soon as you have taken it out of the furnace, whilst it is yet warm, and break it into little bitts, about the bigness of large pease (if you should suffer it to grow cold, it would by attracting the air, suddenly run into an oyl per deliquium.) These pieces of animated iron must be joyned with its contrary, for which you can choose nothing better than a liquor of flints [potassium silicate] prepared in the same manner, which I have taught in the second part of my Furnaces. The glass, wherein you put this liquor of flints must be of the same wideness at the top, as at the bottom, and about an hand-breadth high, and fill'd with the said alkalinous liquor, to which, put your acid concentred by the iron, laying the pieces orderly a thumbs breadth from one another, and place the glass, where it may not be shaken or jogg'd. As soon as these contraries are thus joyned, they begin to act upon one another; but forasmuch, as the one of these contraries is concentred by the iron, and become hard, it cannot mingle it self with its adversary, or destroy it, so they only vex and anguish one another, in doing which, a warmth ariseth between them, and the one contrary pusheth the other to shoot and grow; the hard and dry part, viz. the animated iron drawing so much moisture from its contrary, the liquor of flints, as makes it heave and begin to grow in form of a plant, with root, stock, branches, and twigs, very pleasant to behold, the growth being very swift, so as within an hour and an half, or two hours at the most, the whole glass is fill'd with little iron trees, which grow harder and harder, and when they are hard enough, (which will be in the space of twenty four hours) then the liquor of flints must be let out from it through a hole, left on purpose in the bottom of the glass, and the plant, or little tree, remains. If we desire to make a more pleasant sight of it, we may take several metals, and make them grow up like a tree; iron affords a dark brown, copper a green, lead, tin, and mercury a white and grey, silver a blew, and gold a yellow colour."*

Thus, Glauber understood not only the basic chemistry of the chemical garden, but also its aesthetic qualities, seen in the figures of the present review paper, which make chemical gardens a favorite school chemistry experiment today (albeit not many schools will be able to afford to repeat his experiment with gold salts).

Glauber's widely read book was a source of experimental inspiration for others conducting chemical research in the 17th and 18th centuries,[2] including, notably, Robert Boyle and Isaac Newton. Boyle wrote in his *Of the study of the booke of nature* (c. 1650) of silicate "liquor in which all metalls grow into lovely trees compos'd of roote and branches and the usual parts constituent of those plants".[3] Newton undertook experiments on these first chemical gardens, notes about which we find in his manuscript *Of natures obvious laws & processes in vegetation*, probably written in the first half of the 1670s, in which he writes of metal salts and "their vegetation in a glasse".[4]

It should be noted that in the 17th−18th centuries, different types of growth that share a dendritic morphology, including

DOI: 10.1021/acs.chemrev.5b00014
Chem. Rev. XXXX, XXX, XXX−XXX

chemical gardens, were categorized together under the term "metallic vegetation"; it behoves the modern reader of old texts to check carefully exactly which type of dendritic growth process is being described.

2.2. 19th and Early 20th Centuries

By the 19th century, research on chemical gardens had taken a biological turn. Moritz Traube performed a great deal of work to show the similarities between chemical-garden reactions and biological cells.[5] Traube worked with reactants including copper sulfate and potassium hexacyanoferrate(II), and used techniques such as dipping a glass tube containing one solution into a container of the other, so that a membrane formed at the interface at the end of the tube. Traube's work on artificial cells was widely reported, as can be seen, for example, from a letter Karl Marx sent to his friend Pyotr Lavrov in which he wrote:

> *"My dear Friend, When I visited you the day before yesterday I forgot to tell you an important piece of news of which you may not yet be aware. Traube, a Berlin physiologist, has succeeded in making artificial cells. Needless to say, they are not completely natural cells, being without a nucleus. If a colloidal solution, e.g. of gelatin, is combined with copper sulphate, etc., this produces globules surrounded by a membrane that can be made to grow by intussusception. Here, then, membrane formation and cell growth have left the realm of hypothesis! It marks a great step forward [...]".*[6]

Marx's colleague Engels, in his never-completed book *Dialectics of Nature*[7] wrote of it:

> *"The significance of Traube's "cells" lies in the fact that they show endosmosis and growth as two things which can be produced also in inorganic nature and without any carbon."*

[Endosmosis refers to osmosis in which water enters a "cell" (a space surrounded by a membrane); compare exosmosis.]

Wilhelm Pfeffer developed the Traube cell into the Pfeffer cell, composed of a porous unglazed porcelain container separating two reacting solutions, often of copper sulfate and potassium hexacyanoferrate(II). With this setup, precipitation occurs within the porous matrix, and a mechanically resistant semipermeable membrane is formed between the two solutions (section 3.4), with which he could measure osmotic pressures (Figure 2a). This experimental development, which he wrote about in his 1877 book *Osmotische Untersuchungen* (osmotic investigations),[8] led[10] to Jacobus van't Hoff's work on *The role of osmotic pressure in the analogy between solutions and gases*,[11] 1887, in which he showed how osmotic pressure may be understood in the same way as gas pressure. The first Nobel Prize in Chemistry was awarded in 1901 to van't Hoff "in recognition of the extraordinary services he has rendered by the discovery of the laws of chemical dynamics and osmotic pressure in solutions". Pfeffer's research was carried on and perfected by Morse,[9] who performed an immense amount of extremely careful experimental work with semipermeable membranes he deposited by electrolysis within clay pots (Figure 2b). He affirmed that he could make his electrolytic membranes, again often produced from copper sulfate and potassium hexacyanoferrate(II), perfectly semipermeable, and based on his results it seems a plausible claim. In turn this experimental understanding of osmosis from chemical-garden membranes by Pfeffer and Morse led to work by Gibbs, Nernst, Donnan, and others that laid down the mathematical basis of osmotic phenomena in physical chemistry and bioelectrochemistry (section 5.1).

In the last decades of the 19th century and the first decades of the 20th, a number of researchers worked on chemical gardens to explore, in particular, their relationship with biological growth and form, to follow the line of enquiry begun by Traube. The terms plasmogeny (a coinage of Haeckel championed by Alfonso Herrera[13]) and synthetic biology (favored by Stéphane Leduc[12]) were employed for this exciting new area.[14] Leduc's book *The Mechanism of Life*[12] (1911; see Figure 3) catches this field at its peak; in his chapter 10 on synthetic biology Leduc provides details of the large amount of work then being carried out by researchers across the world, which involved not only chemical gardens but also what we today recognize as being a number of different physical and chemical pattern-formation mechanisms. His enthusiasm for chemical-garden research is clear as he writes:

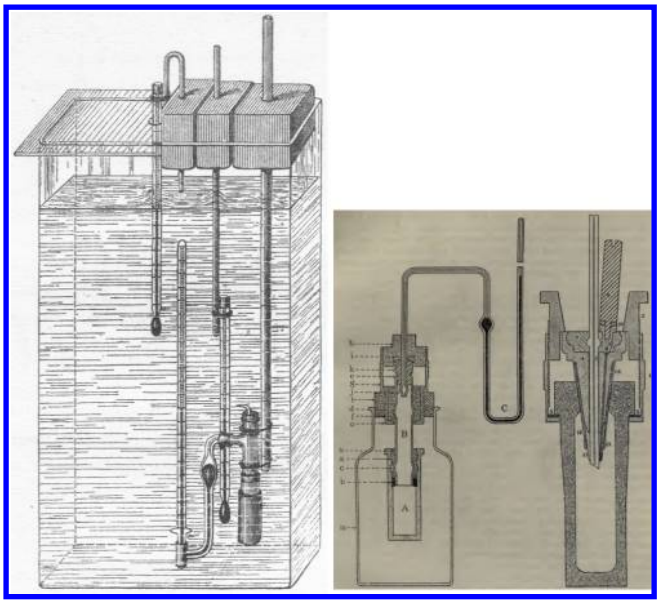

Figure 2. Osmotic pressure measurement cells involving semipermeable chemical-garden membranes deposited within a porous medium of porcelain or clay. (left) Pfeffer's apparatus.[8] (right) Two examples of Morse's apparatus.[9] Reprinted from Pfeffer, Morse (1877, 1914), refs 8 and 9.

> *"The phenomena of osmotic growth show how ordinary mineral matter, carbonates, phosphates, silicates, nitrates, and chlorides, may imitate the forms of animated nature without the intervention of any living organism. Ordinary physical forces are quite sufficient to produce forms like those of living beings, closed cavities containing liquids separated by osmotic membranes, with tissues similar to those of the vital organs in form, colour, evolution, and function."*

2.3. Mid 20th Century

By the time D'Arcy Thompson published the second edition of his classic text *On Growth and Form*[15] (1942), the idea that chemical gardens could tell us something about life was in decline:

> *"...though the reactions involved may be well within the range of physical chemistry, yet the actual conditions of the case may be so complex, subtle and delicate that only now and then, and only in the simplest of cases, has it been found possible to imitate the natural objects successfully. Such an attempt is part of that wide field of enquiry through which Stephane Leduc and other workers have sought to produce, by synthetic means, forms similar to those of living things..."*

The reason for the devaluation is clear: the rise of genetics, culminating in 1953 in Watson and Crick's unravelling of the structure of the DNA molecule.

DOI: 10.1021/acs.chemrev.5b00014
Chem. Rev. XXXX, XXX, XXX−XXX

However, chemical gardens, and the work of Leduc and others, continued to provide fascination beyond science. In *Doktor Faustus*[16] (1947), Thomas Mann wrote extensively of them:

> *"I shall never forget the sight. The vessel of crystallization was three-quarters full of slightly muddy water — that is, dilute water-glass — and from the sandy bottom there strove upwards a grotesque little landscape of variously coloured growths: a confused vegetation of blue, green, and brown shoots which reminded one of algae, mushrooms, attached polyps, also moss, then mussels, fruit pods, little trees or twigs from trees, here and there of limbs. It was the most remarkable sight I ever saw, and remarkable not so much for its appearance, strange and amazing though that was, as on account of its profoundly melancholy nature. For when Father Leverkühn asked us what we thought of it and we timidly answered him that they might be plants: "No", he replied, 'they are not, they only act that way. But do not think the less of them. Precisely because they do, because they try to as hard as they can, they are worthy of all respect'. It turned out that these growths were entirely unorganic in their origin; they existed by virtue of chemicals from the apothecary's shop, the "Blessed Messengers". Before pouring the waterglass, Jonathan had sprinkled the sand at the bottom with various crystals; if I mistake not potassium chromate and sulphate of copper. From this sowing, as the result of a physical process called "Osmotic pressure", there sprang the pathetic crop for which their producer at once and urgently claimed our sympathy. He showed us that these pathetic imitations of life were light-seeking, heliotropic, as science calls it. He exposed the aquarium to the sunlight, shading three sides against it, and behold, toward that one pane through which the light fell, thither straightway slanted the whole equivocal kith and kin: mushrooms, phallic polyp-stalks, little trees, algae, half-formed limbs. Indeed, they so yearned after warmth and joy that they clung to the pane and stuck fast there. "And even so they are dead", said Jonathan, and tears came in his eyes, while Adrian, as of course I saw, was shaken with suppressed laughter. For my part, I must leave it to the reader's judgment whether that sort of thing is matter for laughter or tears."*

Oliver Sacks recalls making chemical gardens as a boy, more or less contemporaneously with Mann's novel, in his autobiographical *Uncle Tungsten: Memories of a Chemical Boyhood*,[17] and some of the authors of this review have similar childhood memories.

The foregoing extract from Mann appears to conflate Leduc's work on osmotic growths with Loeb's coeval work on heliotropic organisms and on osmosis and artificial parthenogenesis.[18] We have seen only one report of classical chemical gardens displaying heliotropism.[19] A modern reading of that somewhat confusing work leads one to the conclusion that localized heating from focusing sunlight in the liquid would have been giving rise to a buoyant plume that could entrain chemical-garden tube growth. For modern heliotropic chemical gardens, however, compare section 7.4. Mann's choice of salts should also be commented upon: copper sulfate is commonly used to produce chemical gardens; potassium salts, however, are not, because of their great solubility. In this case the potassium salt provides the dichromate ion — in the original German it is clear that he means potassium dichromate — that can react with the copper from the other salt, along with the silicate from the waterglass.

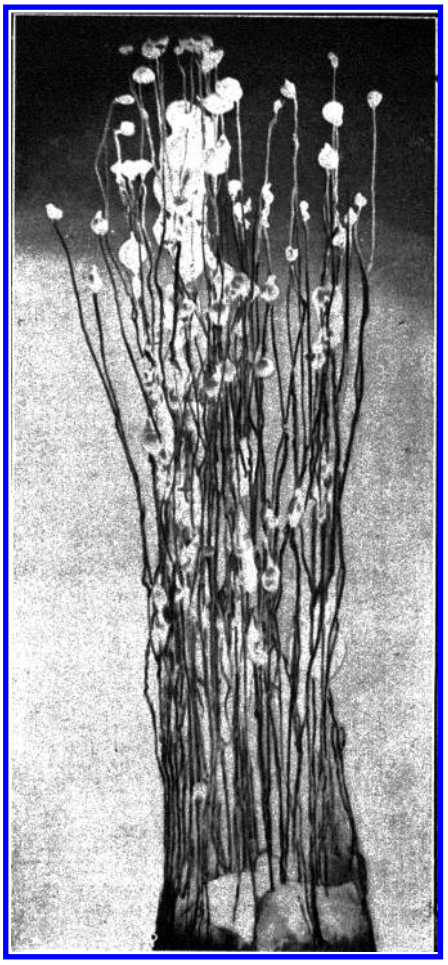

Figure 3. Example of Leduc's work: "Osmotic growth produced by sowing a mixture of $CaCl_2$ and $MnCl_2$ in a solution of alkaline carbonate, phosphate, and silicate. The stem and terminal organs are of different colours." The vertical size is some tens of centimeters. Reprinted from Leduc (1911), ref 12.

By the time J. D. Bernal wrote on the theme in *The Origin of Life*[21] in 1967, post Watson and Crick's work on DNA, chemical gardens were passé:

> *"To a scientist of the last century speculating on the origin of life, the first task as he saw it, was to produce something that gave the forms of what seemed to be characteristic of primitive life; to imitate life by means of various precipitates of inorganic or organic substances; to show that even silicates could produce globular and filamentous forms which mimicked many of the features of life as did, for instance, Leduc's algae and mushrooms".*

The discovery of the genetic mechanisms of inheritance led biology away from looking for the origin of life in the inorganic world; meanwhile osmosis was now considered a well-understood process, and beyond a few prescient early papers that began to detail the physical growth processes,[22−24] chemical gardens were generally relegated to chemistry sets, to the role, so well-described by Mann, of introducing chemistry to children. (For example, see the didactic papers of Eastes and Darrigan[20] and Eastes et al.[25] with aesthetic pictures reproducing some of the experiments of Leduc one century on; Figure 4.) Despite their beauty, however, teaching is a role for which they are ill-suited, since they are so complex and little understood.

DOI: 10.1021/acs.chemrev.5b00014
Chem. Rev. XXXX, XXX, XXX−XXX

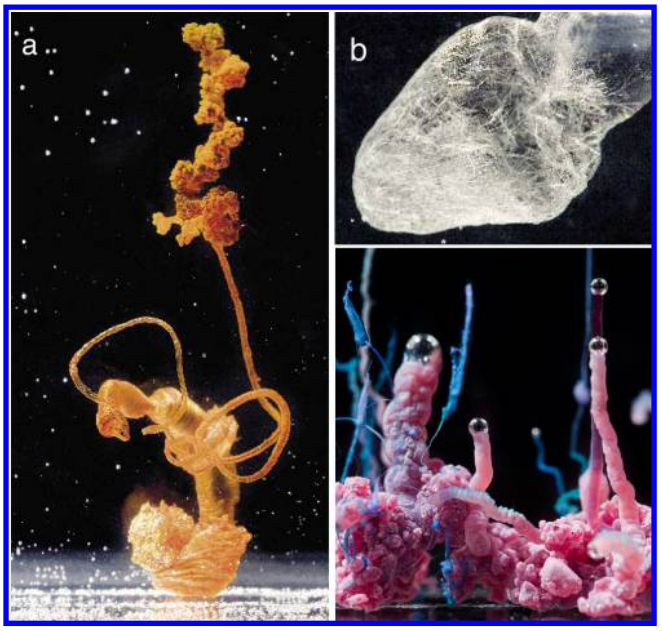

Figure 4. Examples of Eastes and Darrigan's modern recreations of Leduc's work. (a) Sodium silicate solution with an iron(III) chloride seed. (b) Sodium carbonate and sodium phosphate solution with a calcium chloride seed. (c) Sodium silicate solution with a cobalt chloride seed. Images courtesy of Stéphane Querbes.

It was only toward the end of the 20th century that research interest in chemical gardens revived, beginning with the 1980 paper of Coatman et al.,[26] which stemmed from David Double's interest in cement hydration (section 7.2). The work we report here springs from this modern resurgence of interest in chemical gardens, which, moreover, readdresses the interrelated physical, chemical, and biological themes present in chemical-garden research since Glauber.

3. INVENTORY OF EXPERIMENTAL METHODS

The classical chemical garden, described by Glauber in section 2.1, uses a solid metal-salt seed in an aqueous solution of a suitable anion. Through a self-organized growth process of semipermeable membrane formation, osmosis, buoyancy, and tube growth, this produces what is known as a chemical garden. As well as using this classical seed-growth mechanism (section 3.1), one can utilize a variety of experimental techniques to explore various aspects separately. One part of this process, tube formation, can be studied by injecting one solution into another at a given rate (section 3.2). One can also use gas bubbles as buoyancy-driven guidance for tube growth (section 3.3). The precipitation membranes themselves can be deposited in controlled conditions and studied separately (section 3.4). The entire reaction can be studied within a gel (section 3.5). The importance of buoyancy forces can be explored by performing experiments in variable gravity; either in the microgravity of space, or in greater than Earth gravity using a centrifuge (section 3.6). The dimensionality of the system can be reduced using a Hele-Shaw cell to produce growth in almost two dimensions (section 3.7). All of these experimental methods are contributing to our understanding of the chemical-garden system, as we shall describe below.

3.1. Seed growth

In many chemical-garden experiments, the structure forms as a solid "seed" of a soluble ionic compound dissolves in a solution containing another reactive ion (Figure 1). In the classic experiment, a hydrated metal-salt seed is submerged in a sodium silicate solution (Figure 5). The solid seed could be a single crystal but equally could be a polycrystalline aggregate with any size of constituent crystals. Note that the usage of this term in chemical gardens differs from that of crystal growth. Here, the word seed is making use of the common English language definition of "an initial stage from which something may develop".

Traditionally the external solution is a waterglass solution, an aqueous solution of sodium metasilicate,[28] where the Na^+ salt is highly soluble at the external and internal pH and does not form insoluble compounds with the counterion of the metal-salt seed. Owing to the polymerization tendency of silicate,[28] there is not only one silicate anion in the external aqueous solution that can precipitate in contact with the seed metal cation and at the pH of the internal solution. In general any alkali silicate solution can be used due to their high solubility at high pH. The cation should not precipitate with the counterion of the metal salt used as seed

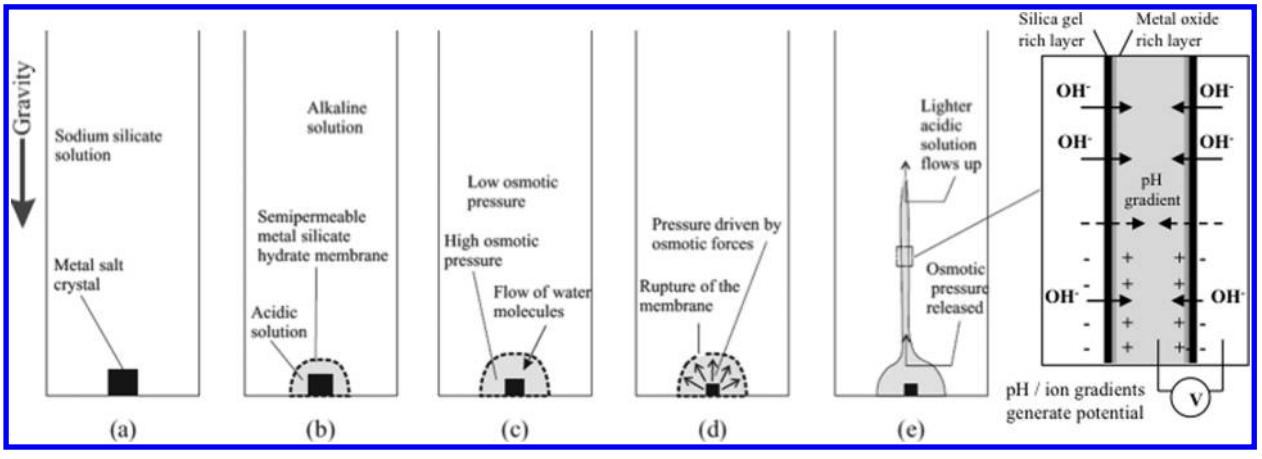

Figure 5. Mechanism of growth of a classical chemical-garden structure from a metal-salt seed placed in sodium silicate solution. (a) Setup at the start of the reaction. (b) Membrane formation between acidic and basic solutions. (c) Osmotic pressure is higher within the membrane than outside it, so the membrane expands. (d) Under osmotic forces, the membrane ruptures. (e) A tube forms. Hydroxide (OH^-) is preferentially drawn into the interior of the membrane. The ionic and pH gradients across the membrane give rise to a membrane potential, as there is a difference in charge between the inner and outer solutions. Adapted with permission from ref 27. Copyright 2002 Elsevier.

DOI: 10.1021/acs.chemrev.5b00014
Chem. Rev. XXXX, XXX, XXX−XXX

and this should be taken into account before using other silicates. Other anions can be used in the external solution, such as phosphates, carbonates, oxalates, etc., as we shall discuss in section 4. In general these anions should satisfy at least two conditions: (i) they should form a semipermeable membrane with the seed and (ii) they should form precipitates in contact with the cations of the internal solution at the pH of the internal solution. These anions can form a stable microstructure and join with the oxide-oxyhydroxides precipitated in the internal solution glueing the particles to stabilize the walls of the structures of chemical gardens.

In the early stages of seed dissolution, the metal (M) ions readily react with the aqueous sodium silicate. This leads to the formation of a colloidal membrane around the seed

$$M^{2+}(aq) + Na_2SiO_3(aq) \rightarrow 2Na^+(aq) + MSiO_3(s)$$

The semipermeable membrane restricts the exchange of ions and molecules between the surrounding silicate and the seed. Thus, a semipermeable membrane forms between the inner solution and the outer solution. Note that this semipermeability is generally not absolute; a real membrane is almost never perfectly semipermeable,[29] as we discuss in section 6. Because the inner solution maintains its high concentration until the seed is completely dissolved, an osmotic pressure is imposed across the membrane which is released by rupturing, the membrane constantly healing itself across the front between the different fluids. Buoyancy forces then cause the inner solution to flow upward, and the membrane continually ruptures and reprecipitates at this fluid interface.

The inner solution has a lower pH than the external solution. Then, when both solutions are in contact, the silicate of the external solution precipitates when it encounters the lower pH medium. The metal (M) cations of the inner solution will precipitate in the inner part of the wall when they encounter the high pH of the external solution, forming, e.g., metal hydroxides

$$M^{2+}(aq) + 2OH^-(aq) \rightarrow M(OH)_2(s)$$

In conjunction with the aforementioned processes, the above reaction steps lead to steep concentration gradients and possibly even a layering or the wall constituents within the tubular structure.

As it grows, the membrane takes on a classic chemical-garden morphology; the structure extends upward (with some sideways deviations) from the metal-salt seed with a characteristic compositional gradient: a more silicate-rich layer on its exterior and a more metal-rich layer on its interior. Chemical gardens may be generated in this way using a variety of different solids or fluids, as so well illustrated by Leduc[12] a century ago (Figure 3).

Variants of the seed method use more controlled and well-characterized sources of the metal salt that still transfer reactive ions to the system via dissolution and/or diffusion. For example Jones and Walter[30] utilized a mechanical injector that extruded a small slug of a strong calcium chloride solution thickened to a paste with fumed silica. An even simpler modification of the seed experiment involves the direct use of pellets[31−33] (an idea that was already in use in the earliest experiments; section 2.1). This method has certain advantages over the use of solid seeds because the latter can yield poor experimental reproducibility owing to a typically unknown surface-to-volume ratio and an unknown degree of polycrystallinity. Another seed method for reactant delivery involves the use of polymer beads. Makki et al.[34] used a simple emulsification technique to produce agarose microbeads that were subsequently loaded with copper sulfate solution, and once these beads were brought in contact with silicate solution, they spontaneously formed a spherical shell of precipitate and small tubes (diameters ∼3 μm) grew from the bead surface. An example of this microbead technique is shown in Figure 6. Yet another variation of the seed technique is to use a gel loaded with one of the reagents as the seed.[35] This work is in turn a return to techniques that were more common a century ago; see Leduc[12] and Lüppo-Cramer.[36]

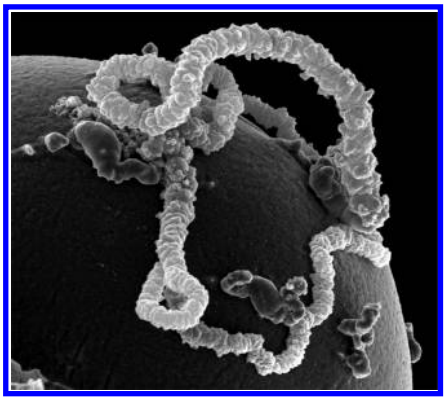

Figure 6. Scanning electron micrograph of a hollow tube produced by exposing a $CuSO_4$-loaded agarose bead to sodium silicate solution. The outer diameter of this tube is approximately 10 μm. Reprinted with permission from ref 34. Copyright 2009 Wiley-VCH Verlag GmbH & Co. KGaA.

The structures formed in seed chemical-garden experiments can vary widely, sometimes changing morphology, at macro- or microscales, within the same structure. For example, in the microbead study noted above it was observed that with decreasing growth velocities the tube changed from a smooth to a brick-like texture, and bead-mediated tube growth occurred only if the product of bead radius and loading concentration exceeded a critical value.[34] There are many other examples of morphology transitions in the chemical-garden literature (e.g., Leduc,[12] Barge et al.,[37] Haudin et al.,[38] etc.) and the precise causes of these changes are still only partially understood.

Typically in these experiments, the solid seed is composed of the metal salt, and the surrounding solution contains the anion (e.g., silicate). However, "reverse" chemical gardens are also possible in which a silicate seed is mechanically held in the upper portion of a metal-ion salt solution. As in the preceding experiments, a precipitated membrane forms between the silicate and metal ions, this time around the silicate seed, and the membrane bursts under high osmotic pressure. The silicate seed continues to dissolve, producing an interior silicate solution which jets out as the membrane ruptures. Precipitation at the changing fluid interface forms a tube, which grows downward, rather than upward, because the silicate solution is denser than the surrounding fluid. The mechanism of formation of reverse chemical gardens is much the same as that in the classic experiment: the semipermeable precipitated membrane forms between different fluids, and the metal ion precipitates at the interface due to the sudden pH change while silicate ions remain on the inside.

An interesting example of a reverse silicate garden is described in a recent publication by Satoh et al.,[39] who studied the effects of pumping an alkaline solution leached from cementitious building materials through fractured low-porosity granitic rocks. This

DOI: 10.1021/acs.chemrev.5b00014
Chem. Rev. XXXX, XXX, XXX−XXX

experiment resulted in the precipitation of calcium silicate hydrate (C−S−H) colloidal membranes and the formation of tubular structures, which grew downward. These structures were attributed to a reverse silicate garden phenomenon; the calcium-rich alkaline solution reacting with silica from the granitic rock and forming C−S−H membranes and tubular growths, with the silicate inside the tubes.

More exotic solutions, such as polymers, have been used to grow chemical gardens: Bormashenko et al.[40] studied the formation of chemical gardens by placing iron(III) chloride seeds in solutions of potassium hexacyanoferrate(II) with cellulose hydroxyethyl ether of different molecular weights. This polymer is joined to the external surface yielding a higher mechanical stability of the tubular structures. For the low-molecular-weight experiments, traditional chemical-garden growth was observed; however, for the high-molecular-weight experiments, the $FeCl_3$ seed floated on top of the solution and formed a downward-growing chemical garden.

In the 19th century, similar or more complex solutions for chemical-garden growth were used by those investigating plasmogeny and synthetic biology, including complex biological solutions of albumen, gelatin, and protoplasm; see Leduc.[12] The use of thickening and gelling agents to increase viscosity and/or density is a technique that was extensively tried in the past, presumably to obtain "better" tubes and vesicles, and ought to be explored more in current work. Perhaps the closest current approach is the gel work of Ibsen et al.[35]

See also section 7.4 for polyoxometalates used as seeds.

3.2. Injection Growth

A main property of seed chemical-garden experiments is that initially, when the fluid is not moving under buoyancy or osmosis, the delivery of the inner reactant is diffusion controlled. Regardless of whether it is the acidic (metal) ion or the alkaline (e.g., silicate) ion, this transport by diffusion controls the dissolution of the seed. Even in the microbead method described in section 3.1, the reactant is supplied by diffusion out of the loaded beads and that method is therefore a similar process. However, the formation of the chemical-garden precipitate membrane occurs at an interface between solutions of contrasting chemical composition and pH, and this precipitation can also occur if one solution is simply injected into another.

Injection methods typically utilize a syringe pump to feed one solution into a reservoir of the other at a flow rate of the experimenter's choosing. In this case the chemical garden grows directly out of the injection aperture in a manner otherwise similar to that observed with the seed method, except that the internal fluid pressure is now supplied mainly by the pressure of the injection rather than by osmosis. In injection experiments, just as in seed experiments, the differences in the water activities of the solutions on either side of the precipitate membrane drive osmotic flow of water across the membrane, followed by subsequent membrane rupturing, reprecipitation, and growth. In either case, a self-assembling precipitate structure is formed.

Injection experiments allow the experimenter to determine precisely the ionic concentrations of both solutions; the concentration of the injected ion solution is known and can be kept constant, unlike in seed experiments where the composition of the inner solution is difficult to measure and is constantly changing. Moreover, the injection method can be used to grow chemical gardens in reactant systems that are not possible with a seed, e.g., different solutions containing several precipitating ions, or precipitation reactions between dilute reactants. The injection method is a descendent of Traube's[5] and Pfeffer's[8] osmotic experiments using two solutions discussed in section 2.2. Injection-driven precipitation also forms the basis of many natural chemical gardens; see section 8.

Injection experiments offer a greater degree of control over both physical parameters (e.g., internal fluid pressure; growth directions) and chemical parameters (e.g., interior ion concentrations; pH gradients). Use of this method has allowed a more controlled study of the growth of chemical-garden structures. Thouvenel-Romans and Steinbock[42] studied the growth of tubular precipitation structures in experiments that involved the injection of aqueous copper sulfate into a large reservoir of 1 M silicate solution. The flow rate of the injected solution was kept constant, and the solution was delivered through a glass capillary at the bottom of the silicate reservoir. This setup produced single, upward-growing tubes in a reproducible fashion. In this study, the authors identified three distinct growth regimes: "jetting", "popping", and "budding", which were shown to be related to the decreasing buoyancy difference between the less dense, injected fluid and the denser silicate solution as metal-salt concentration in the injection was increased. Jetting, occurring at low copper sulfate concentrations, was produced by tubes forming around a buoyant jet of injected solution. At intermediate concentrations, tubes grow in an oscillatory fashion, which involves the periodic capping of the tube tip, the expansion of this membrane cap into a balloon-like structure, and the abrupt release of this balloon: this regime is called popping. At high concentrations, the growth was also rhythmic, but the balloon-like segment remained attached and gave rise to the formation of new "buds" through small breaches: for this reason, this regime is termed budding (cf. Figure 7).

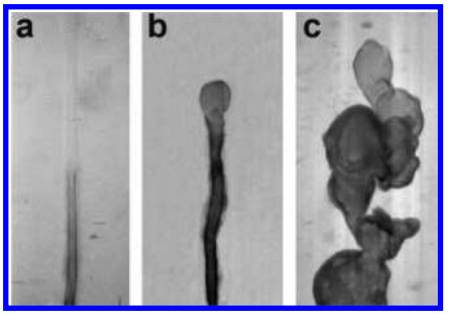

Figure 7. (a) Jetting, (b) popping, and (c) budding tubes in the $CuSO_4$/silicate system. Fields of view: (a) 2.6 × 6.4 mm (a) and (b,c) 7.3 × 15.0 mm. Reprinted with permission from ref 41. Copyright 2004 European Physical Society.

Jetting growth can be understood as a templating process. In Thouvenel-Romans et al.,[41] it was shown that the outer tube radius was well described by the radius of a buoyant, nonreactive jet of one viscous fluid in another. The corresponding equation for flow-rate-dependent radius involves viscosities, densities, and the radius of the cylindrical reservoir; see section 6.1. As of 2015, no quantitative models for the radius selection of popping and budding tubes exist. In popping growth, and possibly also budding growth, volume appears to increase at the same rate with which new reactant solution is delivered. A simple model for the period of popping oscillations was suggested in Thouvenel-Romans and Steinbock.[42] This model identified the process as relaxation oscillations and assumed the existence of a characteristic tensile strength of the freshly formed material. Fits of this

DOI: 10.1021/acs.chemrev.5b00014
Chem. Rev. XXXX, XXX, XXX−XXX

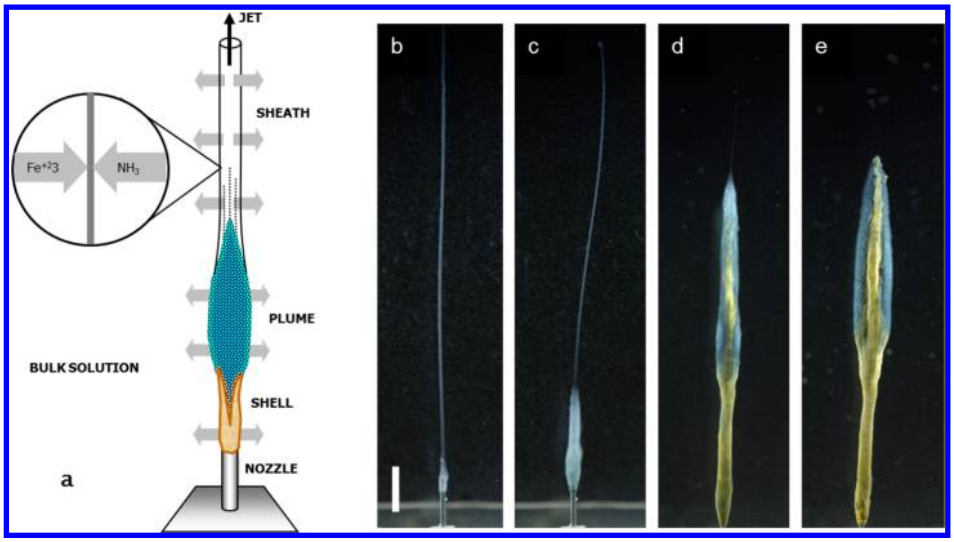

Figure 8. Precipitation templated by a fluid jet. (a) Schematic representation of the stages of growth around a jet of aqueous ammonia injected into an iron sulfate solution and the subsequent oxidation of the precipitate. (b) 1 min after start, (c) 5 min, (d) 45 min, and (e) 125 min. Scale bar is 5 mm. Reprinted with permission from ref 43. Copyright 2005 American Chemical Society.

parameter have yielded good agreement between the model and the experimental data; see section 6.4.

Another injection experiment in a quite different chemical system also followed the basic growth model of Thovenel-Romans and Steinbock. Stone et al.[43] injected an ammonia solution into iron(II) sulfate. However, they saw two new morphological transitions over time in the same system; Figure 8. After the jetting stage, which they referred to as formation of a white, diaphanous "sheath", they observed the gradual development of a much thicker "plume" of a bluish flocculant. Then this stage transitioned to a thinner, but denser orange "shell". These color transitions are in keeping with the progressively more oxidized precipitates of iron in aqueous solutions exposed to air, namely white rust or iron(II) hydroxide, bluish green oxy-hydroxides, and finally iron(III) oxy-hydroxide. This example of tubular chemical gardens illustrates a novel variation in the thickness and complexity of wall growth mirroring that found in earlier work on tubular growth in an electrochemical setting.[44]

The concentration threshold for tube formation has recently been investigated. Batista et al.[45] studied iron−sulfur tubes formed by injection of sodium sulfide into an iron(II) chloride solution. These tubes formed only above a critical reactant concentration, which was widely independent of the employed injection rate. Below this concentration threshold, Batista et al. observed the formation of colloidal particles that did not aggregate to a solid tube but rather followed hydrodynamically controlled plume structures. At the transition concentration, the system initially produced a plume conduit which then thickened in the upward direction to generate a mechanically extremely weak tube. A similar injection technique has been used by Clément and Douady,[46] with iron(II) sulfate and sodium silicate, at larger flow rates. It was evidenced that the tubes produced can grow from a fracture in a symmetrical way on both sides.

The injection approach has also been modified to form precipitates in the reverse scenario:[26] for example, injection of sodium silicate solution into a reservoir of copper sulfate solution.[47] Owing to the density differences between these two solutions, the denser silicate solution was injected in a downward direction to form downward-growing tubes. These structures tended to be more gel-like than the tubes synthesized in Thouvenel-Romans and Steinbock,[42] and also revealed an additional growth regime called "fracturing" in which segments broke off the growing structure. These experiments are a good example of how parameters that would spontaneously vary in a seed growth experiment can be controlled using the injection method.[48] A seed growth experiment with this system might have produced a combination of all three or four growth regimes resulting from variations in the metal-salt concentration in different parts of the structure. Injection methods can also allow for simulation of natural chemical-garden processes; for example, the growth of precipitates around jets of fluid at hydrothermal vents;[49,50] see section 8.

A variant of the injection technique is produced by dripping one solution into another. This method allows control of the initial droplet concentration and also of the initial membrane structure. The dripping method has been studied in detail for one particular set of concentrations of calcium chloride solution dripped into sodium silicate solution.[51] For drops falling from small heights the metal-salt solution is encapsulated by a continuous membrane, while for large heights a broken or scattered precipitate structure forms. After the encapsulated drops were produced, osmosis drove the growth of open tubes. The dependence of the membrane shape on the drop height occurs, in part, because as a drop falls its shape oscillates between prolate and oblate, and the shape of the drop at impact greatly affects the shape of the membrane that forms around the drop.

We shall discuss the specific case of injection into 2D geometries in section 3.7.

3.3. Bubble Guidance

Already early papers noted that many precipitation structures are guided by the buoyancy of an attached air bubble (Figure 9). In 1941 Hazlehurst[23] described this air-capped growth as typically erratic and stated that tube growth without a leading air bubble is observed only if the growth process is very rapid or crystallization is slow. It is not clear whether these criteria are correct since the idea has not yet been pursued in quantitative studies. However, Hazlehurst[23] also described an interesting modification of the underlying phenomenon, which is induced by floating a solid seed (such as iron(II) chloride) upon the silicate solution, utilizing its surface tension. The resulting gelatinous membrane

DOI: 10.1021/acs.chemrev.5b00014
Chem. Rev. XXXX, XXX, XXX−XXX

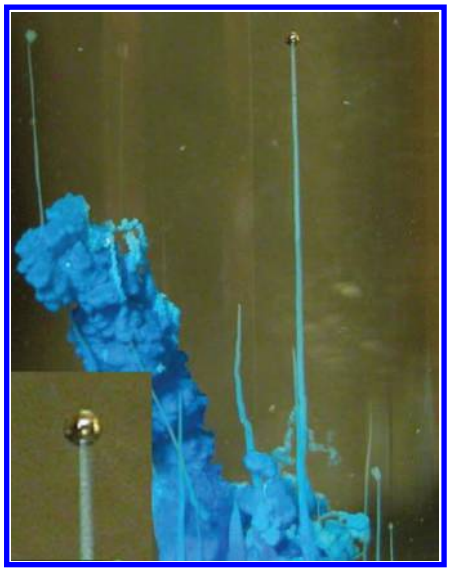

Figure 9. Tube growth with a bubble at the tip; the inset photo shows a magnified view of an air bubble during the vertical growth process. Field of view: 1.9 × 2.5 cm; inset: 2.4 × 3.2 mm. Reprinted with permission from ref 52. Copyright 2005 The Royal Society of Chemistry.

cup initiates tube formation in a downward direction. During this "hanging growth", the solid seed remains at the closed base of the tube while the length-extending reaction zone is at the air−liquid interface. Apparently, the inner salt solution does not come in direct contact with the surrounding silicate and all reactions occur at or close to a thin, continuously forming membrane. Consequently, this experiment can be considered to probe the limiting case of tube growth at very large bubble radius.

Gas bubbles can also be used in the injection method of section 3.2 to increase the overall straightness of the resulting tubes. In this method, a gas bubble is pinned to the growth zone at the tip of the tube where the inner solution is injected. As the inner fluid is injected, a precipitate tube grows, and the gas bubble remains connected to the top of the precipitate structure, moving ever upward as more precipitate is formed. Buoyancy forces cause the bubble to rise directly upward, thus forcing the tubes to grow vertically. In Thouvenel-Romans et al.[52] the tube radius was tightly controlled by the bubble radius with bubble-to-tube radius ratios in the range of approximately 0.8−0.95. It was shown that the rate of increase in tube volume matched the rate of reactant injection, and thus the vertical growth velocity of the tube could readily be predicted and controlled.

The bubble-guidance method has also been used to study the evolution of precipitation membranes, and to control the layered composition of a tube wall.[53] Roszol and Steinbock[54] studied the kinetics of radial wall growth for bubble-directed tubes formed by injection, focusing on silica−copper hydroxide and silica−zinc hydroxide structures. In this study, tubes were formed by bubble guidance, but the injection of metal-salt solution was continued for up to 2 h after the tube had initially formed, to drive continued growth of the precipitate walls. Optical data showed that further wall growth occurred only in an inward direction, and, for copper sulfate injection, that the wall-thickness increase over time obeyed a square-root dependence. This finding suggested that the process of wall thickening in the copper sulfate system is diffusion-controlled, and occurred as a reaction−diffusion front that propagated in the direction of lower reactant concentration[54] (the simplest case of such a front, for the reaction A + B → C, was studied theoretically by Galfi and Racz[55]). For zinc sulfate injections, however, the tube wall radius remained essentially constant over time. This constancy is thought to be a result of the amphoteric character of zinc hydroxide.[54] Subsequent flow of reactants through an already-formed tube can be used to synthesize tubes with layered walls; for example, Roszol and Steinbock[54] synthesized tubes with layered walls consisting of amorphous silica, copper hydroxide, and zinc hydroxide. It seems likely that this layering approach, employing successive injections of different metal-salt solutions in bubble-directed experiments, may be extended to a wide variety of materials for technological purposes.

The bubble-guidance method has been extended to control the vertical growth velocity of a precipitation tube formed by injection.[56,57] In these experiments, a large gas bubble was moved upward at given speeds using a motor-controlled glass rod. The tube radius was selected according to the injection rate of the inner solution, but the vertical growth velocity of the tube was determined by the externally controlled movement of the attached bubble. Moving the bubble upward caused extension of the precipitate tube, and, interestingly, the length extension only occurred either directly underneath the pinning gas bubble or slightly above the injection nozzle, not along the entire tube length. In addition, Makki and Steinbock[56] performed experiments in which the speed of the rod and bubble was alternated periodically between two values. The resulting tubes from this fast−slow bubble growth had corresponding small and large segments whose radii could be predicted from volume conservation of the injected reactant. In transition regions formed during the nearly instantaneous fluid deceleration, numerous nodules were formed on the outer tube surface, presumably in response to the abrupt increase in internal fluid pressure that could not be accommodated by an increase in tube radius. Typical examples of these structures are shown in Figure 10.

Figure 10. Tube growth under externally controlled oscillations of the linear growth velocity. These two representative, dried samples were obtained by alternating the speed between 2 and 6 mm/s. The nodules seem to occur as the result of rapid deceleration. Scale bars: 1 cm. Reprinted with permission from ref 56. Copyright 2011 American Chemical Society.

The same method has been used to trap CdSe/ZnS quantum dots (semiconductor nanocrystals that are small enough to exhibit quantum mechanical properties) in the tube wall.[58] In these experiments, luminescent nanoparticles were dispersed in the injected zinc sulfate solution. The otherwise hydrophobic particles were modified by ligand exchange with dihydrolipoic acid appended with poly(ethylene glycol) prior to injection. Analyses of the dried tube structures showed that quantum dots were distributed nearly homogeneously within the wall at a number density of 10^{10} particles per millimeter of tube length. Chemical quenching experiments with the rehydrated tubes revealed that the large majority of the nanoparticles are accessible to ions such as $Cu^{2+}(aq)$ but do not leach into solution. This

DOI: 10.1021/acs.chemrev.5b00014
Chem. Rev. XXXX, XXX, XXX−XXX

study suggests possible applications of tubular precipitation structures as sensor platforms in microfluidic devices.

3.4. Membrane Growth

Another experimental technique that isolates one aspect of chemical-garden formation is to produce precipitation membranes between different aqueous solutions by introducing the two solutions on either side of an inert carrier matrix:[59] e.g., parchment paper, cellophane, gel, or dialysis tubing. This "artificial" chemical-garden membrane setup dates back to the Pfeffer cell[8] of the 19th century (section 2.2), which used an unglazed porcelain matrix for the same purpose. The idea is to produce a precipitation process between any two solutions similar to that in a seed or an injection experiment. The use of a precipitation template between the different solutions structurally supports the resulting precipitation film in reaction systems where formation of a self-supporting membrane is not possible, meanwhile allowing access to solutions on both sides of the precipitate membrane for analysis of pH, ion, and electrochemical gradients. Recently experiments have been performed in this fashion with carbonates, phosphates, silicates and sulfates[37,60−63] (Figure 11).

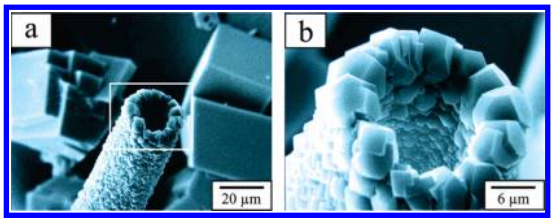

Figure 11. (a) SEM image of a tubular aggregate of calcium carbonate formed on a cation-exchange membrane. (b) The magnified image of the rectangular area in panel a. Reprinted with permission from ref 60. Copyright 2006 American Chemical Society.

Precipitation membranes generated in this manner are similar to the walls of a self-supporting chemical-garden structure: they exhibit compositional and morphological gradients across the membrane, are selectively permeable to ions (and can be cation- or anion-selective), and generate a spontaneous electrical potential difference (section 5.1). Interest in the structure of these semipermeable membranes dates back a century,[64,65] and the membranes have been studied in numerous metal-salt systems.[59,66−76]

The two-cell setup of experiments that form precipitate membranes allows for a much more detailed electrochemical characterization of the precipitate than is possible in a chemical-garden system, since electrodes can be placed very close to the membrane surface as well as in both bulk solutions. Inorganic precipitate membranes have been studied both as analogs of biological membranes and as ion-exchange membranes that could be useful for industrial applications (e.g., electrodialysis, membrane electrodes, fuel cells). The use of a matrix to support the precipitate membrane also allows one to conduct studies on the permeation of ions through the membrane. The two-cell setup allows the experimenter to replace the electrolyte solutions on either side, and thus to study the membrane's behavior when it is placed between any two solutions (e.g., in a concentration gradient of Na^+ or K^+). Measurement of membrane potential as a function of electrolyte concentration gradient across the membrane can determine the relative selectivity for specific ions and the ion transport mechanism.[59,67,68,72−75]

Since the self-assembling inorganic membranes formed between different solutions exhibit compositional gradients, they can also be composed of layers of positive and negative fixed charge, and can be bipolar.[66] Experimental studies of inorganic membranes have revealed that they have many unusual and interesting properties (see, e.g, van Oss[77] and references therein), and therefore it is likely that seed chemical-garden membranes also exhibit similar characteristics, although the nature of seed chemical-garden experiments makes it quite difficult to investigate in the same manner.

3.5. Growth in Gels

What if a gel matrix between different aqueous solutions, such as we discussed in section 3.4 above, were made large enough to allow a complex dynamics to develop within it? There are studies in gels of chemical reactions that form semipermeable membrane precipitates within the gel upon the reaction of two solutions. The reactions can produce complex dynamics, including spirals and target patterns;[78−83] see Figure 12. The reagents involved

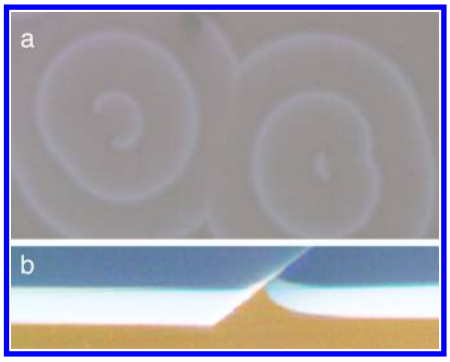

Figure 12. Traveling precipitation waves, including counterrotating spiral waves, are observed in the precipitation reaction of $AlCl_3$ with NaOH. (a) Image, taken from above, of waves in a gel disk within a Petri dish. (b) Image of a wave traveling in a gel containing the pH indicator bromothymol blue (with front illumination). Reprinted with permission from ref 86. Copyright 2013 American Chemical Society.

include hexacyanoferrates and hydroxides reacting with metal salts. That is to say, these are systems which, when placed as a seed in a liquid, produce classical chemical gardens. It should not therefore surprise us that it has been proposed from conductance and impedance measurements that the reaction is precipitating in the gel a membrane semipermeable to some ions.[84,85] A mathematical model has recently been proposed for a example of this class of systems, in which the semipermeable nature of the membrane is essential to the pattern formation.[86]

Given the semipermeability and the presence of different species on the two sides of the membrane, there ought to be osmotic forces operating within the gel. However, there have not been any studies of this point. These gel systems have not hitherto been connected conceptually with chemical gardens; however, given the formation of a semipermeable membrane in these systems, we may consider them to constitute chemobrionic systems in gels. We must note that these are not Liesegang patterns; while Liesegang rings are formed by aqueous solutions diffusing into gels, they differ fundamentally in not involving any semipermeable membranes.[87]

3.6. Varying Gravity

Buoyancy in chemical gardens is a consequence of density gradients that, in classical seed experiments, vary both spatially and temporally during the formation process. It is a major source

DOI: 10.1021/acs.chemrev.5b00014
Chem. Rev. XXXX, XXX, XXX−XXX

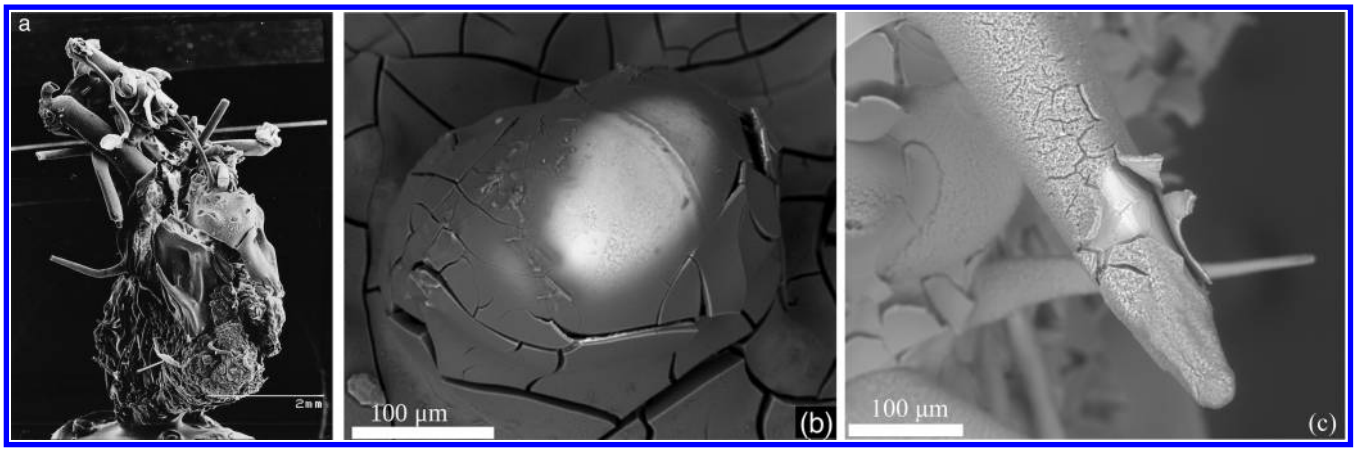

Figure 13. Chemical gardens grown in 0 g; SEM micrographs showing (a) growth under microgravity of a cobalt salt with sodium silicate. Reprinted with permission from ref 30. Copyright 1998 Elsevier. (b) MnCl in 6 M silicate. The brighter region is rich in MnO_2 and the darker in $MnSiO_3$. (c) $NiSO_4$ in 2 M silicate, the external dark layer is SiO_n and the bright internal layer is nickel silicate. Reprinted with permission from ref 33. Copyright 2011 American Chemical Society.

of complexity that affects the composition, morphology, and structure of the resulting garden. It is then an interesting idea that by performing such experiments in space the gravity will be effectively removed and the physics much simplified. Since there is no buoyancy, the only force driving the experiment is the difference of osmotic pressure across the membrane, which can now be studied in isolation. Over the last two decades, the results of two experiments performed in microgravity conditions have been published, by Jones and Walter[30] (see also Jones[88,89]) and Cartwright et al.[33] (A technical description of the experimental setup for the first chemical garden sent into space was published earlier by Stockwell and Williams,[90] who, unfortunately, did not publish the results they obtained. The results of another chemical garden grown in space were lost in 2003 along with the Space Shuttle Columbia.)

The primary objective of microgravity experiments is to isolate the effects of forced convection from those of buoyancy, so as to understand better the roles of osmosis and buoyancy in the growth process.[27] In the presence of Earth gravity the precipitation tubes usually grow upward, as the metallic solution is less dense than the silicate solution in which the seed salt is immersed. However, in the absence of gravity there is no upward direction and tubes grow out from the solid seed apparently randomly, without any preferred direction. Jones and Walter[30] grew two microgravity chemical gardens not with a solid seed at all, but with a paste made of a solution of the metal salt, thickened with finely fumed silica. Tube growth in microgravity generally follows straight lines until the container wall is reached. At a wall, either the growth ends or, in some cases, the tube rebounds off the wall and continues its growth in an opposite direction.[30,33]

The most evident effect of microgravity, other than the different growth-orientation behavior, is the reduced growth rate.[88] An average chemical garden experiment that takes minutes to complete on Earth can take several days in microgravity. This decrease in growth rate is a consequence of the depletion of reactive species around the growth area. As the growth progresses by precipitation of metal silicates, a concentration gradient is developed for the reagents in solution. In the absence of convection, the concentration profiles of species diffusing to the reactive interface are smooth. In the presence of convection, the profile changes: it has high spatial gradients in a concentration boundary layer near the interface and low spatial gradients in the bulk fluid. The high gradients near the interface are responsible for the fast transfer of species and thereby the faster growth observed under gravity.

As well as the normal tubes, unique forms can be observed in microgravity experiments. The absence of buoyancy-driven convection in microgravity not only slows down the overall growth rate, but also has surprising effects on the growth morphologies. In the presence of gravity the membrane is formed and inflated quickly enough so that it cannot thicken much before bursting. In the absence of gravity, everything is slowed and a much thicker membrane forms. This membrane is more resilient and in some instances will not burst, instead it will bulge outward in any region with an excess of pressure. As soon as a bulge is formed the stretched membrane wall becomes weaker and more flexible, presenting less resistance to the inner pressure and further growing outward forming an elongated shape like a plastic finger. This growth regime is termed plastic deformation, as opposed to the usual tubes found in chemical gardens grown on Earth.[30,33] This growth regime is, it seems, unique to microgravity experiments and produces very irregular shapes. The effect was observed in both published reports using two different experimental setups[30,33] (Figure 13).

As a conclusion we can say that eliminating buoyancy-driven convection, by removing gravity, simplifies in part the experiments. However, it also introduces a new source of complexity, the plastic deformation regime, which makes chemical gardens in microgravity a whole new very interesting phenomenon requiring and deserving further research.

One can also force an opposite effect if chemical-garden experiments are performed with gravities larger than 1 g. A stronger gravity increases the influence of buoyancy-driven convection during chemical-garden growth. Density differences become more relevant and define the growth morphologies.

Nearly all chemical gardens are grown under normal gravity. The growing fibrils might initially wander, due perhaps to local fluid flow during their solidification, but once free of such perturbations a fibril should grow directly upward against gravity. Even if a garden generates a mass of growing fibrils, a chemist would expect them to grow upward vertically, spreading around a statistical pattern centered on that vertical. This is not always the case. An extreme example is shown in Figure 14, which is a chemical garden grown from a cobalt sulfate crystal under 1 g. It is very obvious that the fibrils avoid the vertical rather strongly; most of them are at 45° to the vertical. Accordingly, it is of

DOI: 10.1021/acs.chemrev.5b00014
Chem. Rev. XXXX, XXX, XXX−XXX

Figure 14. Cobalt sulfate chemical garden grown at 1 g with sodium silicate displays tubular growth deviating from the vertical by preferred angles; a phenomenon as yet unexplained. The size is some tens of centimeters. Image from David Jones.

interest to observe fibril directions in chemical gardens grown under gravities different from 1 g. There are two ways of doing this. A garden grown on an Earth satellite is under microgravity. But it is also possible to grow a chemical garden under centrifugal force in addition to normal gravity. A chemical garden grown in a centrifuge under 100 g shows fibrils grown parallel to each other, and directed straight toward the center of the centrifuge. A less extreme experiment can mount a chemical-garden cell on a platform spinning at 78 rpm. This gives a combination of gravity and centrifugal force equal to about 1.5 g. If the rotor is arrested during the experiment, while allowing the garden to go on growing, changes in the orientation of the fibrils might be observed. Such experiments have not so far clarified the observations.

3.7. Growth in Quasi Two Dimensions

Another means to tease out the complexity of chemical gardens into separate strands is to reduce the dimensionality of the system.

Chemical gardens may be grown upon injection of solutions into a so-called Hele-Shaw cell, a quasi-two-dimensional reactor consisting in two parallel plates separated by a small gap. This geometry is frequently used in laboratory-scale studies of viscous fingering phenomena that occur when a less viscous solution displaces a more viscous one.[91−94] The technique was utilized with a seed in Cartwright et al.,[27] where it was used to enable images to be taken using Mach−Zehnder interferometry. More recently, it has been used with injection.[38]

The Hele-Shaw cell is placed in a horizontal position on a light table providing a diffuse illumination and the dynamics is recorded from above in transmission, using a digital camera. The setup uses aqueous solutions of metal salt injected radially from a source point into aqueous solutions of sodium silicate with a syringe pump. A large variety of patterns can be observed depending on the concentrations of the two reagents, as displayed in Figure 15.[38,95,96] Since the cell is horizontal and

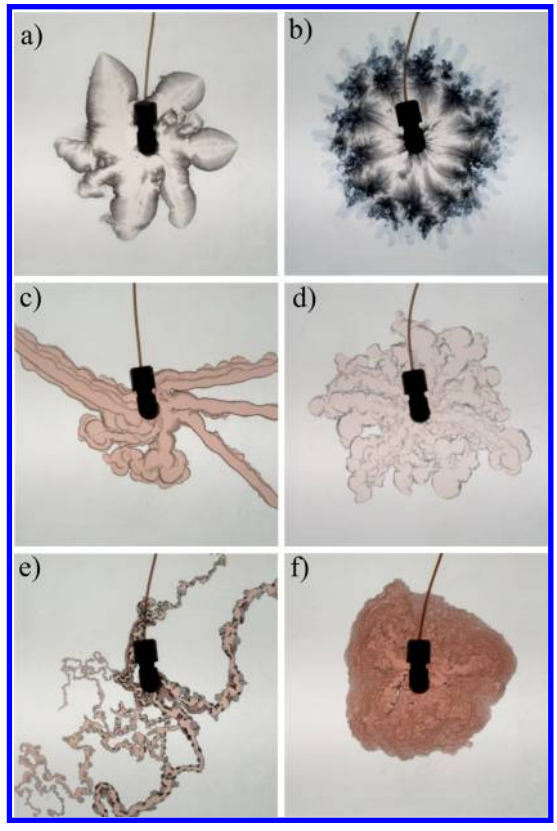

Figure 15. Quasi 2D chemical gardens: Patterns obtained after t = 30 s for cobalt chloride injected into sodium silicate in a Hele-Shaw cell for various concentrations at a fixed flow rate. The field of view is 15 × 15 cm. Images from Florence Haudin.

with a very small gap, the effect of gravity in the vertical direction and of related buoyancy-driven instabilities is negligible. The patterns obtained result thus from an interplay between the precipitation reaction and mechanical and displacement processes.

Although some reaction-driven patterning has recently been evidenced experimentally in displacements within Hele-Shaw cells without[92,94] or with precipitation,[93,100] the large variety of

DOI: 10.1021/acs.chemrev.5b00014
Chem. Rev. XXXX, XXX, XXX−XXX

different modes of growth observed in the case of chemical gardens is quite remarkable. Changes in the injection rate and of concentrations strongly affect the precipitation process and the morphology of the precipitation structures formed in the reaction zone between the two reagents. The flow strongly influences the spatiotemporal dynamics.

In some concentration ranges, spirals are obtained[38] and, as seen in Figure 15a, for a low concentration of the metallic salt and a quite concentrated sodium silicate solution, the pattern looks like a flower, formed of spiral-like buds. The membrane between the two reagents is expanding over a quite large area, with small details looking like eyelashes. In Figure 15b, for a more concentrated and also more viscous sodium silicate solution, we can see the signature of green viscous fingers ahead of the black region with precipitate. When increasing the concentration of cobalt chloride and decreasing that of sodium silicate, small spirals growing isotropically are obtained (Figure 15d). If the concentration of the metallic salt is further increased, worm-like structures with periodic bottlenecks develop in given directions (Figure 15c). For a larger silicate concentration, the pattern is made of small, fast growing intestine-like structures (Figure 15e). Other concentrations can lead to many other patterns, like for example that of Figure 15f, with a quite radial growth of the injected cobalt chloride solution, with the new material growing close to the predeposited one. The resulting structure looks like a stratification, giving an optical impression of terraces of material not completely filling the gap of the cell.

These results show that a wealth of new spatiotemporal dynamics and modes of growth are still to be studied in quasi-two-dimensional geometries. The advantage of using Hele-Shaw cells is to reduce the number of spatial degrees of freedom and to be able to use all characterization tools developed in the vast literature on reaction-driven hydrodynamic instabilities[91,101] to analyze the new patterns. A Hele-Shaw cell also allows an easier analysis of the relevant importance of the various physicochemical and mechanical processes at play in these instabilities.

In addition to experiments performed in Hele-Shaw cells there are further types of structures that can be considered quasi-two-dimensional.[97−99,102−104] These structures form in a 3D system, similarly to classical chemical gardens; however, unlike classical chemical gardens, they do not grow upward. One instance occurs when the buoyancy of the inner solution is negative with respect to the surrounding fluid, and precipitation covers the floor of the container, as shown in Figure 16. Another instance that forms quasi-two-dimensional structures is found when precipitate reaches the surface of the solution and continues to be deposited there. Examples of patterns formed in the Cu^{2+}−phosphate system are shown in Figure 17. See also section 3.3 and the "hanging growth" method,[23] which uses an infinitely large bubble: the atmosphere, or, more precisely, the menisci of the two separate solutions, so the initial precipitation occurs continuously at the air interface.

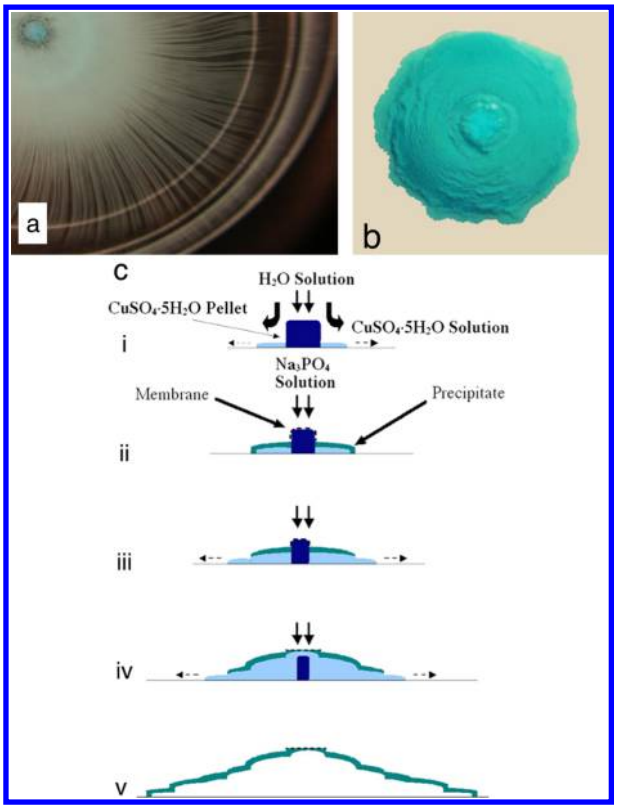

Figure 16. (a) Horizontal structure in the Cu^{2+}−oxalate system;[97] the initial pellet is visible. The structure is about 10 cm in diameter. (b) The structure that grows on the bottom of the experimental dish in the Cu^{2+}−phosphate system.[98] The structure forms a dome with successive layers visible. The structure is about 10 cm in diameter. (c) Sketch of growth dynamics of copper−phosphate structure.[97] (i, ii) The copper pellet dissolves forming a solution with greater density. This solution flows to the bottom under gravity and spreads out. On the top of the solution the membrane/precipitate is growing. It stops spreading of the solution. (iii) Osmotic pressure forces water inside the membrane, lifting a layer of the structure up. (iv, v) The solution spreads, further membrane is formed, and the process repeats. Reprinted with permission from refs 97 and 98. Copyright 2009, 2003 American Chemical Society, Elsevier.

4. MATERIALS CHARACTERIZATION

Chemical-garden structures precipitate in steep chemical and pH gradients, and their composition on the microscale reflects the solution gradients and compositions. A complete understanding of the composition and structure of these precipitation membranes at micro- and nanoscales is still not available, and will be necessary in order to control the self-assembly process to make useful complex materials (section 7). Most of these nanostructures are fragile, poorly crystallized and with very small crystal size, making their characterization difficult. In the past few years analytical equipment is becoming more sophisticated and capable of higher resolution. This presents a good opportunity to use these techniques to obtain deeper information about the complex nanomaterials that are formed in these chemical gardens.

For a summary of the different anions, cations, and experimental setups used in chemical-garden experiments, see Table 1. The properties of the materials formed depend strongly on the physical and chemical conditions. Nevertheless, we can distinguish two main aspects in the characterization of these materials: morphology (section 4.1) and chemical composition (section 4.2), as we shall describe below.

4.1. Morphology

An initial step for characterizing the materials produced from chemical gardens is to investigate their morphology. In the first place the morphology of chemical gardens has been observed simply by eye or by optical microscope. This morphology is highly dependent on the concentration of the external solution, the nature of the salt cations, and, in the case of injection, the flow rate of the injected solution. A variety of analyses have been performed to elucidate the nano- as well as the microscopic

DOI: 10.1021/acs.chemrev.5b00014
Chem. Rev. XXXX, XXX, XXX−XXX

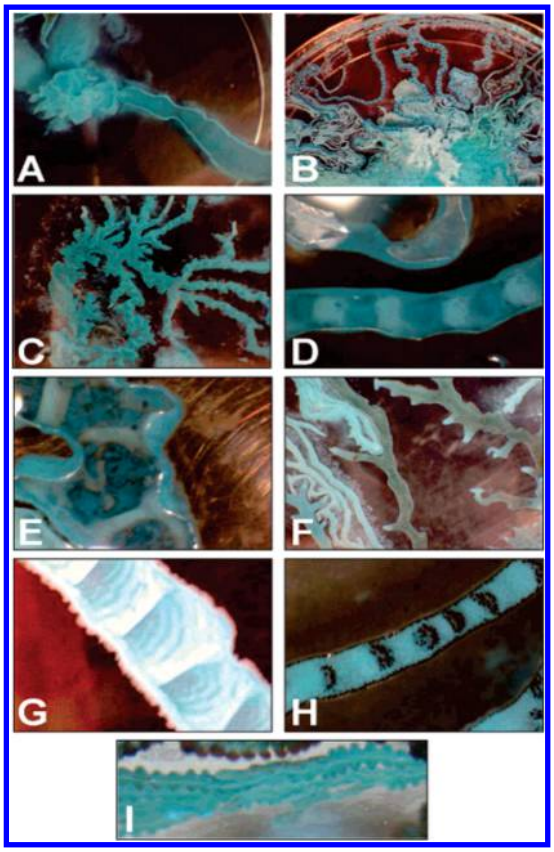

Figure 17. A variety of complex structures growing on the surface in a Cu^{2+}–phosphate system. After reaching the surface the membrane forms half-pipes. Many of these structures are made from a number of connected basins. Some structures have very pronounced periodic features, as seen in d, e, g, and h; that in g has a double periodicity. a, b, e, g, h and i have 1 cm diameter; b has 10 cm diameter. Reprinted with permission from ref 99. Copyright 2007 American Chemical Society.

structure of these materials. In addition to classical optical microscopy, scanning electron microscopy (SEM) can show the morphology of the nanostructures of chemical gardens. More details of the nanostructure of these materials can be obtained by using transmission electron microscopy (TEM). Most of these techniques have been used in many of the works referenced in this review; in this section we will cite only some specific examples. The morphology of crystals can be observed with high-resolution TEM (HRTEM).[131] The use of the electron microscope at different scales can detect some hierarchical structures (e.g., tubules-within-tubules) for these tubes.[35,119] Crystalline phases formed in these materials can be detected and identified by using X-ray diffraction (XRD).[131]

Some chemical-garden precipitates can be extracted from the reaction vessel without their collapse or breakage, enabling physical and chemical analysis after rinsing in water and gentle drying. Observing the morphology, we can identify the regime of the tube growth (jetting, budding, popping, or fracturing; section 3). In silica gardens, the external surface is initially smooth but becomes rougher during the aging process (Figure 18a,b). For instance, a comparative study carried out by Pratama et al.[125] used a downward injection of sodium silicate solution into different solutions of calcium chloride. In this experiment, the four precipitation regimes for the copper–silicate system (jetting, budding, popping, and fracturing) were also observed in the calcium–silicate system. Interestingly, the fragments from the calcium–silicate system yielded tubular fragments (0.5–2 mm in length) that were much harder than those in the reverse copper–silicate system studied by Thouvenel-Romans and Steinbock,[42] and approximately four times larger as well (with tube walls typically measuring ~40 μm in width). SEM analysis of the fracturing tubes in the Pratama et al.[125] work revealed that the exterior surfaces contained micrograins (5–20 μm), and the interior surface exhibited spatial cracks and patterns reminiscent of alligator skin (Figure 19).

We should mention the carbonate–silica microstructures studied by Noorduin et al.,[142] also called biomorphs and induced-morphology crystalline aggregates. Although these structures share the same carbonate and silicate chemistries from which chemical gardens can be formed,[143] the two phenomena are quite a long way apart. The microstructures of Noorduin et al.[142] seem to be a phenomenon linked to crystal morphology; they are microscopic forms for this reason, whereas chemical-garden forms are not linked to the microstructure of the membranes, but to the macroscopic forces of fluid physics. The carbonate–silica microstructures studied by Noorduin et al.[142] are thus not directly relevant to chemobrionics.

4.2. Composition, Porosity, and Postsynthetic Changes

Due to the large number of possible reactants, it is difficult to identify major trends and universal features in the composition of chemical gardens. We remind the reader that it might be well possible to create chemical gardens from all (sufficiently stable) salts with the exception of the salts of the alkali metals. Also the anions needed for the crucial precipitation step are not limited to a single species but can be silicates, phosphates, carbonates, borates, sulfides, hydroxide, and most likely many other compounds. Moreover, most materials characterizations have been performed on dried tube samples and sometimes dried powder. The first step in these investigations is the washing and drying of the tube samples. Surprisingly many reactions and reaction conditions yield tube samples that do not collapse or disintegrate during these steps. However, the drying process and exposure to atmospheric oxygen can alter the sample composition, as reported for iron–sulfur tubes.[45,63]

A meaningful distinction is whether the precipitation process involves two major reactants or more. The classic demonstration experiment that relies on waterglass creates tubes that consist of an outer layer rich in amorphous silica and inner layer of metal hydroxide and oxides. Accordingly these experiments involve at least four reactants, namely silicate and hydroxide ions from the solution reservoir and hydronium (hydroxonium, H_3O^+) and metal ions from the dissolving seed (or inner solution). Other experiments such as those by Batista et al.[45] are based on only one reacting metal ion (Fe^{2+}) and one counterion (sulfide). This decrease in the number of reactants is perhaps most obvious in the formation of calcium carbonate tubes on nafion membranes but even in this simplest case the tubes consist of different polymorphs.

A variety of different techniques have been employed to analyze the chemical composition of the product material in chemical gardens. The standard methods are energy dispersive spectroscopy (EDS), Raman spectroscopy, X-ray diffraction (XRD), thermogravimetric analysis (TGA), and transmission electron microscopy (TEM). The first two are often employed in ways that yield micrometer-scale resolution and can hence distinguish compositional differences between the inner and outer wall surface. This approach was extended by Roszol and Steinbock[54] for the example of silica-based structures using

DOI: 10.1021/acs.chemrev.5b00014
Chem. Rev. XXXX, XXX, XXX–XXX

Table 1. Precipitating Anions and Cations Used in Chemical-Garden Experiments[a]

anion	cation	setup	refs
aluminate	Ca^{2+}	solid	26
arsenate(III)	Cu^{2+}	solid	105
	Mg^{2+}	solid	105
arsenate(V)	Co^{2+}	solid	105
	Cu^{2+}	solid	105
borate	Fe^{3+}	solid	23
carbonate	Ba^{2+}	solid	35,105
	Ca^{2+}	solid	35,105−107
		liquid	19,60,61,106
	Co^{2+}	solid	105
	Cu^{2+}	solid	35,107,108
	Cu^{2+}, Zn^{2+}	solid	35
	Sr^{2+}	solid	35,105
	Zn^{2+}	solid	35
carbonate, hydroxide	Al^{3+}	solid	109
carbonate, phosphate	Ca^{2+}	solid	12
carbonate, phosphate, silicate	Ca^{2+}	solid	12
carbonate, phosphate, sulfate	Ca^{2+}	solid	12
chlorite, thiourea	Pb^{2+}	solid	102
chromate	Ag^{+}	solid	105
	Ba^{2+}	solid	105
hexacyanoferrate(II)	Cu^{2+}	solid	12
		liquid	5,8,9,110
	Fe^{3+}	solid	26,40
		liquid	8
hexacyanoferrate(III)	Al^{3+}	solid	111
	Cd^{2+}	solid	111,112
	Co^{2+}	solid	111,112
	Cr^{2+}	solid	111,112
	Cu^{2+}	solid	111,112
	Fe^{3+}	solid	111,112
	Ni^{2+}	solid	111,112
	Pb^{2+}	solid	111,112
	Sn^{2+}	solid	111,112
	Zn^{2+}	solid	111,112
hydroxide	Al^{3+}	liquid	109
oxalate	Ba^{2+}	solid	105
	Ca^{2+}	solid	105
	Cu^{2+}	solid	104
	Sr^{2+}	solid	105
		liquid	97
phosphate	Ba^{2+}	solid	35
	Ca^{2+}	solid	14,35,105
		liquid	8
	Cu^{2+}	solid	98
	Fe^{3+}	solid	23
	Sr^{2+}	solid	35
	Zn^{2+}	solid	35
phosphate, silicate	Fe^{2+}	solid	37
POM	Phen. salt, Imid. salt	solid	113−115
	Phen. salt, Phen. dimer salt, Ruth., Meth.	liquid	116−118
silicate	Ag^{+}	solid	1,22,36
	Al^{3+}	solid	13,22,119−121
		liquid	121
	Au^{3+}	solid	1
	Ba^{2+}	solid	22,31
	Ca^{2+}	solid	13,22,26,31−33,122−126
		liquid	51,95
		paste	30,88,89
	Cd^{2+}	solid	22
	Ce^{3+}	solid	22

DOI: 10.1021/acs.chemrev.5b00014
Chem. Rev. XXXX, XXX, XXX−XXX

Table 1. continued

anion	cation	setup	refs
	Co^{2+}	solid	22,24,26,27,30,32,33,36,88,89,122,127−130
		liquid	38,95,96
	Cr^{3+}	solid	22
	Cu^{2+}	solid	1,13,22,34,36,122,127,131,132
		liquid	41,42,47,48,52−54,56,95,133
	Fe^{2+}	solid	22,26,36,122,127
		liquid	46
	Fe^{3+}	solid	1,22,23,134
	Hg^{+}	solid	1,22
	Hg^{2+}	solid	22
	Mg^{2+}	solid	22,135
		paste	30,88,89
	Mn^{2+}	solid	22,32,33,36,132
	Ni^{2+}	solid	22,32,33,122
		paste	30,88,89
	Pb^{2+}	solid	1,13,22
	Sn^{4+}	solid	1
	Sr^{2+}	solid	22,31
	$[UO_2]^{2+}$	solid	22,36
	Y^{3+}	solid	22
	Zn^{2+}	solid	22,48,58,132,136
		liquid	48,54,58,137
	Zr^{4+}	solid	22
silicate, sulfide	Fe^{2+}	liquid	49,50,138
stannate	Co^{2+}	solid	105
	Cu^{2+}	solid	105
	Mg^{2+}	solid	105
sulfide	Fe^{2+}	liquid	44,45,57,62,63,139−141
sulfate	Ba^{2+}	solid	105
	Ca^{2+}	solid	105
	Sr^{2+}	solid	105

[a]The experimental setup is a liquid (a solution) together with either a solid (a seed, as described in section 3.1, or other solid) or a second liquid (an injection setup, as in section 3.2, or other liquid); paste refers to a setup in which the injected material is liquid during injection and solid thereafter (see Jones' microgravity experiments in section 3.6). The table should not be taken as being exhaustive, particularly for older literature. (Imid., Imidazophenanthridinium; Meth., Methylene Blue; Phen., Phenanthridinium; POM; Polyoxometalate; Ruth., Ruthenium(II) Complex)

SEM/EDS for the measurement of elemental distributions across fractured tube walls. The latter work along with other studies show, perhaps surprisingly, that although silicon has been observed in the walls of chemical-garden tubes grown from silicate, the silicon contribution is surprisingly low. Thus, the frequently used alias "silica gardens" is slightly misleading. Silica usually precipitates in a very thin layer and only longer experiment times seem to induce an aging process of silica accumulation on the external surface of the tube.[32]

In silica gardens, the external surface of the tube is smooth but it becomes more rough during the aging process (Figure 18a,b). In some cases, layers with different chemical compositions can be distinguished clearly (Figure 18c,d); in other cases this separation is less clear, and metal silicate interfaces (crystalline $Ni_3Si_2O_5(OH)_4$ in the case of nickel) have been detected.[32,33] In the cases of separate silica layers, the tetrahedral oxygens of the SiO_4 layers are completely coordinated with the Si atoms, and no chemical bonds are likely to be formed between the external silica layer and the internal metal oxide−hydroxide layer. In other cases one of these Si−O oxygens oriented to the internal surface can be coordinated with the metal hydroxide clusters nucleating the formation of a metal silicate interlayer in the internal face of tubes.[32] We note that the nickel−silica and cobalt−silica tubes can show interesting color variations due to different oxidation states of the metal ions.[32,38]

Another example of a more extensive materials characterization has been provided by Batista et al.,[45] who studied iron−sulfur tubes formed by injection of sodium sulfide into iron(II) chloride solution. Analyses of the dried tubes by X-ray diffraction showed the presence of the iron compounds greigite and lepidocrocite. Balköse et al.[122] characterized tube samples formed from waterglass and seed particles of Ca, Fe, Co, Ni, and Cu salts. They reported that group 7 metal(II) tubes were amorphous, whereas groups 2 and 11 metal(II) tubes were partially crystalline. Balköse et al.[122] also performed surface area measurements using N_2 adsorption. The reported values are in the range of 8 to 249 m^2/g. Iron-containing silica tubes were also studied by Makki and Steinbock.[57] From XRD measurements and Mössbauer spectroscopy, the authors concluded that their samples contained magnetite.

A carefully chemical characterization of these tubes at the nanoscale level is important to know the growth mechanism. Ibsen et al.[35] characterized tubes grown in anionic solutions of phosphates and carbonates from seeds of gels containing chloride salts of alkaline-earth and Zn and Cu cations, finding that the tubes of alkaline-earth cations are formed by phosphate or carbonate, whereas the tubes of Zn are formed by $Zn_5(OH)_8Cl_3{\cdot}H_2O$ and no significant amount of carbonate was found.

DOI: 10.1021/acs.chemrev.5b00014
Chem. Rev. XXXX, XXX, XXX−XXX

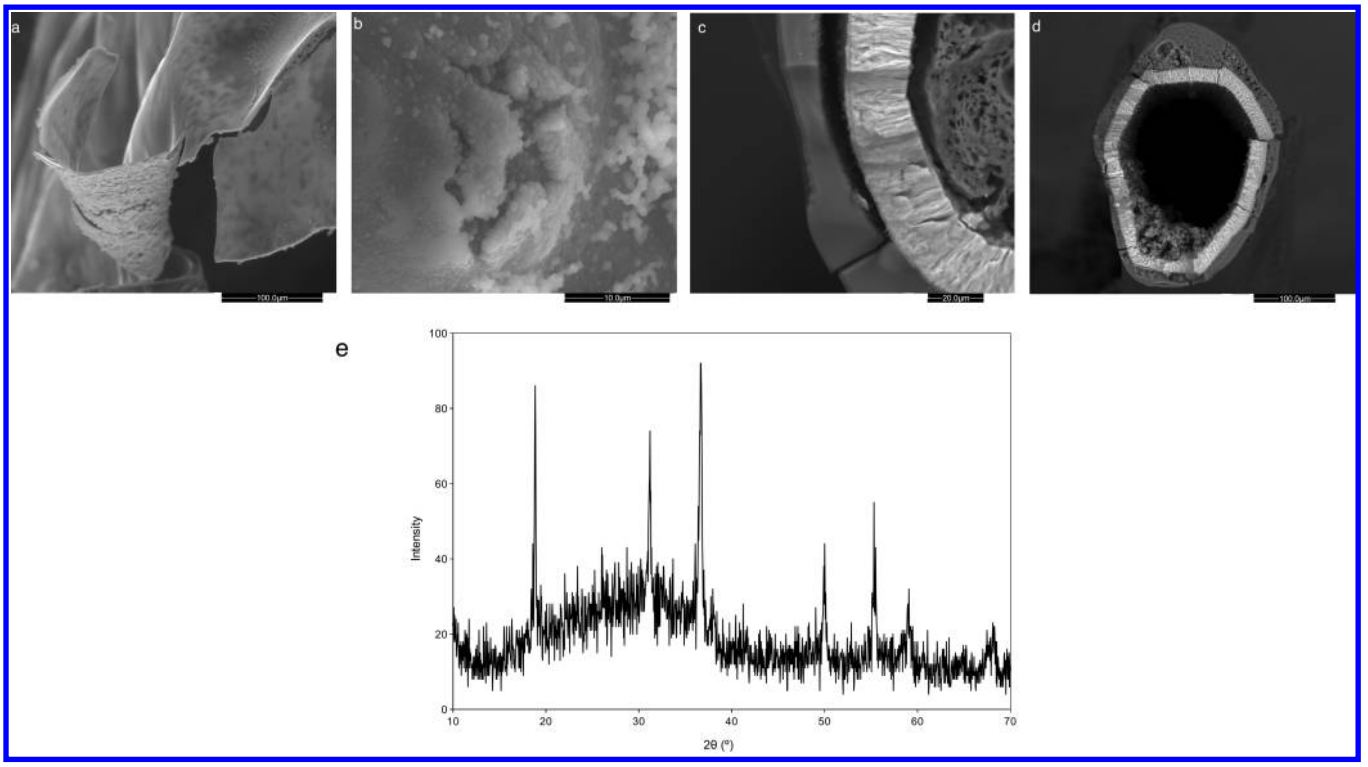

Figure 18. SEM images of tubes from silicate and (a, b) Ca, (a) smooth external surface, and (b) nanoaggregates during aging, and (c, d) SEM images using a backscattering solid-state detector from Mn. (e) XRD pattern of the tube corresponding to hydrated manganese oxide crystals placed in the bright zones of c and d. Adapted with permission from ref 32. Copyright 2011 American Chemical Society.

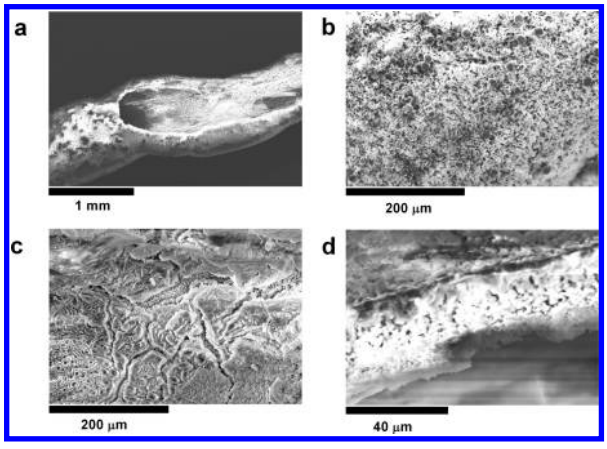

Figure 19. SEM images of (a) single fracturing precipitation tube, (b) exterior surface, (c) interior surface, and (d) tube wall. Adapted with permission from ref 125. Copyright 2011 Elsevier.

Collins et al.[120] studied chemical gardens formed from aluminum nitrate seeds in sodium silicate solution. The as-synthesized structures had a BET (Brunauer–Emmett–Teller) surface area of 148 m^2/g, pore volumes of 0.36 cm^3/g, and showed a broad distribution of pore diameters in the range of 3–100 nm. The authors also exposed their samples to NH_4Cl at elevated temperatures followed by calcination to yield H^+-exchanged material with Brønsted acid catalytic properties.[144] Porosity measurements on these and other processed samples revealed only small decreases in the BET surface area, pore volume, and average pore size.

Some studies evaluated the postsynthetic modifications other than the ones reported by Collins et al.[120] Pagano et al.[137] heated tubular structures consisting predominantly of silica and zinc hydroxide to create decimeter tubes with a thin outer silica layer supporting ZnO nanostructures on their interior surface. After modification these tubes became photoluminescent and photocatalytically active, as demonstrated with the decomposition of an organic dye. Roszol and Steinbock[53] studied postsynthetic changes to silica-copper tubes. The original blue samples consisted predominantly of silica and amorphous $Cu(OH)_2$. We note that the lack of $Cu(OH)_2$ crystallinity does not fully agree with the results of Balköse et al.;[122] however the employed reaction conditions in these two studies were different. Heating of the tubes resulted first in black silica-CuO and then in crimson-red silica-Cu_2O tubes. XRD measurements revealed that the latter two copper compounds were present in crystalline forms. TGA measurements showed that the chemical transitions occurred around 550 and 900 °C. Despite these high temperatures, the tubular shapes remained intact in most experiments. The authors also demonstrated the transformation of silica–Cu_2O tubes to tubes containing metallic Cu(0) particles. This transformation was accomplished by exposure to sulfuric acid and resulted in brownish tubes.

5. ENERGETIC PHENOMENA

Gradients of density and ion concentrations across a semipermeable membrane make chemical gardens a source of energy. Such energetic properties have a number of exciting potential applications in various fields. Early work tried to control chemical-garden growth and emphasized its dynamic character; these works also began to understand chemical gardens' electrical nature. We are returning to these aspects of chemical gardens in the latest works. In this section we discuss the electrochemical (section 5.1), magnetic (section 5.2), and dynamical (section 5.3) properties of chemical gardens.

DOI: 10.1021/acs.chemrev.5b00014
Chem. Rev. XXXX, XXX, XXX–XXX

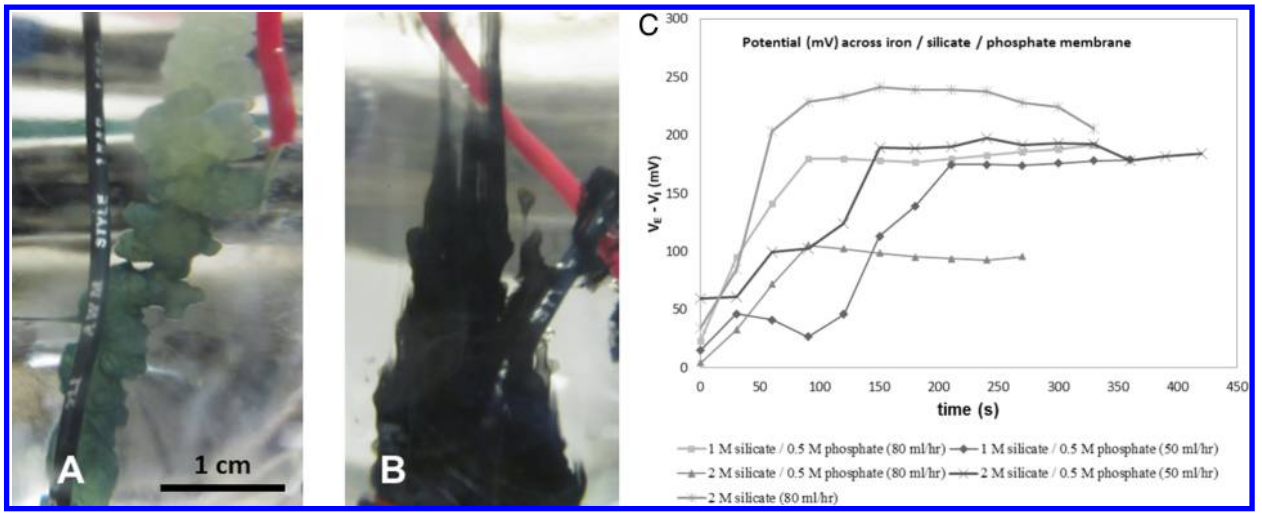

Figure 20. Chemical-garden structures grown via injection of (a) acidic $FeCl_2$ solution into alkaline silicate solution; and (b) alkaline sodium sulfide/silicate solution into acidic $FeCl_2$-containing solution. A wire was placed near the injection point so that the membrane would envelop the wire as it grew, while a second wire was placed in the outer solution. A membrane potential is generated immediately upon precipitation, and the value of the membrane potential is characteristic of the reactant system and concentrations chosen. (c) Shows potentials generated by Fe(II)−silicate−phosphate chemical gardens formed with varying reactant concentrations and injection rates. (a,b) Images from Laurie Barge; (c) Reprinted with permission from ref 37. Copyright 2012 American Chemical Society.

5.1. Electrochemical Properties and Fuel Cells

Since chemical-garden membranes form at the interface of solutions of contrasting pH and chemical composition, precipitation of the membrane establishes concentration gradients of particular ions, which drives the generation of electrical potentials across the chemical-garden membrane. A great deal of work on membranes from physical chemistry and bioelectrochemistry can be brought to bear upon this matter. The unequal distribution of charged species across a semipermeable membrane is what is called the Gibbs−Donnan effect. The Nernst equation relates the concentration gradient to the electrical gradient and is the starting point for understanding the basis of the membrane potential. The Goldman−Hodgkin−Katz equation determines the potential across a membrane taking into account all of the species and their permeabilities (see, e.g., Schultz[145]). Interest in the electrochemical properties of chemical-garden membranes is by no means recent; potential differences across precipitation membranes have been studied for over a century, and work by Donnan[146] led to the theoretical work described above.[59,77] Interest in possible links between the electrochemical properties of chemical gardens and the technologies of batteries and fuel cells is not only recent, either. A connection between chemical gardens and lead−acid batteries was postulated by Julian.[147] Morse,[9] on the other hand, as we described in section 2.2, found that by passing a current chemical-garden membranes might be deposited electrolytically with little difficulty.

In the case in which a hydrated metal-salt seed is dissolved in a silicate solution, the inner solution becomes more acidic, and thus a pH gradient across the inorganic membrane is established as dissolution and osmotic growth proceeds. In the example in Figure 5, as OH^- ions from the outer alkaline solution diffuse toward the interior, they are precipitated with the metal salt, forming a layer of metal hydroxides. The depletion of OH^- ions from the outer solution establishes a net charge difference between the inner and outer solutions, which can be measured as an electrical potential, if electrodes are placed in the interior of the chemical-garden structure and in the outer solution.

Measuring electrical potential across chemical-garden membranes is experimentally challenging because of the fragile nature of chemical-garden structures and the small volume of liquid in the interior, but electrochemical measurements have been accomplished utilizing a variety of methods. Injection methods have induced chemical gardens to grow directly around one electrode placed near the injection point, thus immersing one electrode in the inner solution.[37] In addition, inorganic membranes have been forced to grow from pellet dissolution in an open cylindrical morphology so that an electrode could be placed inside the structure.[130] Another technique is to produce precipitate membranes between different aqueous solutions by introducing the two solutions on either side of a porous dialysis membrane template in a fuel-cell setup so that the precipitate only forms on this template. This "artificial" chemical-garden membrane setup, which dates back to the Pfeffer cell[8] of the 19th century (section 2.2), produces the same precipitation process between any two solutions as it occurs in an injection experiment, and electrochemical gradients are generated in the same manner. This type of experiment allows for easier analysis of the actual membrane structure itself once precipitation is completed, as well as inner and outer solution chemistry.[62]

By whatever means it is achieved, the placement of an electrode inside a chemical-garden structure allows for the measurement of electrochemical parameters including voltage, resistance, and electrical current. Each of these properties has a bearing on the chemical garden's ability to generate gradients and thereby free energy on both short and long time scales. Figure 20 shows examples of two chemical-garden reactant systems (iron(II) silicate and iron(II) sulfide−silicate) grown around electrodes, and an example of potential generated by iron(II)−silicate−phosphate chemical gardens. Figures 20a and b are examples of two reactant systems of opposite orientation: in the iron−silicate system, the acidic iron chloride solution was injected into the alkaline silicate solution; in the iron-sulfide/silicate system, the alkaline sodium sulfide/silicate solution was injected into the acidic iron-containing solution. While the directionality of the voltage in chemical-garden experiments is determined by the orientation of the pH gradient between inner

DOI: 10.1021/acs.chemrev.5b00014
Chem. Rev. XXXX, XXX, XXX−XXX

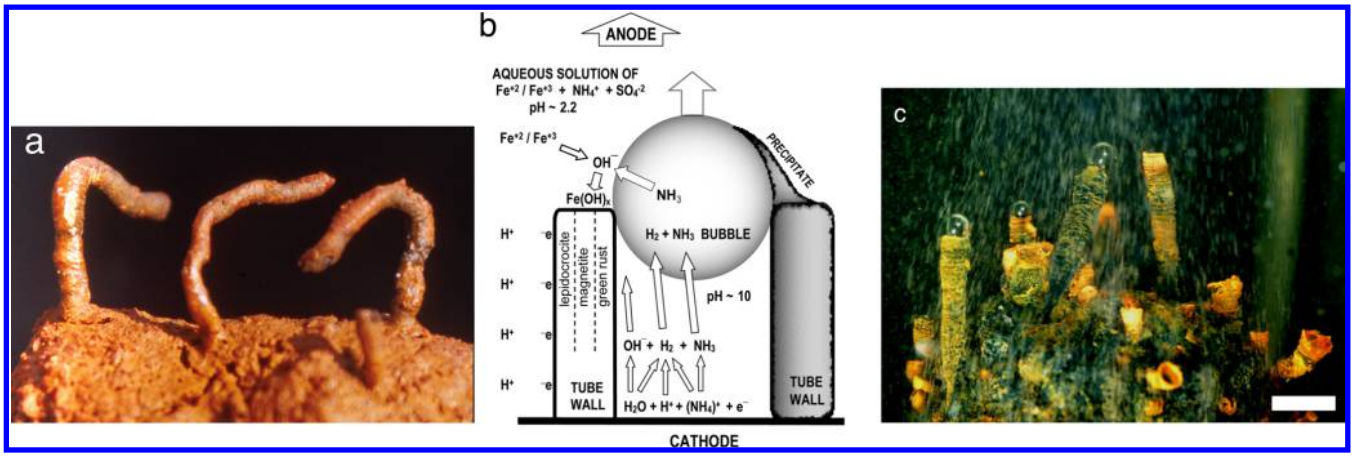

Figure 21. (a) Curved tubes approximately 1 cm long of precipitating magnetite, with an outer layer oxidized to orange lepidocrocite, grown on a negatively charged magnet in a solution of iron(III) ammonium sulfate. (b) Schematic diagram of the bubble and tube walls growing on the cathode. (c) Growing tubes with bubbles emerging (scale bar = 5 mm). Reprinted with permission from ref 44. Copyright 2004 National Academy of Sciences, U.S.A.

and outer solutions, the absolute value of the voltage is dependent upon chemical parameters such as the choice of reactants and their concentrations. For example, using a "Beutner rig",[110] the Fe–sulfide chemical garden generated significantly more electrical potential (0.5–0.6 V) than the Fe–silicate chemical garden (−0.2 V), even though the concentrations of reactive ions were similar in both experiments (~0.1 M).[37,141]

In injection chemical-garden experiments where the total inner solution is injected in less than 1 h, the voltage measured has been observed to maintain itself for several hours.[148] In some cases, chemical-garden voltage has been maintained for over 24 h.[37] This indicates that, for a time, the chemical-garden membrane has a very low permeability to hydronium and hydroxyl ions. In iron–silicate and iron–sulfide–silicate chemical gardens, electrical resistances of 130 to 210 kΩ and 8.5 to 11.5 MΩ were measured, respectively, indicating that the chemical-garden membranes in these cases, though moderately insulating, appear to be capable of electron conduction. However, the establishment of an electrical potential gradient between the inner and outer solutions may be due to ion concentrations and not to electron transfer (conduction or electron tunneling). Nevertheless, it is possible that the precipitate membrane itself could store energy in the form of compositional or redox gradients; particularly if composed of particular materials such as molybdenum–iron sulfides that are capable of transferring two electrons at once toward two electron acceptors with very high and very low redox potentials, thus enabling a wider energetic variety of possible redox reactions.[141,149,150]

Compositional gradients between inner and outer chemical-garden membrane surfaces are commonly observed in chemical-garden experiments (e.g., Cartwright et al.,[27] Ibsen et al.,[35] Barge et al.,[37] McGlynn et al.[138]); see section 4, and in precipitates such as iron sulfide where different layers of precipitate have different degrees of oxidation, there may be a redox gradient present across the membrane as well.[50] It is not known whether there is a surface charge present on the inner and outer membrane layers in chemical-garden experiments; that is, whether the observed electrical potentials are dependent on the inner and outer solutions being present or if the electrochemical gradient would persist independently within the membrane.

The chemical-garden system is in disequilibrium during the membrane growth phase, when the interior solution is still rupturing and reprecipitating upon meeting the outer reactive ion, and so long as disequilibrium is maintained, a voltage will continue to be generated by ion gradients. However, once the solutions are spent and precipitation ceases, or the inner solution is no longer being injected or the seed is completely dissolved, the system will decay toward equilibrium.[130] In the experiments shown in Figure 20, the membrane potential was maintained for many hours after the injection was stopped and slowly decayed over 1–2 days. While the system is in disequilibrium, however, chemical gardens can be thought of as analogous to membrane fuel cells; in effect, utilizing a selectively permeable membrane with inner and outer surfaces of different composition separating two solutions of contrasting reduction potential E_h and pH.[63,151] In a real membrane fuel cell, the catalytic electrodes on either side of the semipermeable membrane would be of specific composition designed to catalyze reactions in either half of the cell, and electrical potential would be applied to those electrodes to drive the reactions. It is not yet known whether chemical-garden systems that generate their own electrical potential, with possibly charged or redox active membrane surfaces (such as iron sulfides), might also be able to drive chemical reactions in this fashion, but it is a possibility inviting further experimentation.

In typical chemical-garden experiments, the out-of-equilibrium phase only persists for as long as it takes the seed to dissolve or until the cessation of injection. However, in a system where the disequilibrium could be maintained for very long periods of time, such as in the natural chemical-garden structures precipitated at hydrothermal vents, it is worth considering the energy that might be generated across the inorganic membranes at those locations and its possible applications to the design and operation of "natural" fuel cells as well as its implications for the emergence of life (see section 8.1).

5.2. Magnetic Properties

Under some conditions magnetic fields can affect precipitative tubular growth in at least two ways. First, when a charged particle with an electric charge, q in a solution moves with a velocity $\mathbf{v}$ in a magnetic flux density $\mathbf{B}$, it will experience a Lorentz force perpendicular to both $\mathbf{v}$ and $\mathbf{B}$, $F = q\mathbf{v} \times \mathbf{B}$. The Lorentz force induces circumferential convection of the solution as the force acting on the charged particles is transferred to the surrounding solvent molecules in the solution. This convection is called magnetohydrodynamic (MHD) convection. This movement of the solution can affect local ion concentration gradients, which in

DOI: 10.1021/acs.chemrev.5b00014
Chem. Rev. XXXX, XXX, XXX–XXX

turn can create nonuniform deposition of material on the growing tube.

In a specific example,[44] when a conductive magnet is also the negatively charged cathode immersed in a solution below the anode, a swirling, horizontal ring of solution is created above the polar face where the curving magnetic field crosses the vertical electric field. Second, at the same point where the field curves toward the other pole, any ferromagnetic precipitating particles, if of sufficient size to have a single domain, will be oriented by the field as they are deposited on the growing lip. This nano-orientation can scale up to the macro level with the result that the entire tube follows the field "lines"; see Figure 21. This process is not unlike the common school demonstration of the pattern of curved lines taken by iron filings spread across a sheet of paper over a magnet. However, within the realm of chemobrionics, even such seemingly simple processes can interact in a synergistic way to create complex three-dimensional patterns mimicking organic growth.

Several groups have been working on growing chemical-garden tubes in magnetic fields, and one finding is that magnetic fields can induce 3D-morphological chirality in membrane tubes.[127,132,135,136,152,153] An example is tubes grown by the reaction of sodium silicate solution and zinc sulfate seeds. When no magnetic field is applied, the tubes grow upward (Figure 22a),

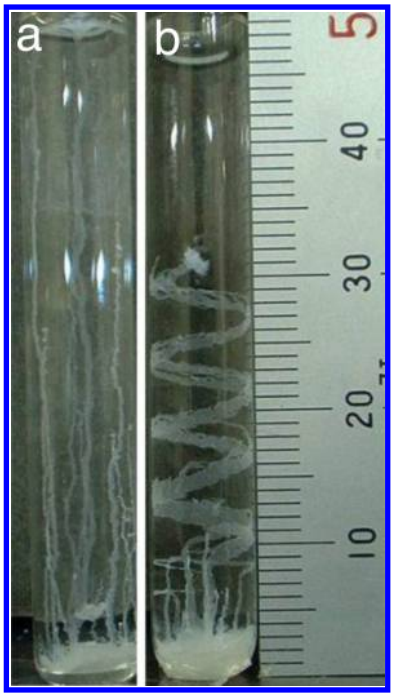

Figure 22. Magnetic field effects: a chemical garden reaction in a bore tube of a superconducting magnet. Vertical field: (a) 0 T, (b) 6.3 T. The scale is in millimeters. Adapted with permission from ref 136. Copyright 2004 American Chemical Society.

but in the presence of a vertical magnetic field the tubes near the inner surface of the glass vessel grow helically (Figure 22b). The direction of the magnetic field also controls the chirality of the tubes: when the field is inverted, the tubes grow helically in the left-handed direction, whereas previously they were exclusively right-handed. Surfaces also appear to have an effect on tube chirality. When a small round bar (0.3 mm diameter) was inserted in the solution, helical membrane tubes with left-handed chirality grew on the outer surface of the bar, and tubes grown apart from vessel wall were also twisted to the left-handed direction. The tube tops were observed to grow circumferentially, and this was concluded to be due to Lorentz forces, i.e., that ions in the solution expelled from the tube in a magnetic field gain rotational forces. This conclusion was further confirmed from the in situ observation of the solution motion during reaction. In the magnetic field remarkable circumferential convection was observed, whereas no appreciable convection was observed at a zero field. It was determined that the effect is explainable by the boundary-assisted Lorentz force-induced convection, where the direction of convection is controlled by the relative orientation of the tube top and the wall of a vessel or a bar.[132]

Chemical gardens can also be grown to be constituted mainly of magnetic components. Makki and Steinbock[57] reported the synthesis of silica-magnetite tubes by injection of an iron(II,III) solution into a solution containing sodium silicate and ammonium hydroxide. The growth velocity of the tube was controlled by pinning a gas bubble, which could be moved upward with a glass rod at 1.5−6 mm/s, to the tip of the tube rod. The resulting tubes were washed, dried, and characterized, and it was found that they contained magnetite nanoparticles 5−15 nm in size. Magnetite is typically ferrimagnetic but magnetite nanoparticles show this cooperative phenomenon only below a characteristic blocking temperature. For the silica−magnetite tubes this temperature was reported to be 95 K. Above this temperature the material is superparamagnetic, which implies that the magnetization can randomly flip due to thermal effects; the magnetic susceptibility, however, is much larger than for common paramagnetic substances. A surprising finding of this study was that the magnetic properties depend on the applied injection rate and the controlled growth speed. For instance, below the blocking temperature, the remnant magnetization increased with injection rate but decreased with growth speed while the coercivity showed the opposite trends.[57] A likely explanation for this mechanical control of magnetic properties is that injection rate and growth speed affect the size of the magnetite nanoparticles.

These types of experiments can yield information about the processes of self-assembly and also help to develop techniques for creating chemical gardens for materials applications. Since the growth of chemical gardens can be controlled by an external magnetic field, and the precipitates themselves can have magnetic character, which is also controlled by applied magnetic fields as in superparamagnetic materials, these magnetic chemical gardens hold the promise of having some interesting and useful applications.

5.3. Chemical Motors

The internal fluid pressure changes that cause chemical gardens to grow and rupture can produce rhythmic movement in these structures, a phenomenon known as "chemical motors". The mechanism is that of the budding and popping regimes of chemical-garden growth. After formation of the membrane, pressure inside the membrane increases, causing the stress on the membrane to grow until it reaches a failure point whereupon the membrane ruptures and solution is ejected from the rupture site. The interior solution reacts with the exterior solution and a new membrane is formed, sealing off the interior. These repeated ruptures cause variations in pressure on the inside of the membrane, and these oscillations in pressure cause oscillations in membrane stress which in certain conditions result in movement of the structure. In some cases this movement is periodic, and

DOI: 10.1021/acs.chemrev.5b00014
Chem. Rev. XXXX, XXX, XXX−XXX

such "chemical-garden motors" have been observed to oscillate for hundreds of oscillations. This phenomenon was already reported in the 19th-century literature.[12]

A similar mechanism, the buildup of osmotic pressure in a closed compartment that later will lead to an explosion, is used by some plants, e.g., dwarf mistletoe (*Arceuthobium*), squirting cucumber (*Ecballium elaterium*), for spreading their seeds.[154−158]

A chemical motor in the Cu^{2+}−CO_3^{2-} system is shown in Figure 23a. Here a pellet of copper chloride was immersed in a solution of sodium carbonate. The pellet began to dissolve and immediately copper carbonate precipitated forming a semipermeable membrane layer that covered the pellet. Water diffused into the pellet by osmosis, increasing the pressure inside the membrane. This pressure increase caused a part of membrane to be ejected entirely, upon which the pellet was again exposed to carbonate solution and the process was repeated. This motor was very regular, as is shown in Figure 23b. Another chemical motor is shown in Figure 24a. In this experiment, after submerging a pellet of calcium chloride in silicate solution, a three-armed

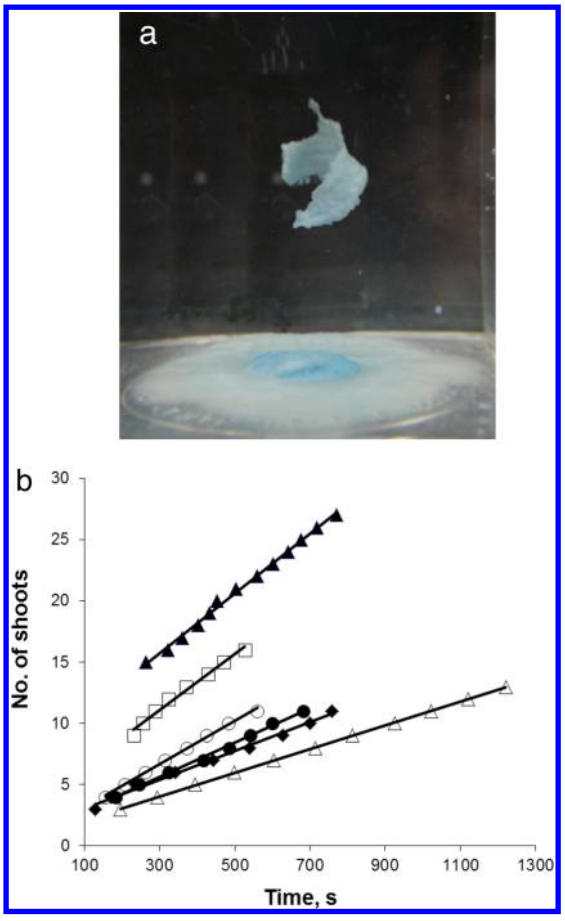

Figure 23. (a) A pellet of copper chloride in a solution of sodium carbonate leads to the formation of a precipitate structure that is periodically ejected from the pellet. The period is about 1 min and the process may continue for 1 h. The width of the image corresponds to 5 cm. (b) The number of membrane pieces that have been ejected as a function of time for various carbonate concentrations. The $[CO_3^{2-}]$ molarity is black triangles, 0.16 M, open squares, 0.13 M, open circles, 0.11 M, black circles, 0.09 M, black diamonds, 0.07 M, open triangles, 0.06 M. Note that the data are linear and the slope is increasing with the concentration of carbonate. Reprinted with permission from ref 108. Copyright 2005 Springer Science and Business Media.

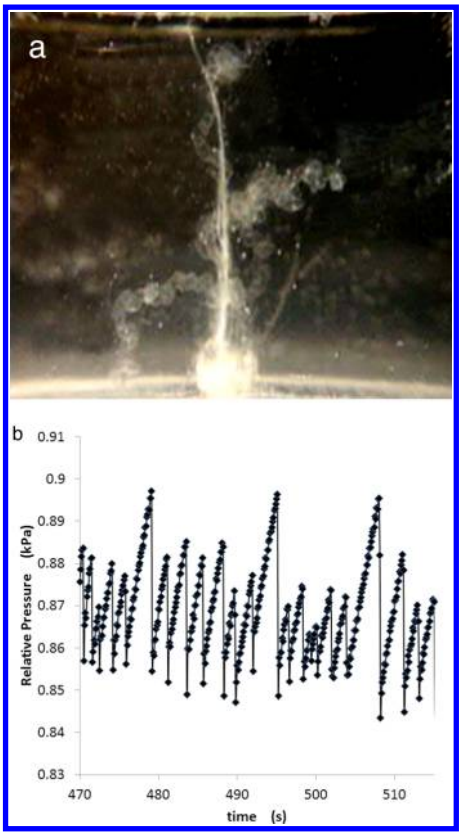

Figure 24. (a) Example of a moving structure with three "arms". The two horizontal arms move up and down in synchronized motion. The pellet at the bottom of the structure has a diameter of 1 cm.[123] (b) Changes of pressure inside the moving structure as a function of time.[124] Reprinted with permission from refs 123 and 124. Copyright 2007 and 2009 American Physical Society.

structure grew. The two almost horizontal arms were observed to "flop" regularly. Pressure inside the structure was measured as a function of time (Figure 24b) and was found to increase linearly until it reached a critical value, which suggests that the membrane stretching is predominantly elastic. It is important to note the very fast change from pressure drop to linear pressure increase, which indicates that the kinetics of membrane formation are very fast, too fast to be discerned in these measurements. A mathematical model of these systems, which allows prediction of the period of oscillations as a function of system parameters, is presented in Pantaleone et al.[123] and described in section 6.4.

These chemical motors possess varying properties depending on the parameters of the system in which they formed; relative fluid densities, reactant type and concentration, and pH gradients. Different chemical motors may therefore fulfill different functions, such as producing a cell that moves periodically up and down, or another cell that may rotate or flip over, or another that moves like slime,[109] or yet another system that may produce precipitation rings with controlled inner and outer diameters.[102] The chemical "cannon" of Figure 23a expelled part of the structure with a controllable frequency. The structure shown in Figure 24, with synchronized movement of two arms, might form a swimming structure if it were disconnected from the pellet.

Even more complex behaviors have been observed in other systems. In a system with $AlCl_3$, periodic ejection of longer slender arms has been observed.[109] In a system with $AlCl_3$−Na_2CO_3−NaOH, at the beginning of the experiment, the

DOI: 10.1021/acs.chemrev.5b00014
Chem. Rev. XXXX, XXX, XXX−XXX

injected solution spreads out on the bottom of the vessel and forms a membrane. After a time, a small cell grew from part of the membrane and eventually detached from the bottom membrane and moved upward toward the surface. After reaching some height, the rising cell membrane changed direction and fell back to the bottom of the vessel. This process repeated periodically. This motor, then, could periodically carry material to the top and back to the bottom: i.e., it took CO_3^{2-} from the solution and converted it to CO_2 gas which carried the cell upward until released. For a simple self-assembling chemical system, these are rather complex machines.

6. MATHEMATICAL MODELING

Most work on the modeling of chemical gardens has hitherto decoupled the chemistry and fluid mechanics. Although this simplification is only valid when the time scales for fluid motion and chemical transformation are very different, it gives us insight into the limiting behaviors of the system and allows the rationalization of some experimental measurements. The flow of a nonreactive jet or plume of one viscous fluid rising in another is governed by momentum and mass conservation. For incompressible, Newtonian fluids, these properties are expressed by

$$0 = -\nabla p + \eta\nabla^2\mathbf{u} + \rho\mathbf{g}$$
$$\nabla\cdot\mathbf{u} = 0 \qquad (1)$$

Here $\mathbf{u}$ is the velocity vector, p is pressure, $\mathbf{g}$ is the gravitational acceleration, and η and ρ are the viscosity and density of the fluid, respectively. The first relation demonstrates a balance between pressure, viscous and buoyancy forces and is valid for slow, low Reynolds number flows for which the acceleration of the fluid is negligible (this is the classical Stokes' equation). For an axisymmetric configuration, the rising inner fluid forms a cylindrical jet; see Figure 25. This jet drags the nearby surrounding external fluid upward. In an environment of finite vertical extent, the rising fluids spread out radially at the top surface, creating a recirculating toroidal cell around the jet. In laboratory experiments, the jet fluid may be removed at the top of the environment.[41] This complex flow requires a two-dimensional solution of eq 1, with boundary conditions at the interface of the two fluids expressing continuity of stress, pressure and velocity; further conditions are needed at all the boundaries of the environment.

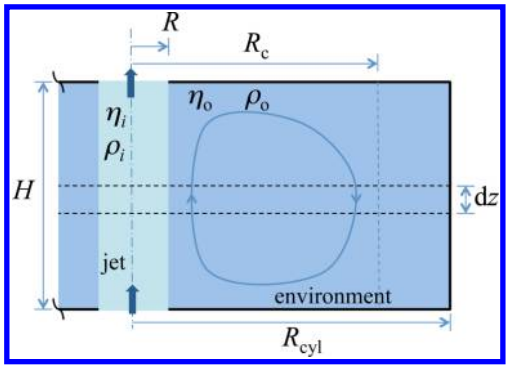

Figure 25. Sketch of the model setup with a fluid jet and recirculation of the fluid in the environment around it, that leads to eqs 2, 4, and, with $\eta_o \to \infty$, 5

Simple approximate solutions of eq 1 have been obtained by assuming a one-dimensional vertical flow, in both the jet and the environmental fluids and no net vertical transport of fluid in the environment;[41] these solutions focus on the flow in the jet and surroundings away from the bottom and top boundaries of the environment. Using these assumptions, integration of eq 1 in the radial direction leads to the vertical volumetric flow rate in the jet

$$Q = \frac{\pi}{8\eta_i}\Delta\rho g R^4\left[4\frac{\eta_i}{\eta_o}\left(\ln\frac{R_c}{R} - \frac{1}{2}\right) + 1\right] + \frac{\pi}{8\eta_i}\frac{dP}{dz}R^4\left[2\frac{\eta_i}{\eta_o} - \frac{\eta_i}{\eta_o}\left(\frac{R_c}{R}\right)^2 - 1\right] \qquad (2)$$

Here R is the radius of the jet, z denotes height, $P = p+\rho_o gz$ is the reduced pressure, $\Delta\rho = \rho_o - \rho_i$ is the density difference between the outer environmental and inner jet fluids, and η_i and η_o are the inner and outer fluid viscosities, respectively. The radius of the recirculating cell R_c is defined here by one requirement only, that of no net vertical flow in the environment; in reality R_c is a function of the aspect ratio of the environment (height/radius H/R_{cyl}), as well as dP/dz and the properties of the fluids, but this function cannot be specified by a simple one-dimensional approximation of the flow. We see that there are two forces driving the fluid flow upward (more commonly) in a chemical-garden tube: pressure and buoyancy. As precipitation occurs and the chemical tube becomes more viscous, $\eta_o \to \infty$, the viscous terms in the brackets reduce to zero; this solution corresponds to flow in a solid tube. We can thus identify four limiting behaviors, according to the driving force for flow, either pressure or buoyancy, and according to the viscosity of the outside fluid, either finite or infinite, the latter representing a solid. The experiments of Thouvenel-Romans et al.[41] are compatible with a model of coupled buoyancy and pressure driven flow in a viscous environment. These results are presented in section 6.1. The experiments of Kaminker et al.[121] are compatible with a model of pressure-driven flow in a solid tube; these results are presented in section 6.2. In general, in a chemical garden both buoyancy and pressure work together in driving flow and precipitation. The dominant effect will depend strongly on the chemistry and concentration of the reagents. While the buoyancy forces arise from the fluid density differences, the pressure forces result from osmotic effects and the elasticity of the membrane formed at the interface of the two reacting fluids in a chemical garden (see Figure 5).

Flow driven by osmotic effects has been studied for over a century in the context of biological, chemical and physical applications. While the early works of van't Hoff[111] and Rayleigh[159] explained osmosis in terms of the work done by the rebounding molecules of solute on a selective (semi-permeable) membrane, the same phenomenon was later described by Gibbs onward in terms of the free energy and chemical potential.[160] Different disciplines have preferred one or the other of these approaches to derive the classical thermostatic result, but the kinetic and thermodynamic theoretical treatments are entirely equivalent.[161] However, it is the effect of osmosis on a mesoscale involving many colloidal particle lengths or even on the macroscopic scale of a tube that is important to understand its role in chemical-garden growth. At present, all works to model osmotic flow in a porous medium at the continuum level ultimately derive from the semiempirical 1958 formulation of Kedem and Katchalsky.[162] According to Kedem–Katchalsky, for dilute solutions, the molar flux of solute (species 1), N_1, and volume flux of solvent (species 2), u_2, across a membrane permeable to the solvent but only partially permeable to the solute, are

DOI: 10.1021/acs.chemrev.5b00014
Chem. Rev. XXXX, XXX, XXX–XXX

$$u_2 = L_o(-\delta p + \sigma_o R_u T \delta c_1)$$
$$N_1 = -w R_u T \delta c_1 + (1 - \sigma_o) u_2 c_1 \quad (3)$$

These relations were obtained from irreversible thermodynamics under the assumption of linearity between the fluxes and the driving forces. Here R_u is the universal gas constant and the temperature T is assumed constant; δp and δc_1 are the pressure and molar concentration differences across the membrane, and L_o is a transport coefficient. The reflection coefficient σ_o measures the fraction of solute molecules that are reflected by the membrane,[163] taking the value of one for a perfectly semipermeable membrane and zero for a completely permeable one. For the more common partially semipermeable membrane, which reflects some solute molecules but not all, $0 < \sigma_o < 1$.[29] The solute permeability coefficient w is null for a semipermeable membrane ($\sigma_o = 1$). The phenomenological coefficients w, σ_o, and L_o are measured, for a given solute and membrane, by carefully designed experiments.[164] Cardoso and Cartwright[165] performed a momentum balance at the molecular level to derive the minimal continuum-level equations for the flow of a binary mixture in a porous medium in the presence of osmotic effects. They showed that the simplified, semiempirical form above for the transport equations is valid in the limit of dilute, ideal solutions, and that the solute permeability coefficient, w, is related to the momentum transfer at the entrance and exit of narrow pores. It is important to note here that eqs 3 demonstrate the transport of solute by both advective and diffusive mechanisms. For solutions of electrolytes, more complex semiempirical equations taking into account electrochemical effects have been proposed[164] (see section 5.1).

There have been a few analyses of osmotic effects in precipitate membranes. Sørensen[166] inquired about the stability of the planar form of a semipermeable precipitate membrane including the osmotic transport of the solvent into the membrane. He showed theoretically that solid growth could occur preferentially at wavelengths shorter than the thickness of the concentrated ion layer ahead of the growing membrane, thus suggesting a regular pattern for chimney development. However, the model did not include pressure effects, nor the elastic properties of the membrane, and was thus unable to predict a finite wavelength with maximum growth. Jones and Walter[30] observed complex morphologies in chemical gardens formed in laboratory experiments under microgravity, for which buoyancy-driven convective transport is negligible and the reactants move mainly by diffusive and osmotic mechanisms. They suggested an analogy with the instability of a solidification front advancing in a supercooled melt. More recently, Pantaleone et al.[123] considered the motion of a semipermeable chemical-garden membrane arising from osmotic flow driven by the solute concentration difference across the membrane, as presented in section 6.3 below. Semipermeable membranes formed in chemical gardens can exhibit oscillatory growth (section 6.4) owing to the periodic rupture under osmotic or externally imposed pressure forces and resealing by precipitation of new solid (section 6.5). These periodic processes can lead to very complex precipitate morphologies. Some simplification is observed by restricting growth to two dimensions, which leads in one particular case to spiral growth that may be modeled with a geometric model; section 6.6.

We have highlighted above that in most models of chemical gardens the fluid mechanics has been treated separately from the precipitation chemistry. The only study to date coupling the advective and diffusive transport of the solute with the chemistry of the precipitation is that by Stone et al.[43] Theoretical and experimental results for chimney growth are presented in section 6.7 below in the context of templating by a fluid jet. However, a full model of reactant transport driven by pressure, buoyancy and osmotic forces toward a site of localized precipitation as occurs in a chemical garden has not been developed as yet.

6.1. Tube Width

Jetting growth (Figure 7; section 3.2) can be understood as a hydrodynamically controlled templating process. In Thouvenel-Romans et al.,[41] it was shown that the outer tube radius R_0 is well described by the radius R of a buoyant, nonreactive jet of one viscous fluid in another. The experimental data from this study show a continuous increase of R_0 with the employed pump rate Q. The range of the latter quantities was approximately 80−230 μm and 1−80 mL/h, respectively. These data agree surprisingly well with a simple fluid mechanics model, as described by eq 2, with the additional boundary condition of zero velocity at the outer solid wall of the environment at radius R_{cyl}. The authors obtained a general analytical but cumbersome result for the $Q(R)$ dependence. In the physically relevant limit of a cylindrical container (the environment) that is much larger than the fluid jet (i.e., $R_{cyl} \gg R$), their model leads to

$$Q = \frac{\pi}{8\eta_i}\Delta\rho g R^4 \left[4\frac{\eta_i}{\eta_o}\left(\ln\frac{R_{cyl}}{R} - 1\right) + 1\right] \quad (4)$$

The viscosities $\eta_{i,o}$ and the densities $\rho_{i,o}$ can be obtained from independent measurements. Since the environment diameter is also known, this yields a unique relation between Q and R without any free parameters; see Figure 26.

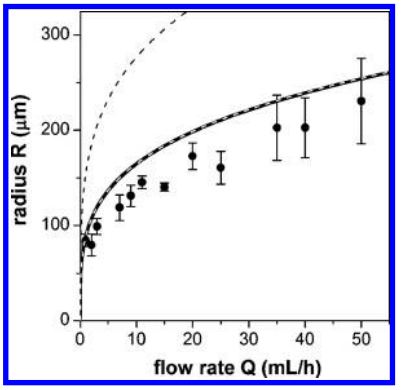

Figure 26. Jetting data are shown along with the solutions of purely hydrodynamic equations. The lower curve corresponds to a model specified in eq 4. The upper dashed curve corresponds to the stiff tube model, i.e., eq 4 for $\eta_o \to \infty$. Reprinted with permission from ref 41. Copyright 2004 European Physical Society.

6.2. Tube Pressure

When tubes grow in chemical gardens, it is because there is a force driving the interior fluid along the tube. This force typically comes from the pressure produced by the pump, be it osmotic or mechanical. The pressure driving the flow can be easily measured in pumping experiments by attaching a pressure sensor to the tube leading to the fluid chamber. Such pressure measurements are critical for understanding the dynamics of tube growth.

Figure 27 shows some recent experimental results[121] for the base pressure as a function of the tube height for upward growing tubes. The measured pressure grew smoothly and linearly with the tube height, and the rate of pressure growth depended on the

DOI: 10.1021/acs.chemrev.5b00014
Chem. Rev. XXXX, XXX, XXX−XXX

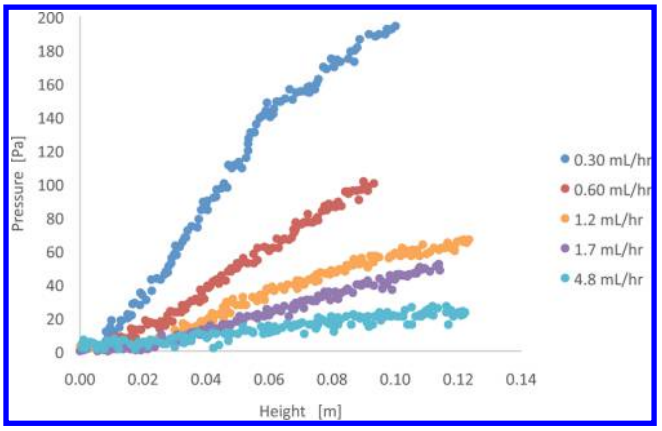

Figure 27. Measurements of base pressure versus tube height for growing tubes made by pumping 0.50 M $AlCl_3$ plus 0.75 M NaCl into 1.5 M sodium silicate. The different data sets correspond to different pumping rates, as indicated in the legend. The initial pressure and tube height have been arbitrarily set to 0 for all measurements. Data from the experiments discussed in ref 121

pumping rate. Qualitatively, the smooth growth tells us that the tube end is open at the top (compare Figure 27 with the pressure measurements in Figure 24 for closed tube growth). To understand quantitatively the connection between the rate of pressure change and the pumping rate, a model of flow down a tube is needed. For a cylindrical, vertical pipe of internal radius R_i, the change in pressure at the base of the tube, P_b, with height of the tube, h, is given by

$$\frac{dP_b}{dh} = \frac{8\eta_i}{\pi}\frac{Q}{{R_i}^4} - \Delta\rho g \tag{5}$$

The first term is the standard Hagen−Poiseuille laminar viscous pipe drag and the second term is due to gravity. For the experiment shown in Figure 27, $\Delta\rho$ was negligible so only the first term needs to be considered. The external radius of the tubes, R_0, was observed to depend on Q as $R_0 \propto Q^{\gamma}$ with $\gamma = 0.43 \pm 0.09$, so taking the internal radius R_i proportional the external radius R_0 predicts that dP_b/dh scales with Q as the power $1-4\times 0.43 = -0.72$. This predication is in reasonable agreement with the data, where the observed scaling exponent was −0.81. Thus, the decrease in dP_b/dh with the flow rate as observed in Figure 27 occurs because the tube radius increases quickly with the flow rate.

Note that the observed dependence of the external radius, R_0, with Q in this experiment is different than that observed for the jetting growth discussed in section 6.1, which would have $\gamma = 0.25$. This is because jetting growth was observed using very low concentrations of metal salt solution where the tube growth was templated by a fluid plume of mostly nonreacting metal salt solution. However, for the experimental measurements discussed here the metal salt concentration was an order of magnitude higher and there were no nonreactive plumes.

These observations of dP_b/dh have important implications for what happens when multiple tubes grow simultaneously from the same base.[121] Multiple tube growth is common when tubes branch or when tubes grow from an extended source such as a pellet. The flow rates down the different tubes are coupled together because they have the same base pressure and because they share the flow coming out of the base. As these tubes grow, dP_b/dh will generally be different for the different tubes and so the distribution of flow between the tubes will change continuously as they grow. The change in flow down the ith tube with time can be described by a nonlinear differential equation similar to the continuous logistic equation, but with the opposite sign[121]

$$\frac{dQ_i(t)}{dt} = -\xi_i(t){Q_i}^{\delta}(t)[\beta_i - {Q_i}^{1-\delta}(t)] \tag{6}$$

with $0 \le \delta \le 1$. Here β and ξ are slowly changing parameters and $\delta = 2-4\gamma$ is a scaling exponent. This equation can be solved exactly to find the tube radii and flow rates as a function of time, however its qualitative implications are apparent. While the logistic equation has a stable, nonzero fixed point, because this equation has the opposite sign that fixed point is now unstable and the equation predicts that flow rates are either driven to extinction or to the maximum possible flow. This is readily understandable from Figure 27 where we see that narrow tubes (small flow rates) have a larger dP_b/dh and so their resistance to flow grows more quickly than wide tubes (large flow rates), which further reduces the flow rate down the narrow tubes making them narrower. It is interesting to note that these dynamics are qualitatively similar to that of another fluid system coupled by pressure and volume conservation, the popular two-balloon demonstration.[167]

6.3. Osmotic Growth

The flow of water and ions across a semipermeable membrane can be driven by physical forces on the molecules and/or by statistical processes from concentration differences across the membrane. For silicate gardens the precipitation membranes have been observed to only support physical pressure differences of order 10−1000 Pa before they rupture[121,123,124] (see, e.g., Figures 24 and 27). This is far smaller than the typical osmotic pressures resulting from the concentration differences of the chemicals used to form the membrane, which are typically of order 10^7 Pa. Thus, the flow of solution across the membranes in chemical gardens is primarily determined by concentration differences.[123] Neglecting everything but the statistical processes, the total flow across the membrane and into a chemical garden structure can be written as

$$\frac{dV}{dt} \approx \kappa \int_S dA[\Pi_i - \Pi_o] \tag{7}$$

Here dV/dt is the volume flux across the entire membrane, the integration is over the area of the membrane, S, Π_i and Π_o denote the osmotic pressures on the interior and exterior of the membrane, and κ is a rate constant. It has been assumed that the membrane is uniform so that the rate constant can be taken outside of the integral. Using that the osmotic pressures are approximately proportional to the solute concentrations, eq 7 can be rewritten as

$$\frac{dV}{dt}(t) \approx \mu' \int_{S(t)} dA[C_i(\mathbf{r}, t) - C_i^*] \tag{8}$$

Here the concentration of the interior solution is denoted by $C_i(r,t)$; the dependence on the exterior concentration is contained in C_i^* the interior concentration when the osmotic pressures balance across the membrane, and μ' is a rate constant. The interior concentration will generally vary with position, $\mathbf{r}$, and time, t, inside the structure. The exterior solution typically has a much larger volume and is not confined to narrow tubes, so its variation in space and time has been neglected.

In situations where the growth of a structure comes entirely from osmosis, eq 8 can be used to construct a model for the

DOI: 10.1021/acs.chemrev.5b00014
Chem. Rev. XXXX, XXX, XXX−XXX

growth rate of the structure.[123] This is the case for closed tubes growing from a seed. It is assumed that at a time when the seed is fully dissolved the structure consists of a base with volume V_B and area A_B, and a tube of radius R and total length $h(t)$, so that $V(t) = V_B + \pi R^2 h(t)$ and $A(t) = A_B + 2\pi R h(t)$. To simplify the integration the crude assumption is made that $C_i(\mathbf{r},t)$ is independent of position. Then eq 8 can be rewritten as

$$\frac{dh}{dt}(t) \approx \mu' \frac{A(t)}{\pi R^2}\left[(c_0 + c_F)\frac{V_b}{V(t)} - (C_i^* + c_F)\right] \quad (9)$$

Here c_0 and c_F are constants which depend on the total number of moles in the seed and on the amount of solute per unit area used to form the membrane.[123] The volume of the membrane has been neglected. For typical values in chemical garden experiments, this equation predicts that the tube initially grows at an approximately constant rate while eventually approaching a constant value equal to the maximum tube length. The total tube length is finite because there is only a finite amount of the interior solute and this constrains the growth. This maximum tube length occurs at the fixed point of eq 9, when $dh/dt = 0$, so that it is independent of the rate constant but depends only on how much interior solute goes into forming the membrane and how much is needed to balance the exterior osmotic pressure. Note that because the structure was assumed to be uniform, $h(t)$ describes the total tube length which may actually consist of several tubes. This model is not appropriate for injection experiments because the mechanical pumping adds to the volume of the structure.

6.4. Relaxation Oscillations

The growth of chemical gardens is not always continual. It has been known for a long time[12,13,23] that sometimes it is discrete, with new bits of the structure appearing quickly at somewhat regular intervals. The driving mechanism here is the same as in all chemical gardens: the pump (osmotic or mechanical) increases the volume inside the membrane, causing an outflow of liquid. However, what is unique to the irregular growth is that the membrane seals itself extremely quickly so that growth occurs via repeated rupturing of the membrane and fluid extrusion. The slow buildup of pressure in the solution enclosed by the membrane followed by its quick release when rupturing occurs, as shown in Figure 24b, is a classic example of a relaxation oscillation.

Many different types of structures can be produced by this growth mechanism. Sometimes the ruptures appear at apparently random locations around the membrane, producing structures that resemble a hedgehog. At other times the ruptures occur repeatedly at the same location, producing long, irregular tubes of approximately constant radius that can grow for hundreds of oscillations, see Figure 24a. The type of structure produced depends on the choice of chemicals and their concentrations. Also the two types of structures mentioned can appear in the same system, although not generally at the same time.

This discrete growth mechanism can be described quantitatively by examining the physics of membrane rupture. The membrane has a tensile stress, σ', when the internal pressure is larger than the external pressure. Rupture occurs when this stress reaches a critical value, σ_c'. The stress in the membrane at the end of a growing tube is approximately

$$\sigma' \approx \frac{\Delta P R}{2w}$$

where R is the tube radius, w the membrane thickness, and ΔP is the pressure difference across the membrane. When a rupture occurs, ΔP drops to zero, but after the membrane seals inflow increases the interior fluid volume causing the membrane to stretch, causing ΔP and σ' to increase. As expected from general considerations,[123] ΔP has been observed[124] to be linear in time t, and can be expressed as $\Delta P = \zeta Q t$, where Q is the volume inflow rate and ζ is a pressure response parameter for the system. The stress at the tube end increases more slowly than linear because the newly formed membrane there is growing in thickness. Observations of membrane growth with time[54] suggest that the thickness can be parametrized as $w=(D_e t)^{1/2}$ where D_e is the effective diffusion parameter for flow through the membrane that observations suggest is about 3 orders of magnitude less than that of water.[54] The lack of any length scale to set the tube radius, R, suggests that it is determined dynamically and can be related to the oscillation period, T, as $R = c(QT)^{1/3}$, where c is a dimensionless geometric parameter that observations[123,124] find to be about 1. Putting this all together, the average oscillation period and tube radius can be calculated from the system parameters and the flow rate as[123]

$$T = \left[\frac{4D_e\sigma_c'^2}{\zeta^2 c^2}\right]^{3/5} Q^{-8/5} \quad (10)$$

$$R = \left[\frac{4D_e\sigma_c'^2 c^3}{\zeta^2}\right]^{1/5} Q^{-1/5} \quad (11)$$

Other observable quantities, such as the pressure change at rupture, can be calculated too in a straightforward manner from this model. Direct observations of the pressure inside the structure can be used to deduce the elastic modulus of the membrane.[124]

This simple model agrees with current observations of periodic tube growth. However, comparisons between theory and experiment can be difficult for systems growing from relaxation oscillations. Note that the above equations depend directly on the pressure response of the system, ζ. This is a *global* parameter depending on how the membrane over the entire structure stretches. This parameter depends on the shape of the structure and will evolve slowly in time as the membrane thickens. The global nature of this membrane stretching can be observed directly in the periodic "twitching" of the entire structure observed in some chemical-garden systems such as that shown in Figure 24a.

6.5. Fracture Dynamics

Rhythmic phenomena are not limited to the stretching of the precipitation membrane but can also affect more solid tube segments and are best described as fracture or rupture events. Fracturing dynamics is observed only for low flow rates and high density differences. The sequence of snapshots in Figure 28a presents an example for this type of tubular growth. During very long periods, the tubular growth is growing downward in steady fashion and devoid of the jetting of sodium silicate at the interface of the dilute metal salt solution. The steady growth is capable of being interrupted by break-off events, two of which are discerned in the third and final snapshots of Figure 28a. During these latter events, long cylindrical segments split off and sink to the bottom of the reservoir.

One important material property of chemical-garden tubes is that they can continually fracture and "heal" themselves. Studies of fracturing dynamics of injection-produced tubes show that tubular precipitation structures exhibit an ability to regenerate their colloidal membrane tube during a break-off event; a process

DOI: 10.1021/acs.chemrev.5b00014
Chem. Rev. XXXX, XXX, XXX−XXX

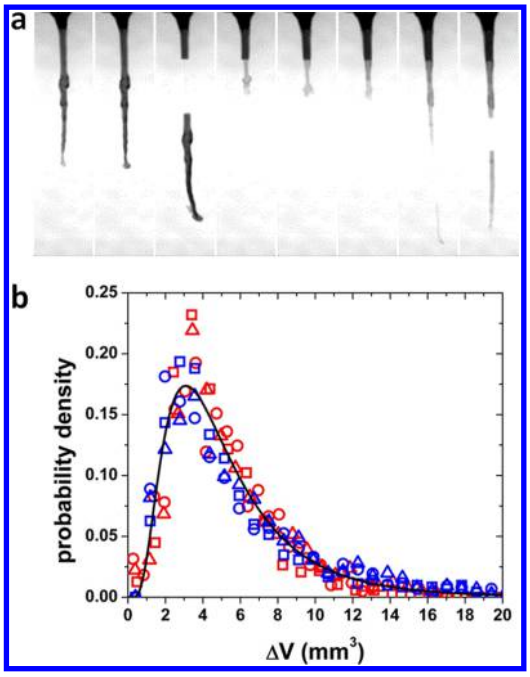

Figure 28. Reverse tubular growth in the fracturing regime. Copper sulfate solution is injected from the top down into a reservoir of sodium silicate solution. (a) Sequence of images spaced at 15s intervals. The image area is 1.3 × 5.4 cm^2 and the flow rate equals 1.1 mL/h. The copper and silicate concentrations are 0.075 and 1.0 M, respectively. (b) Probability density of fracturing events as a function of the volume ΔV, which is calculated from the length distribution of the ruptured tube segments (blue data) and the time distribution of the growth duration between subsequent rupturing events (red data). The continuous line is the best-fit log-normal distribution. Reprinted with permission from ref 47. Copyright 2007 American Chemical Society.

termed "self-healing". This property has been observed in both a reverse injection chemical garden system[47,125] and in experiments that involve reactant-loaded agarose beads.[34] A quantitative model has been reported for the reverse copper-silicate system using the lengths of broken-off tube segments Δh and the time difference between break-off events Δt. Detailed measurements revealed that Δh and Δt obey log-normal distributions

$$f(x) = \frac{1}{x\sigma\sqrt{2\pi}} \exp\left\{-\frac{(\ln x - \mu)^2}{2\sigma^2}\right\}$$

where μ and σ are the mean and standard deviation of the variable's logarithm, respectively.

Furthermore, it was found that the maximum of the Δh distribution is independent of the flow rate Q, while the maximum of the Δt distribution shifts to larger values with decreasing Q.[47] This study suggests that the stochastic aspects of fracturing growth do not result from external noise but rather from intrinsic features of the system.

The approximate range for fracturing tube radii was 0.41 mm and seemed to be independent of three different flow rates (i.e., 0.8, 1.1, and 1.4 mL/h). The critical length and time were described by their most frequent, modal, values. For distributions of the log-normal type this value yielded $\exp(\mu_{\Delta h} - {\sigma_{\Delta h}}^2)$ and gave rise to the critical volume $V_{crit} = \pi r^2 \exp(\mu_{\Delta h} - {\sigma_{\Delta h}}^2)$. The critical volume for time between break-off events was described by $V_{crit} = Q \exp(\mu_{\Delta t} - {\sigma_{\Delta t}}^2)$. Finally, a single master distribution was plotted in terms of the variable ΔV which was calculated from the Δh and Δt distributions as $\Delta V = \pi r^2 \Delta h$ and $\Delta V = Q\Delta t$, respectively. This master curve is shown in Figure 28b. Blue and red markers correspond to ΔV data obtained from length and time distributions, respectively. The different marker symbols distinguish between experimental data measured at three different flow rates. Overall the agreement between the measurements and the fitted log-normal distribution is very good. Accordingly, all features of the Δt distribution are determined by the ΔL distribution. The origins of the latter spread in lengths are not understood but could reflect random variations in the tube thickness, composition, and crystallinity.

Reverse silica gardens are an interesting example that can be studied quantitatively using the injection technique. Moreover, tubes that are characteristic of the fracturing regime break because of their increasing mass. Additionally, experiments of this type did reveal that the fracturing tubes essentially conserve the volume of the injected solution within their expanding structures. Future studies may perhaps include other reactant pairs along with the development of externally forced systems. The latter experiments could provide some information which may allow for the understanding of precipitation tubes in artificial and natural systems.

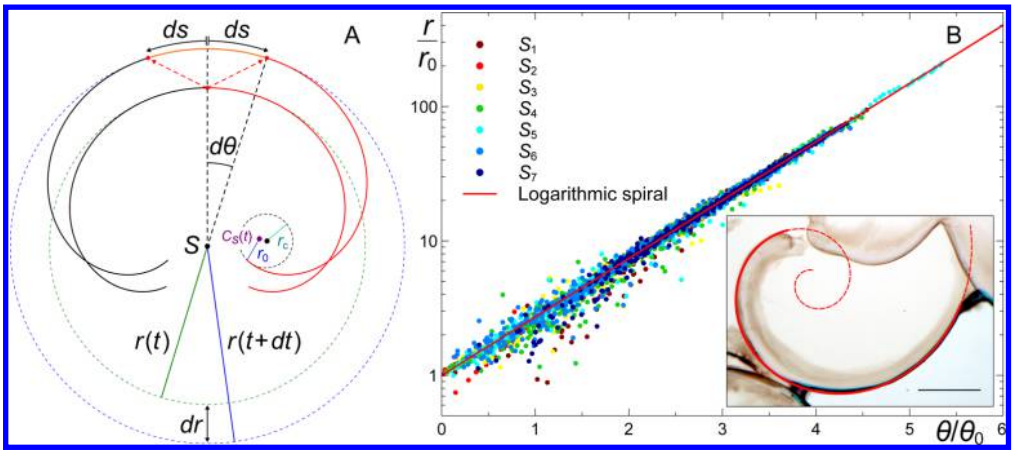

Figure 29. (a) Schematic explaining the growth mechanism of the spiral-shaped precipitates during an infinitely small interval of time dt during which $r(t)$ is the radius of the bubble of injected reagent and S is the point source. (b) Scaling law for 173 experimental analyzed sprials: measured radial distance $r=r_0$ as a function of the scaled angle $\theta=\theta_0$ (for 9 experiments and 7 pairs of concentrations). (Inset) Spiraled precipitate with evidence of the corresponding logarithmic spiral. (Scale bar, 2 mm.) Reprinted with permission from ref 38. Copyright 2014 Haudin et al.

DOI: 10.1021/acs.chemrev.5b00014
Chem. Rev. XXXX, XXX, XXX−XXX

6.6. Spirals in Two Dimensions

As we discussed in section 3.7, when chemical gardens are confined to grow in two dimensions, many novel morphologies appear. Prominent among them is spiral growth, which has been modeled with a geometric argument.[38]

Let us consider a source of reagent 1 injected at a point into reagent 2 in a two-dimensional system. Initially the contact zone between them will be a circle of arbitrarily small radius, r_0. Precipitation will occur at the contact zone, and with continued injection, as the precipitate breaks, the bubble of liquid 1 continues to expand within liquid 2, and the contact zone between them continues to expand in radius. Hence the new solid material being added will have the radius of curvature of the bubble of liquid 1 within liquid 2 at that time. In other words, the material at the distance s along the curve where fresh material is being precipitated (s thus being the arc length of the curve) will correspond to a bubble of liquid 1 within liquid 2 of radius of curvature R, and this gives us the relation $R \propto s$ between the radius of curvature and the arc length of the curve. This is the Cesàro equation $R = bs$ (b being a constant), which describes a logarithmic spiral.

In more detail, the equation of the precipitation zone is obtained by looking at two infinitesimally close time steps as displayed in Figure 29a. At time $t + \mathrm{d}t$, the precipitate layer formed at time t is pushed away by the newly created precipitate and rotates by an angle $\mathrm{d}\theta$. The length $\mathrm{d}s$ of this new segment of precipitate is proportional to the increase in length of the expanding bubble of reagent 1, namely

$$\mathrm{d}s = \theta_0[r(t + \mathrm{d}t) - r(t)] = \theta_0 \frac{\mathrm{d}r(t)}{\mathrm{d}t}\mathrm{d}t \tag{12}$$

where $\theta_0 = \mathrm{d}s/\mathrm{d}r$ is a constant growth rate controlling the length of the precipitate layer created as the bubble radius increases. A large value of θ_0 corresponds to a length $\mathrm{d}s$ for the new segment of precipitate large compared to the radial increase of length $\mathrm{d}r$ and produces a spiral that is more coiled. As seen in Figure 29a, the length $\mathrm{d}s = r(t + \mathrm{d}t)\,\mathrm{d}\theta$ is given to first order in $\mathrm{d}t$ and $\mathrm{d}\theta$ by

$$\mathrm{d}s = r(t)\mathrm{d}\theta \tag{13}$$

Substituting eq 12 into 13 we obtain $\mathrm{d}\theta = \mathrm{d}s/r = \theta_0(\mathrm{d}r/r)$ which is readily integrated to give

$$r = r_0 \mathrm{e}^{\theta/\theta_0} \tag{14}$$

where r_0 is a constant of integration. Equation 14 builds a logarithmic spiral in polar coordinates and quantitatively describes spiralled structures in nature (seashells, snails, or the horns of animals)[15] where the growth mechanism preserves the global shape by the simple addition of new material in successive self-similar steps. To validate this, spiral radii from 9 experiments and for 7 pairs of concentrations have been analyzed as a function of the polar angle; see Figure 29b. The radial distance and polar angle are rescaled by r_0 and θ_0 respectively. As seen in Figure 29b, all spiral radii converge onto an exponential master curve, proving that indeed the spirals are logarithmic to a good accuracy. The dispersion observed at low θ (near the spiral center) is due to the fact that the experimental spirals emerge from an arc of an initial tiny circular section of radius r_0, and not from a point as in the model.

Spiral growth goes on only as long as the produced precipitate can pivot within the cell; spiral growth stops when the structure becomes pinned by encountering a wall or another precipitate layer. Then the membrane breaks and a new radial source is generated, leading to a fresh spiral in a periodic, or almost periodic, fashion.

6.7. Templating by a Fluid Jet

While our emphasis here has primarily been on classical chemical-garden chemistry, in previous sections we have mentioned complementary work on tubular growth in electrochemically forced iron sulfate systems.[44] There it was found that tubular precipitates grow through the templating action of hydrogen bubbles (Figure 21) that linger on the cathode in a chamber filled with an iron−ammonium−sulfate solution. It was hypothesized that diffusion of ammonium to the bubble surface triggered the formation of a precipitative film there, a part of which remained after buoyant detachment of the bubble, adding to the tube. As a test of this chemical mechanism, and to study other templating processes, an experiment was set up[43] in which aqueous ammonia was injected into an iron sulfate solution (Figure 8), with the result that indeed a slow-moving fluid jet can act as a template for tubular growth. But the dynamics can be complex, with repeated events of detachment and rehealing of the tube wall over time (Figure 30).

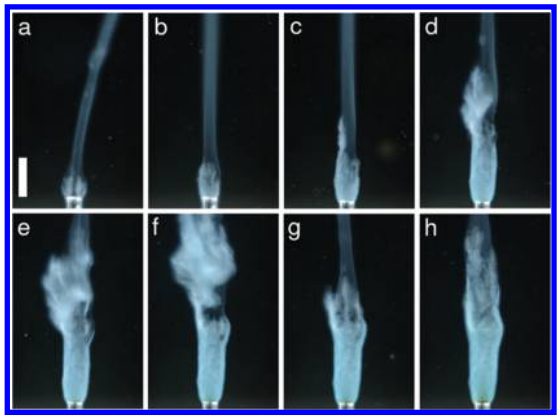

Figure 30. Close-up of a growing tube. The sequence of images spans 5 min with panels d−g taken 15 s apart. Tube growth begins in (a) as precipitate attached to nozzle, followed by transient elongation (b−d), detachment of a section (e, f), and finally, regrowth (g, h). Scale bar is 2 mm. Reprinted with permission from ref 43. Copyright 2005 American Chemical Society.

The primary quantitative results from the experiment[43] are shown in Figure 31a, where we see that the tube height h saturates over time to a value h^* that increases with the volumetric injection rate, or equivalently, the mean injection speed u. Defining a characteristic time τ as that when $h = 0.6h^*$, it was found that there is a good data collapse when the data are plotted as h/h^* versus t/τ (Figure 31b) and that τ and h^* are both approximately linear in u. A simple model with these properties is based on the assumption that it is lateral diffusion of ammonia outward from the ascending jet that controls the precipitation rate, subsumed in the rate constant k, and that that diffusion can be modeled as quasi-two-dimensional in the plane orthogonal to the jet propagation direction. In the simplest kinetic scenario, the rate of growth $\mathrm{d}h/\mathrm{d}t$ of the tube height is given by the excess concentration at the tube end $C(h)$ relative to some threshold value C^*, so

$$\frac{\mathrm{d}h}{\mathrm{d}t} = k[C(h) - C^*] \tag{15}$$

DOI: 10.1021/acs.chemrev.5b00014
Chem. Rev. XXXX, XXX, XXX−XXX

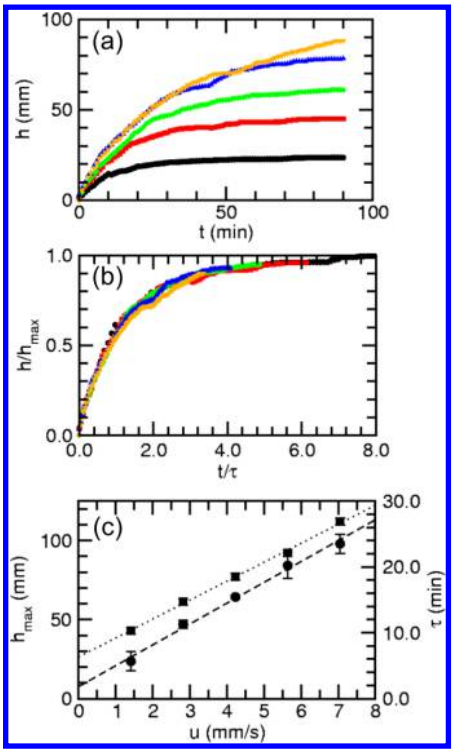

Figure 31. Growth dynamics of tubes. (a) Height vs time at various flow rates: 1 mL/h (blue) to 5 mL/h (orange). Each of the growth curves represents the average of three individual runs. (b) Rescaled height H' as a function of rescaled time s. Function shown in black is from model described in text. (c) Characteristic time (circles) and maximum height (squares) as functions of average fluid velocity of the jet. Linear fits also shown. Reprinted with permission from ref 43. Copyright 2005 American Chemical Society.

where $C(h)$ is taken to be the concentration at the midline of a 2D concentration field that began at time $t = 0$ at the jet nozzle as a top-hat profile

$$C(h) = C_0[1 - \exp(-a^2/4D_m t)] \quad (16)$$

If we now let $t = h/u$ and set $dh/dt = 0$ to find the maximum height we obtain indeed a scaling solution for $H' = h/h^*$ as a function of $s = t/\tau$, with $h^* \propto u$ and $\tau \propto u$ as observed experimentally. Moreover, the diffusion constant D_m extracted from the data is quite consistent with expectations for small molecular species.

7. APPLICATIONS: FROM CORROSION AND CEMENT TO MATERIALS SCIENCE AND TECHNOLOGICALLY RELEVANT PRODUCTS

Though the study of chemobrionics may seem detached from immediate utilitarian applications, this is not so. There are highly applied areas in which the growth of self-assembling tubular structures plays a key role. In some instances, such as corrosion (section 7.1), we should like to inhibit the formation of these structures; in others, like Portland cement (section 7.2) and chemical grouting (section 7.3), they may be intrinsic to the structural properties of the material; and in others, like polyoxometalate tubes (section 7.4), we wish to learn how to control them.

7.1. Corrosion Tubes

The corrosion of steel is a serious problem for many industries, and the morphologies of the resulting oxide formations include processes and products of the types we are discussing here. Indeed, the special cases of tubes, tubercles, and similar hollow forms of corrosion helps elucidate the fundamental chemistry of iron corrosion.

Starting with a publication in 1921, Ackermann[168−171] studied unexpected micro- to millimeter-sized structures formed in the corrosion of small iron particles (thin wires, shavings, and so on of technical grade), Figure 32. In the typical experiment, several

Figure 32. (a) Sketch and (b) optical micrograph of tubular forms of iron rust. Reprinted with permission from ref 168. Copyright 1921 Springer.

of these samples were positioned on a microscope slide in close proximity to a drop of acid and covered by a coverslip. Using an optical microscope, Ackermann observed the condensation of small satellite droplets around the original drop. In the course of the experiments, these droplets formed continuous films on the iron samples and induced precipitation reactions that decreased in rate with increasing distance from the acid source. Ackermann reported that the colloidal corrosion products generated cylindrical stalks on the surface of the metal sample. These stalks were capped by the small solution droplets that often disappeared while the stalk remained. The latter induced the additional formation of even smaller brush-like extensions. In regions with lower precipitation rates, Ackermann also observed colorless, hollow tubes of a gel-like consistency. The interior of these tubes was apparently filled by a fluid and sometimes compartmentalized by membrane-like walls. He reported several other features based on visual inspection, polarization microscopy, and qualitative reactivity. The largest complex structures had a length of 0.5 mm and resembled "jellyfish-like" objects; he reported that the tubes could reach much longer lengths. Pattern formation was observed only below 17 °C. The stability and detailed shape of the structures depended strongly on the relative humidity; for instance, a sudden increase in humidity seemed to induce the (reversible) collapse of the structures to liquid droplets.

In 1958 Butler and Ison[172] described hollow "whiskers" found growing inside mild steel tubes during tests on the effects of water flow rate on internal corrosion, Figure 33. These corrosion structures were less than 0.5 mm in diameter but up to 90 mm in length and grew parallel to the direction of flow. X-ray diffraction indicated that they were made of goethite on the outside surface and magnetite on the inside. This mineralogical layering of different oxidation states of iron minerals resulting from a redox gradient through the tube wall has remained a common characteristic of these structures (cf. section 4). Growth was attributed to diffusion of iron(II) ions from the anodic pit at the base of the whiskers to the rim where contact with the aerated water causes precipitation as iron(III) oxides. In another investigation of corrosion a short time later, a tubular corrosion product was observed at a pH of 12 by Riggs et al.[173] and Sudbury et al.[174] Iron(II) ion transport to the open tip was suggested, with

DOI: 10.1021/acs.chemrev.5b00014
Chem. Rev. XXXX, XXX, XXX−XXX

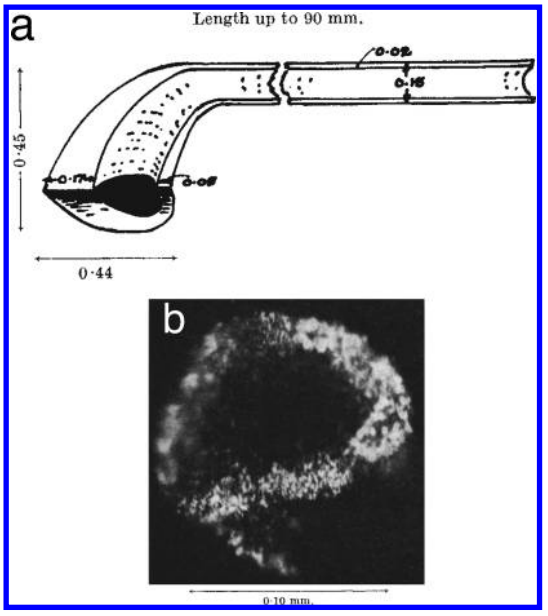

Figure 33. (a) Sketched longitudinal section and (b) micrograph cross section of tubular forms of iron rust. Reprinted with permission from ref 172. Copyright 1958 Macmillan Publishers Ltd.

posterior oxidation to iron(III), Figure 34. Inside the tubes the pH was found to be approximately 3, in keeping with anodic conditions. The work was discussed by Fontana[175] in his textbook *Corrosion Engineering* as an example of the autocatalytic nature of pitting. In this work, as in the earlier one, no bubbles were reported.

Nearly two decades later came a report of corrosion products including hollow nodules and short conical to tubular formations of uniform diameter called "chimneys",[176] Figure 35. Gas bubbles were seen emerging from the open ends and the authors assumed that the gas was hydrogen according to the reaction $3Fe + 4H_2O \rightarrow Fe_3O_4 + 4H_2$. The growth sites for the tubes were apparently cathodic and the material was determined by XRD and SEM to be green rust, magnetite, and lepidocrocite (FeOOH). Like magnetite, green rust contains both Fe(II) and Fe(III) but is a more reduced and more complicated hydroxide that is very unstable, readily converting to more oxidized, simpler, and more stable oxides.[177]

In a 1967 paper, Iverson[112] showed that "hollow whiskers" are formed by the reaction of iron particles or iron alloys in acidified potassium hexacyanoferrate(III) solution; examples are shown in Figure 36. In 1980, as part of their study on silicate gardens and related phenomena, Coatman et al.[26] reported images of tubular structures of iron(III) hexacyanoferrate(II) growing from the surface of a mild steel panel that had been immersed in potassium hexacyanoferrate(II) solution. This was clearly identified as a corrosion process and the tubular growths as corrosion products. It was noted that corrosion products are often colloidal in character and can form a protective skin over the metal surface. For continued reaction to occur there has to be a spalling process (due to pressure generated within or under the skin) to remove it and expose fresh metal to the corrosive environment. It was speculated that such pressures may be osmotic in character due to the semipermeable properties of the colloidal skin and hence there may be a mechanistic connection between corrosion and the processes occurring in the growth of silicate gardens.

More than two decades passed before tubular formations of iron oxides were grown for their own sake. In this study by Stone

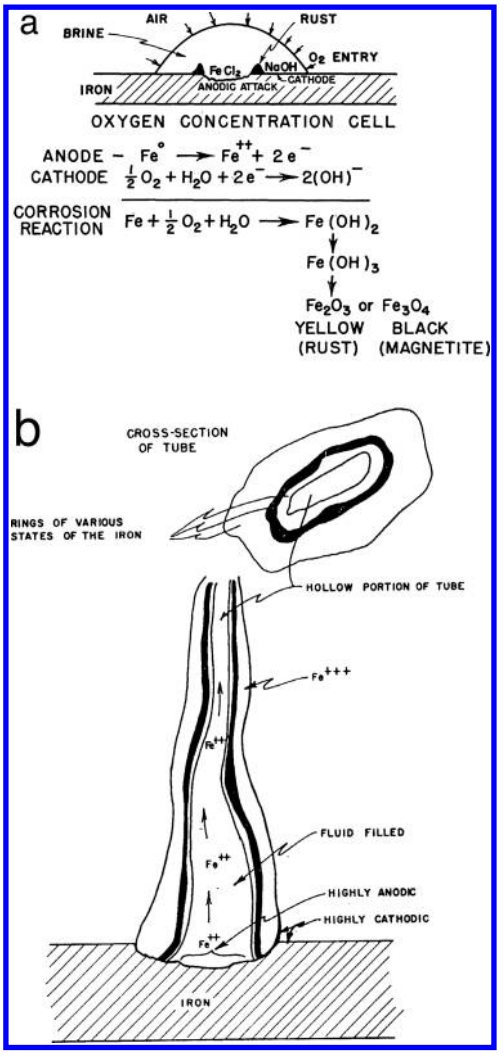

Figure 34. (a) Oxygen corrosion mechanism of iron and (b) corrosion tube growth mechanism. Reprinted with permission from ref 173. Copyright 1960 NACE International.

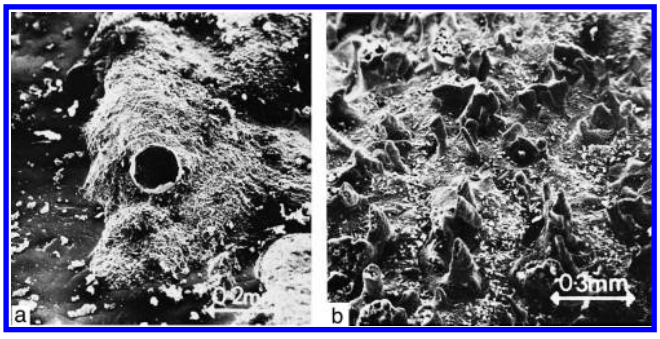

Figure 35. (a) Nodule of Fe_3O_4 and green rust showing vent which formed on gray cast iron in water at 50 °C and 0.44 ppm of O_2 after 7 h (SEM). (b) Open-topped "chimneys" growing out of crusted scale formed after 25 h on gray cast iron in water at 50 °C and 3.00 ppm of O_2 (SEM, 60° tilt). Reprinted with permission from ref 176. Copyright 1979 Elsevier.

and Goldstein,[44] charged electrodes were set up in concentrated solutions of dissolved iron salts to accelerate the precipitation process. The electrochemical cell also allows for a clear separation of the cathode (reducing) and the anode (oxidizing) by an ionic solution. In contrast, in ordinary corrosion the

DOI: 10.1021/acs.chemrev.5b00014
Chem. Rev. XXXX, XXX, XXX−XXX

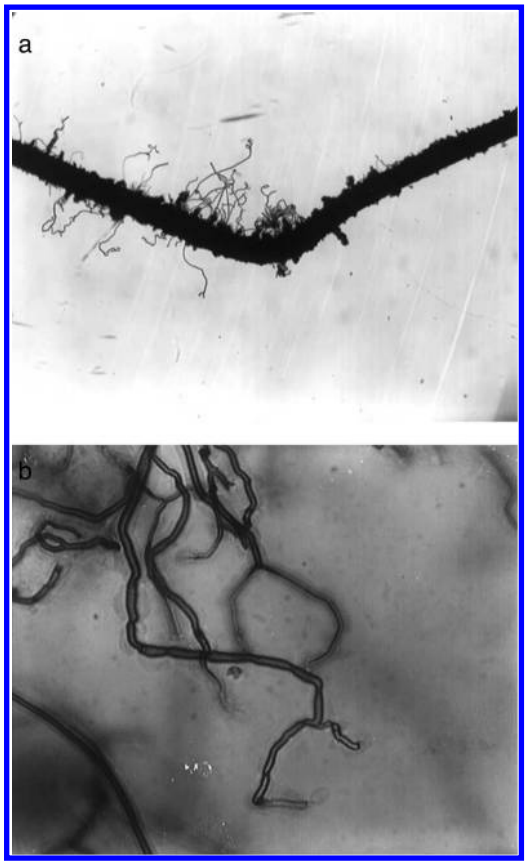

Figure 36. (a) "Hollow whiskers" from fatigued nichrome wire (0.5 cm diameter) in acidified potassium hexacyanoferrate(III) solution (×10). (b) Enlarged view of hollow whiskers (×c.135). Reprinted with permission from ref 112. Copyright 1967 Macmillan Publishers Ltd.

cathodic and anodic sites get set up in an uncontrolled pattern on the metal surface. (Initially, there is a chaotic "flickering" of charges before the pattern gets established.) With an external current the generation of gas bubbles from electrolysis can be greatly increased, although the exact sites of continuous bubble streams cannot be controlled. At the cathode, reduction of water creates hydroxide ions and hydrogen gas while at the anode water is oxidized to protons and oxygen gas. It is important to note that the fundamental redox reactions of both ordinary corrosion and the electrochemical cell are the same. In this electrochemical cell, because iron(II) and iron(III) salts were ammonium sulfates, both hydrogen and free ammonia gas were generated at the cathode's surface (Figure 21). Therefore, green rust more readily precipitated around the bubbles as the ammonia diffused into the surrounding solution. As each bubble detached, a ring of precipitate was left behind at the lip and in this way the tubes grew upward as long as the site at the base of the tube continued to generate bubbles. Despite the intense electrochemical conditions and concentrated solutions, the same wall layering was found as in the earlier study of ordinary corrosion; that is, green rust on the inside and lepidocrocite on the outside with magnetite in between. Recently, this formation mechanism was confirmed in a study of corrosion in cast iron pipes carrying drinking water.[178] The authors rejected other possible causes including active templating by microorganisms or static templating resulting from the minerals themselves.

7.2. Cement Hydration

Although not the first paper to report on the fibrous morphology of Portland cement paste, the classic paper published in 1976 by Double and Hellawell[179] was the first to make a direct comparison between chemical gardens and the fibrillar formations around hydrating cement particles, which they had observed in a "wet" environmental cell in a high voltage transmission electron microscope (TEM). In this and subsequent papers[180−182] they reported that the reaction of calcium silicates with water gives rise to an initial coating of calcium−silicate−hydrate (C−S−H) gel around the cement grains and that this coating develops surface protuberances that grow into densely packed fibrils (Figure 37). It was proposed that the hydration mechanism of Portland cement is analogous to the growth of silicate gardens. The C−S−H gel coating acts as a semipermeable membrane that allows inward diffusion of water and outward diffusion of calcium and hydroxyl ions but not of the larger silicate ions. The development of osmotic pressure in the C−S−H gel coating on the cement grains relative to the solution outside causes the coating to rupture and this is the driving force for the growth of the fibers, some of which were seen to be hollow (Figure 37c).

Birchall et al.[183] published a contemporaneous paper supporting an osmotic mechanism and arguing that a crystallization "through solution" process could not be the primary mechanism of the hydration of Portland cement. A number of subsequent papers by other authors[184−188] have also reported on observations of hollow tubular growths during

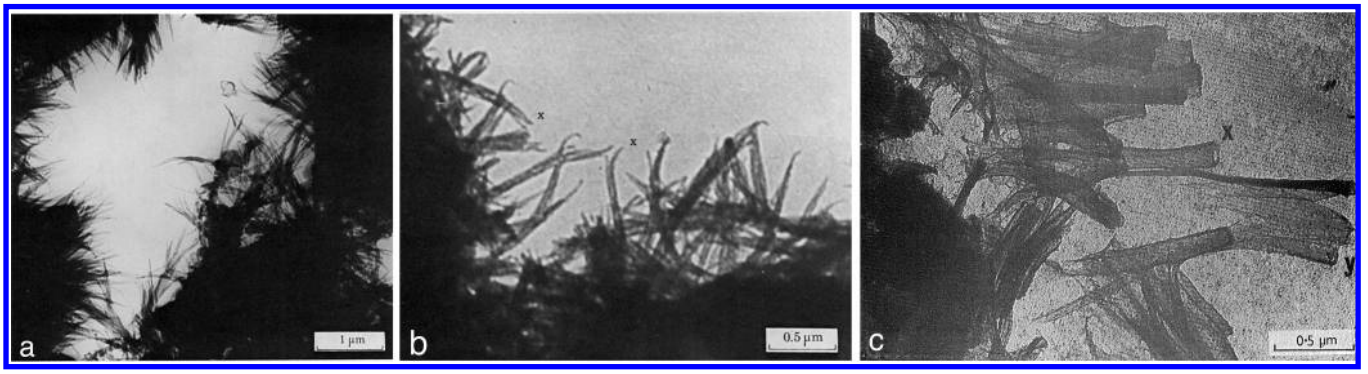

Figure 37. Cement tubes: (a) Cement + water sample after more than 1 day showing the secondary fibrillar development of C−S−H gel around the cement grains. (b) Greater detail of fibers. Environmental specimen stage, high voltage electron microscope. (c) Dried cement sample showing fibrillar C−S−H hydration product, the appearance of which suggests tubular morphologies. Transmission electron micrograph. Reprinted with permission from refs 179 and 182. Copyright 1976 Macmillan Publishers Ltd.; 1978 Silicates Industriels.

DOI: 10.1021/acs.chemrev.5b00014
Chem. Rev. XXXX, XXX, XXX−XXX

cement hydration and attempted to establish to what extent cement tubes were evidence of an osmotic pumping model.

It is a pity that current cement researchers seem to be unaware of, or have forgotten about, this hydration mechanism. For example, a recent cement review[189] reports: "During the 1980s, several papers reported that specific morphological features seem to form during each stage of reaction. The C−S−H needle morphology that typically forms preferentially during the early stages was once seen as a clue to the reaction mechanism, but this has not stood the test of time." However, there is no specific criticism made of the osmotic model. Furthermore, in the same paper, the authors assert that mechanical rupture of the semipermeable C−S−H barrier layer due to osmotic pressure allows trapped silicate ions to react with the calcium-rich solution and that this mechanism is the most consistent with direct experimental evidence from nuclear resonance reaction analysis. This mechanism bears all the appearance of being an osmotic pumping model.

Following the papers on cement morphology, Double and co-workers[190−193] turned their attention to using the osmotic membrane model to explain the effects of admixtures, which are widely used in the cement industry to accelerate or retard setting. From the osmotic model it follows that cement hydration depends on diffusion through protective colloidal membranes around the cement grains. The rate of reaction, and hence the development of the secondary C−S−H gel hydration products, is controlled by the permeability and cohesion of these coatings. It was proposed that changes to the colloidal structure of the C−S−H gel coating will influence hydration kinetics: a more flocculated, poorly adherent coating accelerates hydration, whereas a dense, coagulated coating causes retardation. Hence the ranking of cations and anions as cement accelerators and retarders was linked to the efficacy of flocculation of the colloidal membrane.

The mechanistic connection between chemical gardens, cement hydration, and corrosion[26] has led to an explanation of why many additives that accelerate cement hydration also promote corrosion of steel, and those that retard hydration are usually corrosion inhibitors.[194] These considerations have implications in the search for cement hydration accelerators for use in reinforced concrete, and on the effect of corrosion inhibitors on the properties of reinforced cement mortars, as corroborated in a recent study.[195]

7.3. Chemical Grouting in Soils

In civil engineering work, the reactions of waterglass and other chemicals have been widely used to strengthen foundations, and to prevent liquefaction of embankments and water leakage. Although many different chemical reactions are today used in this chemical grouting,[197] the original Joosten process developed in the 1920s involved two boreholes into which would be injected on the one hand waterglass, or silica gel, and on the other calcium or magnesium chloride solutions.[198] We surmise that the Joosten technique thus must have produced something like a chemical garden in the soil, although we do not know of any work that provides evidence that the results of the injection were in fact chemical-garden-like.

Something like the reverse of this situation is found in naturally occurring laterites that are high in iron. This clay-like material is commonly dug from subsurface deposits in the tropics and shaped into blocks. Upon exposure to the air and wet−dry cycles laterites (Latin for "brick stone") irreversibly harden without heat into a durable building material. Multistory buildings constructed of such blocks in India have withstood the wind driven rain of countless monsoons for centuries. Relevant to our concerns is that laterites typically are not homogeneous but contain numerous nondirectional structures that have been described as "tubular", "cellular", and "vesicular" (Figure 38). The

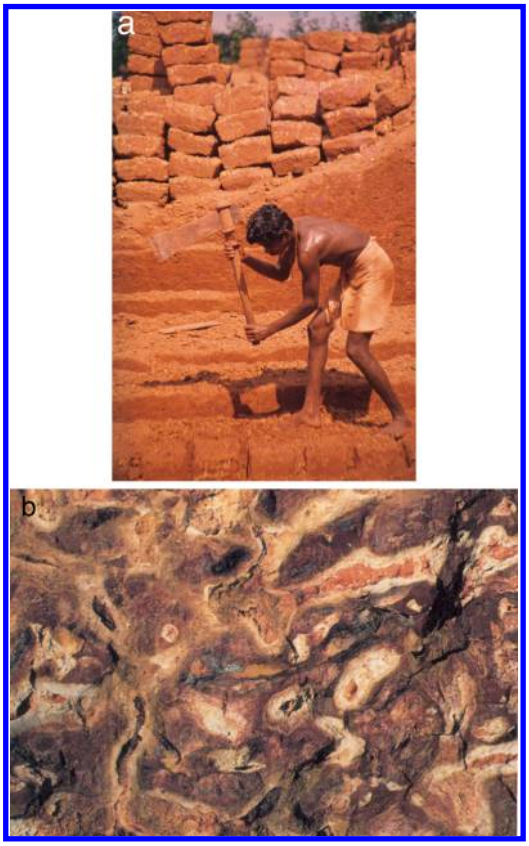

Figure 38. (a) Laterite quarry in Angadipuram, India. (b) close-up view, which spans about 1 dm vertically, of typical laterite showing tubular structures surrounded by various iron oxides. Images from Werner Schellmann. Reprinted with permission from ref 196. Copyright 1994 ISRIC — World Soil Information.

formation of these structures have been attributed to "interstitial, chemically active pore liquids or gases contained within the rock body, or introduced from external sources" that are active during the metasomatic process that replaces the mostly silicic parent material.[196] All this suggests a slow, geological version of the kind of morphogenesis we see in chemical gardens.

7.4. Polyoxometalates: Synthetic Microtubes

Polyoxometalates (POMs) belong to a large family of cluster anions with large variations in molecular and extended structural motifs constructed from transition metal oxo subunits (typically MO_x where M is V, Mo, or W and $x = 4−6$) linked together by sharing of one or more oxide ions between neighbors. POM clusters are extraordinary molecules: they have a high charge, are of nanoscale dimensions, and the metal-oxide cage can encapsulate many types of small templates and can be formed by self-assembly.[199−203] Although POMs have much in common with bulk transition-metal oxides, their molecular nature gives them a vast structural diversity with many applications as redox, catalytically active and responsive nanoscale materials.

The growth of micrometer-scale hollow tubes from polyoxometalate (POM) materials undergoing cation exchange with bulky cations in aqueous solution was initially reported in

DOI: 10.1021/acs.chemrev.5b00014
Chem. Rev. XXXX, XXX, XXX−XXX

2009[113] and has now been shown to be a general phenomenon for POMs within a critical solubility range.[116] As further dissolved material is extruded, either from a small injection aperture or from a rupture in a membrane surrounding a dissolving crystal, the continued aggregation process results in the formation of a hollow tube structure extending from the aperture (Figure 39). The tube continues to grow from the open

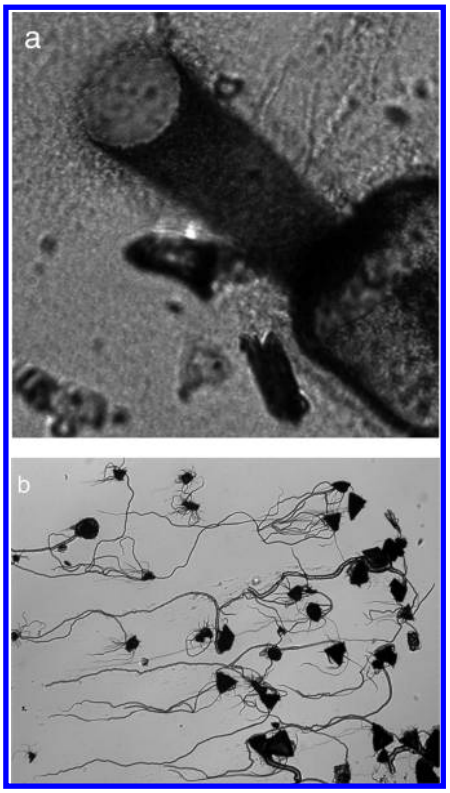

Figure 39. (a) Microtube approximately 50 μm in diameter growing on a glass surface. $(C_4H_{10}NO)_{40}[W_{72}Mn_{12}O_{268}Si_7]\cdot 48H_2O$ POM in *N*-methyl dihydroimidazolphenanthridinium bromide solution. Image from Geoff Cooper. (b) Several microtubes approximately 25−75 μm in diameter under bulk flow conditions, showing the alignment of the growth direction to the flow. Reprinted with permission from ref 116. Copyright 2011 American Chemical Society.

end until the source of POM material is exhausted, a shorter exit route is provided (e.g., from a rupture in the tube closer to the source), or the cation concentration becomes too low for aggregation. POM tube growth has been demonstrated with a wide range of different cations including several dihydro-imidazo-phenanthridinium (DIP) compounds, 3,7-*bis*(dimethylamino)-phenothiazin-5-ium chloride (methylene blue), polymeric poly(*N*-[3-(dimethylamino)propyl]methacrylamide), and even the complex $Ru^{II}(bipy)_3(BF_4)_2$ (bipy =2,2′-bipyridyl).

POM systems are inverted with respect to classical chemical-garden systems, in that POM fragments are anionic and tube growth involves their aggregation in a bulk solution containing cations. Mechanistically, the growth of POM microtubes is so similar to that of classical chemical gardens that the two phenomena must be part of a larger gamut of precipitation-membrane tube-formation mechanisms. It is hoped, that, by analyzing the characteristics of POM microtubes and chemical gardens, we can reach a better understanding of the general mechanisms of osmotically driven tube formation.

In POM tube-growth systems it may be desirable to reduce the solubility of the POM material, so that the slower dissolution and release of POM allows membrane closure to occur and the osmotic pump mechanism to initiate. Also, the ability to grow tubes from more soluble POMs, or from those that do not crystallize readily, finally expands the generality of the tube growth phenomenon to all water-soluble POM species. One way to reduce the POM solubility is to add a less soluble secondary material to the POM pellet, which can act as a retardant to the initial dissolution.[115] Capillary injection can be externally controlled and thus removes many of the uncertainties from tube growth and initiation, for example, there is no requirement for the membrane rupture and osmotic pressure to produce the initial aperture. Also, the positions of the capillary ends in the experiment can be defined or even moved during growth, to control tube morphology.

More precise control of POM microtubes is desirable since then they can be used to make useful patterns or devices. With injection methods, the fluid pressure inside the tube (and hence the rate of POM delivery and rate of aggregation) can be controlled, and this allows adjustment of the tube diameter.[114] When the flow rate is decreased or the concentration of the cation is increased, the material begins to aggregate closer to the aperture and the resulting tube narrows. The opposite is true if the flow rate increases or concentration is reduced. It is also possible to control the direction of the growing tubes (and even multiple growing tubes at once), to create custom patterns. As the POM material is ejected from the growing tube, it is influenced by any liquid flow in the sample such that tubes will always grow along the direction of flow. Thus, the use of electrodes to set up convection currents in the surrounding fluid allows the direction of the growing tubes to be controlled,[114] and by using a dye molecule in the cation solution to allow local heating by absorption of laser energy, a focused laser spot can be used to create a localized flow. This means that an individual tube can be steered reliably and independently by coupling the laser optics to a spatial light modulator (SLM) in a setup more commonly used as "optical tweezers"; the laser light can be split into multiple foci which can be used to control different growing tubes independently within the same sample.[118] Growing a specific structure requires accurate positioning of the laser spots by a user who can react to the progress of the system, and this depends critically on the computer interface used to control the SLM. To achieve this, the microscope image is displayed on a multitouch tablet (Apple iPad), along with markers representing the laser spots.[204] These markers can be dragged around, moving the laser spots to follow the user's fingers, so that multitouch gestures allow the growing microtubes to be controlled (see examples of structures in Figure 40). Laser heating also allows tube walls to be deliberately ruptured, producing branch points, or preloaded capillaries to be unblocked in situ so that extra tubes can be initiated on demand during device construction. The movement of the laser spot can be automated with image analysis and feedback such that a computer can control the laser spot to steer a microtube into a predefined pattern as it grows (Figure 40i).

It is also possible to produce larger hollow architectures, not just microtubes, from POM materials. When the POM solution is very concentrated or the aperture is large (200 μm or greater), the injection of POM into a cation solution does not produce microtube growth but instead produces large membranous vesicles. These inorganic chemical cells, which have been termed "iCHELLs" (Figure 41), are robust, leak-free, spontaneously

DOI: 10.1021/acs.chemrev.5b00014
Chem. Rev. XXXX, XXX, XXX−XXX

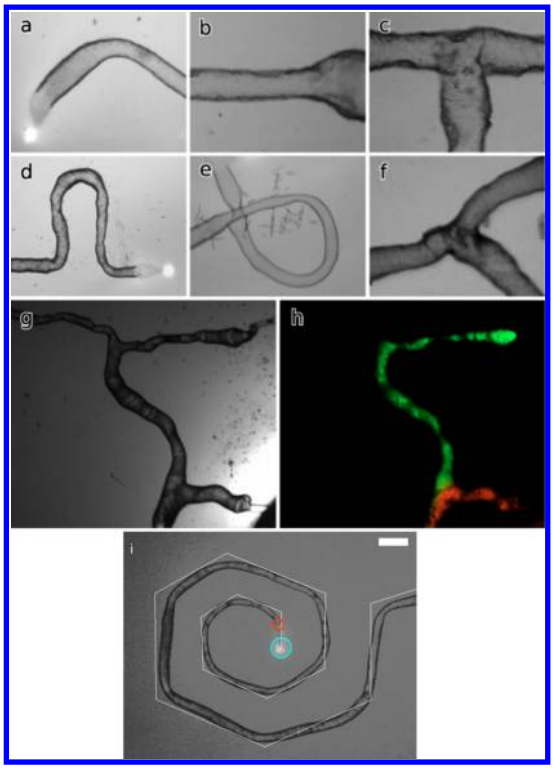

Figure 40. Laser control system can produce devices using a number of basic elements: (a) a wide bend, (b) a change in diameter, (c) a T junction produced by puncturing a growing tube, (d) a sharp bend, (e) tubes crossing, (f) a Y junction produced by merging two tubes, (g) a device comprised of two Y junctions between three individual tubes, and (h) the same device with green (fluorescein) and red (rhodamine B) fluorescent dyes flowing into the junctions. Tubes are between 20 and 50 μm in diameter. (i) Automated control of a laser spot to grow a tube to a specified pattern (a spiral). The blue marker shows the laser spot position, the red marker shows the position of the growing tube (by image analysis) and the white line shows the preloaded pattern. Scale bar is 500 μm. Images from Geoff Cooper.

repairing, and have diameters ranging from 50 μm to several millimeters.[117] iCHELLs display intrinsic physical properties that reflect their molecular building blocks, such as catalytic activity or chiral structure, as well as being able to partition chemical components within a system as miniature reactors. They can be manufactured in bulk or on a microfluidic platform or be nested within one another to produce clearly separated domains within a single structure. Due to the large library of starting materials from which they can be produced, iCHELLs offer a method by which hybrid membranes with various in-built functionalities can be produced at a water−water interface, i.e., without the need for immiscible solvent systems or solid supports. While, initially, iCHELL production does not follow an osmotic growth mechanism, since the growth pressure is externally applied, it is possible to influence the morphology postsynthesis. For example, changing the external cation concentration can be used to change the size of the iCHELLs or even trigger spontaneous morphogenesis into microtubes.

The mechanistic similarity between POM tube growth and classical chemical gardens is striking, and, like the inorganic self-assembly examples described in previous sections, the structures made with POM precipitates are potentially catalytic and technologically useful. Since these microtubes and membranes are formed by simple electrostatic aggregation, and the range of available POM materials is huge, it is easy to see how this approach could be extended to produce materials with radically different functionality, just by changing either of the reagents. This ability to combine the functionalities of both components in a process largely independent of the chemical properties of the species could be of importance for future applications and device manufacture in energy storage, microfluidics, electronics, and catalysis.

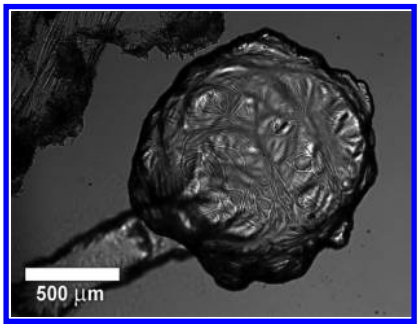

Figure 41. iCHELL composed of $\{PW_{12}\}$ POM and *N*-methyl dihydroimidazolphenanthridinium bromide. Image from Geoff Cooper.

8. CHEMICAL GARDENS IN NATURE AND IMPLICATIONS FOR THE ORIGIN OF LIFE

Up to this point, we have considered chemical gardens in the laboratory and in technological applications; what about in the natural world, in geology and biology? In the geological world, natural chemical-garden structures involving semipermeable precipitation membranes are found in a range of environments. The most studied are hydrothermal vents on the ocean floor (section 8.1), because of the interest and possible implications for the origin of life (sections 8.2−8.3). Recently, it has been pointed out that so-called brinicles formed beneath floating sea ice are another example of a geological chemical garden (section 8.4). Further examples are out there. As for the biological world, of course it is full of semipermeable membranes formed of proteins, but are there in fact any biological examples of biomineral precipitation formed with a chemical-garden pathway? These are being sought. Lastly, we note that the formation of a precipitation film through the templating action of bubbles, discussed earlier in several contexts, also appears in the growth of so-called "soda straws" in limestone caves. These hollow tubes form as calcium carbonate precipitates on pendant fluid drops hanging from the tube end as carbon dioxide outgasses from the water and its pH rises. The same basic chemistry underlies the formation of iconic speleothems such as stalactites, whose growth laws have been studied recently.[205,206] However, the growth of soda straws has not yet been examined systematically; it is not clear to what extent a wall-thickening mechanism for soda straws, growing in air, might emulate that of chemical-garden tubes, growing in solution, and hence to what extent they can be thought of analogous structures.

One of the most fundamental philosophical and scientific challenges for humans is to understand the origin of life: a highly organized system that emerged from self-organizing chemistry, and invariably relies on chemical and electrochemical disequilibria in much the same way that chemical-garden systems do. Chemical gardens were first studied as a possible mechanism for the origin of life, as we discussed in section 2.3, since they adopt biomimetic morphologies. The history of chemical gardens is from the very beginning a history of comparing these structures

DOI: 10.1021/acs.chemrev.5b00014
Chem. Rev. XXXX, XXX, XXX−XXX

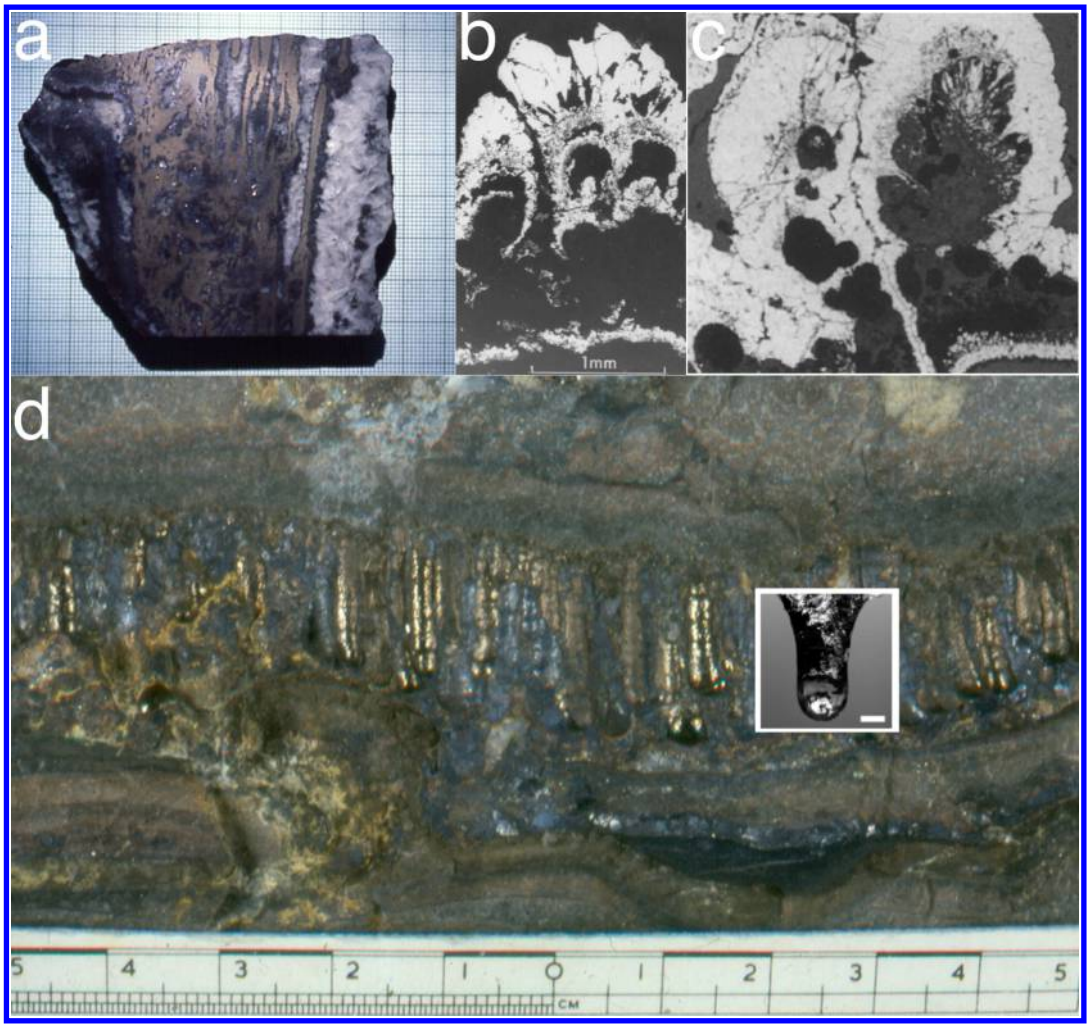

Figure 42. (a) Natural iron sulfide garden from the Tynagh mine, Ireland, now composed of pyrite embedded in barite, produced as a somewhat acidic, iron(III)-bearing buoyant hydrothermal solution invaded a mildly alkaline sulfanide (bisulfide)-bearing brine occupying a void below the carboniferous seafloor ~350 million years ago (Russell and Hall,[141] cf., jetting, section 3.2); (b, c) hollow pyrite botryoids produced as for (a) but perhaps more slowly (Russell and Hall,[141] cf., budding, section 3.2); (d) reverse gardens found at Navan, also in Ireland, whereby a dense sulfanide-bearing surface brine seeped down into an open horizontal joint occupied by iron-bearing mineralizing solution ~350 million years ago.[207] A photograph of a comparable reversed-phase growth of a "hanging" iron(III) sulfide budding tube produced as iron(III) sulfate was passed down into gaseous H_2S is superimposed on the geological sample (cf. Stone and Goldstein,[44] Figure 6 and the reverse chemical gardens of Pagano et al.,[47] section 3.1). Adapted with permission from ref 141. Copyright 2006 GSA.

to biological forms. It is clear why the earliest researchers from Glauber's time used this terminology, because that was all with which they could compare these forms. But to see why in the 19th and early 20th centuries Leduc, Herrera, and contemporaries used the vocabulary of biology, one needs to understand the context of their work a century ago: they were trying to show how biology could arise from the inorganic world of physics and chemistry, from chemical gardens, from osmotic forces, together with diffusion and other physical mechanisms. The piece of the puzzle they were missing is genetics, so that they thought that they might be able to create a single-celled organism simply by mixing components in this way. This field, that they called plasmogeny or synthetic biology, died as proteins and finally DNA were isolated, and the enormous complexity of even a single biological cell became clear. Now, though, the science has come full-circle: while we now understand that chemical-garden structures do not directly result in the formation of biological membranes in the way that was originally thought, the study of these self-assembling structures is today yielding new insights into the processes that may have driven the origin of metabolism on the early Earth.

Surprisingly, even in systems with just two inorganic compounds a vesicle can be formed spontaneously, with a membrane across which chemicals can diffuse from the exterior, to react with chemicals inside, whereon some product may diffuse out. This vesicle sustains itself far from thermodynamic equilibrium.[107] Chemical gardens are essentially membranes formed from the chemical and pH disequilibria between two different solutions, and their self-organizing properties persist only so long as these disequilibria exist. Chemical-garden structures can be considered as chemical reactors: the membranes maintain chemical gradients, but they allow some reagents/ions to permeate through the membrane, and the types of experiments described in the present review demonstrate how the alteration of simple physical and chemical parameters of chemical-garden systems can result in everything from catalytic surfaces, to layered structures, to the generation of electrical potentials and currents. There are natural chemical-garden

DOI: 10.1021/acs.chemrev.5b00014
Chem. Rev. XXXX, XXX, XXX−XXX

structures that form at the interface of hydrothermal fluid and seawater at deep-sea vents, and though these are much larger, more long-lived, and more complex in composition than simple chemical-garden laboratory experiments, the mechanisms of formation, and possibilities for free energy conversion, are much the same.

8.1. Hydrothermal Vents: A Natural Chemical Garden as a Hatchery of Life

Natural examples of chemical gardens that grew around springs (Figure 42a) and seeps (Figure 42b,c) have been found as fossilized structures at the Tynagh and Silvermines base-metal deposits in Ireland and reverse gardens found in the giant orebody at Navan, also in Ireland (Figure 42d).[140,207,208] In a natural system of this type, the injecting solution (hydrothermal fluid) and the reservoir (ocean) would both have complex compositions with multiple precipitating species.

It was the discovery of just such natural chemical gardens that led to the proposal that naturally generated chemical garden electrochemical cells at submarine alkaline hydrothermal vents on the early Earth might have focused redox, osmotic, and chemiosmotic (pH) gradients as the free energy sources that drove life into being.[139,140,209] It now appears that precipitate membranes comprising the ever-renewing outermost surfaces of such a submarine hydrothermal mound would have maintained disequilibria for the order of the 100 000 years the hydrothermal vent was active, though with a pH contrast inverse to the classical acid interior/alkaline exterior garden.[139,210] Reflecting on a comparison with the kind of chemical garden Leduc had in mind to explain life's origin, in the hydrothermal case we can think of minerals in the ocean crust that are compounds that, like those involved in laboratory chemical-garden growth, are comprised of weak acids and strong bases. Although olivine ($\sim Mg_{1.8}Fe_{0.2}SiO_4$) was the dominant mineral of the early Earth's oceanic crust, and is responsible for much of the reduction of water and carbon dioxide, it is the dissolution of calcium from the minor concentrations of diopside ($\sim MgCaSi_2O_6$) that is largely responsible for the high pH (high OH^- concentration) of moderate-temperature ultramafic rock/water interactions.[211−214] Thus, the calcium and silica hydrolyzed by carbonic ocean water gravitating to depth through fractures deputize for the dissolution of sodium silicate to produce an alkaline solution of calcium, minor magnesium, and hydroxide ions where sulfide constitutes a significant proportion of the ocean crust, and then sulfanide (bisulfide, HS^-) joins the alkaline mix.[49,215] The contrasting acidic medium is the Hadean carbonic ocean, which contributes the metal ions, predominantly iron and magnesium along with some zinc, as well as minor nickel and cobalt components.[216−218]

In life, the proton gradient across the membrane from outside to inside the cell, augmented by the membrane potential, is put to work by various types of pyrophosphatase engines sited in the membrane to convert inorganic monophosphates (Pi) to pyrophosphates (e.g., PPi) or adenosine diphosphate (ADP) to the triphosphate (ATP). The resulting pyrophosphates such as ATP drive phosphorylation and polymerization. Osmosis is a feature of all life, coupling, for example, phosphorylation to redox and pH gradients as a means of storing energy within the cell,[219] and it is this conversion of free energy that marks the transition from mere exergonic [i.e., spontaneous and energy-producing] geochemical reactions toward endergonic reactions [those requiring free energy to proceed] that can be driven against the thermodynamic gradient, a requirement of all biochemistry.[220] In the words of Nick Lane, "Mitchell's proton gradients enable cellular metabolism to transcend chemistry".[221]

To detail the system, given the kind of massive submarine chemical-garden structure likely to have been generated at an alkaline submarine spring on the early Earth, a proton gradient would have been imposed across the outer inorganic membranes separating the acidic, carbonic exterior from the alkaline interior (Figure 43). Thus, no pumping enzymes (i.e., respiratory

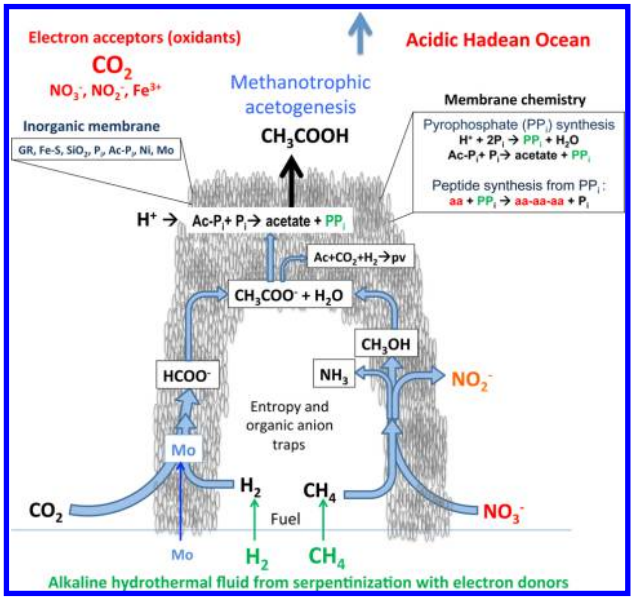

Figure 43. Natural compartmentalized chemical garden (hydrothermal mound) over an alkaline vent (exhaling sulfide containing solution) in the ancient Hadean carbonic ocean (anoxic and therefore enriched in dissolved Fe^{2+}).[49] The chemiosmotic potential is derived from the partial dissolution of the olivine and minor pyroxene comprising komatiite, peridotite, or harzburgite beneath the hydrothermal mound (not shown) to produce an alkaline hydrothermal fluid, against the acidic (carbonic) ocean. Interaction between the two fluids in the green rust (GR)-bearing membrane could have driven the synthesis of formate ($HCOO^-$), acetate (ac, CH_3COO^-), pyruvate (pv), and thereby, amino acids (aa) and peptides (aa-aa-aa)[222−224] while the chemiosmotic potential may have driven pyrophosphate (PPi) formation from orthophosphates (Pi) and acetyl phosphate (Ac-Pi). Redrawn with permission from ref 209. Copyright 2013 the Royal Society.

complexes) would have been required at this early stage for the generation of the pH gradient. A use of this gradient marked the onset of chemiosmosis whereby a proton gradient diffusing across the inorganic membrane drove pyrophosphate condensation from orthophosphates at high ratio to generate the energy currency in the first cellular compartments. Indeed, we speculate that any monophosphate driven into the interlayers of double layer hydroxides such as in green rust (now known as fougèrite, e.g., $\sim[Fe_3^{II}Fe^{III}(OH)_8]^+[Cl{\cdot}2H_2O]^-$), comprising the hydrothermal membranes, may have been driven by the proton gradient to condense to the pyrophosphate.[50,209,225−227] In the low-water-activity environment within the membrane the resulting pyrophosphate might then condense amino acids to peptides, a first step to a biochemical perpetuity. This reaction is inheritable as product could be entrained and flow in the hydrothermal stream to further inorganic compartments developing as the chemical garden continued to grow, fed by the long-lived submarine alkaline spring (cf. Yamanaka et al.[228] and Yamagata and Inomata[229]).

DOI: 10.1021/acs.chemrev.5b00014
Chem. Rev. XXXX, XXX, XXX−XXX

The other main requirement for life to emerge is the fixation of carbon, and we argue that, apart from free energy conversion employing the natural proton force to generate pyrophosphate, the same hydrothermal mound could also act as a carbon fixation engine, fueled by the electron donors (H_2 and CH_4), which are delivered from the exothermic serpentinization reactions.[230] These reactions feed back to augment the thermal gradient driving the open system hydrothermal convection cells supplying the submarine mound mentioned above.[139,231−233] Thus, inorganic carbon in the form of methane is delivered in the hydrothermal solutions while carbon dioxide is delivered to the mound's margins from an ocean in equilibrium with a CO_2 atmosphere and constantly supplied there through currents and/or carburation whereby the speed of hydrothermal flow draws the relatively oxidized ocean water into its stream.[234] The carbon dioxide was reduced to formate ($HCOO^-$) on nickel iron sulfides (e.g., Ni-doped greigite SFeS[Fe_3NiS_4]SFeS), and pyrophosphate converted the formate to carbon monoxide (CO).[150,235,236] At the same time, methane is argued to have been oxidized on iron(II)-rich fougèrite, trébeurdenite ($\sim Fe_2^{II}Fe_4^{III}(OH)_{10}CO_3{\cdot}3H_2O$), first to a methyl group ($-CH_3$) and then to formaldehyde (HCHO), the fougèrite having been oxidized to trébeurdenite by nitrate in the ocean. The formaldehyde was then reduced by hydrothermal hydrogen and the product thiolated to a methanethiol (CH_3SH).[149,150,237,238] The CO and the methanethiol were then assembled on a similar nickel iron sulfide in the membrane to produce thioacetate (CH_3COSCH_3), a substrate lying at the heart of autotrophic metabolism.[239] It is thought that even today hydrothermal chimneys composed of iron sulfide may facilitate electron transport through conductive chemical-garden type structures[240] and thus provide an energy source for chemolithotrophic microbial communities, i.e., those living off electrons derived from reduced inorganic minerals such as mackinawite (FeS).

8.2. Reconsideration as to What Constitutes Prebiotic Molecules

The study of chemical gardens frees us, as it did Leduc,[12] from assuming that organic molecules were the first requirement for life's emergence. While organic molecules would have been sparse, ill-sorted, and mostly inimical to early life, e.g., polyaromatic hydrocarbons and tars, the inorganic precipitates that make relatively durable semipermeable and semiconducting inorganic membranes at submarine alkaline hydrothermal springs in the Hadean would have been ubiquitous. These inorganic membranes would have comprised the kind of mixed-valence iron hydroxides and sulfides previously mentioned, dosed with nickel, cobalt, and molybdenum and minor phosphates, perhaps sitting in a dominantly silica and brucite ($Mg(OH)_2$) membrane. As we have argued above, the hydrogen, carbon, and nitrogen sources were hydrothermal hydrogen, methane, and ammonia and oceanic carbon dioxide and nitrate; the former being the electron donors and the latter the electron acceptors. These were the prebiotic molecules. Under this view, organic molecules were produced on site, with further energy contributed mainly by the ambient proton-motive force and redox gradients though augmented by the thermal gradient imposed across the precipitate membranes juxtaposing acidulous ocean with alkaline hydrothermal solution.[241] While the reduction of carbon dioxide to carbon monoxide through the consumption of an electrochemical gradient has been demonstrated,[222] the presumed oxidation of the methane produced through the serpentinization awaits experimental testing.

The question then arises: by what means were these organic molecules synthesized, given that many of the reductive steps from CO_2 to carboxylic, amino, and nucleic acids are endergonic? One answer, remarked on in section 8.1, is that some of the reductive work will have already been accomplished, though slowly, in the serpentinizing systems feeding the submarine hydrothermal springs. Then the methane produced through the serpentinization of ancient oceanic crust could have been oxidized to organic intermediates such as methanol (CH_3OH), formaldehyde (HCHO), and a methyl group ($-CH_3$) with nitrate (NO_3^-).[150] Experimental support for this view lies in the discovery that methane can be oxidized at room temperature by α-O in Fe-zeolites and released through the hydrolysis of (-Fe-OCH_3)α groups.[242] Interestingly, the α-oxygen is deposited in the zeolite through the decomposition of N_2O at 230 °C.[242] At the same time carbon dioxide may be reduced to formate or carbon monoxide.[237] Huber and Wächtershäuser[243] have assembled an acetyl complex, the basic molecule of metabolism, from carbon monoxide and a thiolated methyl group. Further steps in metabolism can be achieved through aminations and condensations.[244−246]

The way any of these uphill reactions progress in living cells is through the tied coupling with exergonic reactions through enzymes or nanoengines. Those that spring readily to mind are the rotary ATPase, Complex 1, and the methylcoenzyme M reductase engine. The first has been likened to a Wankel engine, the second to a steam engine, and the third to a two-stroke.[247−249] But how could engines, no matter how simple, materialize in a chemical-garden membrane? Two ready-made engines have been suggested.[209,234] The first, situated toward the membrane interior, coupling endergonic with exergonic redox reactions, involves molybdenum, a metal, when ligated to sulfur plus or minus oxygen, with the propensity to be involved in two electron transfer.[237] In certain conditions molybdenum can bifurcate electrons, losing one to a high-potential electron acceptor (e.g., nitrite) while the other is lost to a low-potential acceptor (e.g., CO_2 and methanol).[150,250,251] Such dependency is very much part of life as we know it today, which uses not only molydopterins for such a gambit but can use tungsten in its place at higher temperatures and has invented organic molecules such as quinones and flavins to do the same trick.[250,252] The second, comprising the membrane exterior, is speculated to be green rust or fougèrite.[209,226] This mixed-valence layered oxyhydroxide can expand somewhat when oxidized as the iron(III) atoms repel each other, thus attracting higher charged counterions in place of hydroxide such as orthophosphate. Thus, trapped in a low-entropy site in the interlayer it could be induced to condense to pyrophosphate, driven both chemically by the steep (~5 pH units) proton gradient operating across the membrane and the pyrophosphate then driven toward the interior. Both putative systems are engines in that they only work when tightly coupled to, are dependent upon, exergonic reactions.[234] Such speculations require experimental tests. Nevertheless, it is notable that the chemical reactants called upon in this theory, hydrothermal hydrogen and methane, are both used as fuels by a strain of a single species of *Methanosarcinales* at Lost City.[253] Moreover, nitrite may be the electron acceptor and acetate is emitted as a waste product.[254]

The vision we have outlined reminds one of Leduc's conclusion in *The Mechanism of Life*:

DOI: 10.1021/acs.chemrev.5b00014
Chem. Rev. XXXX, XXX, XXX−XXX

"During these long ages an exuberant growth of osmotic vegetation must have been produced in these primeval seas. All the substances which were capable of producing osmotic membranes by mutual contact sprang into growth, the soluble salts of calcium, carbonates, phosphates, silicates, albuminoid matter, became organized as osmotic productions, were born, developed, evolved, dissociated, and died. Millions of ephemeral forms must have succeeded one another in the natural evolution of that age, when the living world was represented by matter thus organized by osmosis".[12]

8.3. Toward the Origin of Life

What would it take for a Hadean submarine chemical garden to spawn life? Could the chemistry and the chemical and electrochemical gradients driving proton fluxes inward and electron fluxes outward across the walls of such a garden eventually lead to the emergence of biosynthesis, and could this be demonstrated in the lab?[255] The minerals comprising the walls do have structures affine with protoenzymes and there is now some encouraging evidence that two of these, the iron−nickel sulfides and the iron oxyhydroxides, can be coerced into acting, albeit rather inefficiently, as redox and condensation catalysts to drive the endergonic reactions that stand at the gates of an autotrophic metabolic pathway. Using violarite ($FeNi_2S_4$) as the catalyst, Yamaguchi et al.[222] have demonstrated the electrolytic reduction of CO_2 to CO in a reaction that opens the gate to autotrophic metabolism. Violarite has a comparable structure to that of the active center of carbon monoxide dehydrogenase (CODH), the enzyme that does the same job in the acetyl co-A synthase pathway. However, the reduction required an electrochemical boost or overpotential of around 200 mV. These authors account for this requirement by appealing to the ambient proton motive force of three to four pH units which is equivalent to this voltage. It is notable that the efficiency of the catalyst was substantially improved when it was chelated with amines, as in the enzyme itself. The next requirement is for a methyl group to react with the CO to form activated acetate. As we have seen, this reaction has been achieved at high yield by Huber and Wächtershäuser[243] using an FeS−NiS mixture. We surmise that the structure of these FeS−NiS clusters again approximated violarite, affine with the active center of the acetyl Co-A enzyme responsible for the same reaction in the acetogens. We have already suggested that the methyl group was derived through the oxidation of the hydrothermal methane, an idea that awaits experimental investigation.[150] Oxidized fougèrite, trébeurdenite, likely occupying the outer margins of the chemical garden wall, is the candidate catalyst.[256] This form of fougèrite is also stabilized by organic chelates, in this case organic acids.[257] The oxidation of reduced fougèrite involves the eight-electron reduction of nitrate all the way to ammonium.[227,258] Here again we can recall the experimental demonstration of the amination of certain carboxylic acid with ammonium salts dissolved in alkaline solution and catalyzed equally well by both iron sulfide and iron hydroxide.[244]

So, what is missing from this plan? Now we enter much more speculative ground. We know that life depends on an internal free energy currency involving the phosphate−phosphate bond; these days mainly as ATP. Pyrophosphate was the presumed precursor, driven very far from equilibrium from its hydrolysis products.[259] Proton pyrophosphatase has been advanced as the first mechanical enzyme to achieve this disequilibrium, driven again by the ambient proton motive force. The structure of this enzyme has now been elucidated.[260,261] Constructed from protein loops and trans-membrane helices, it is thought to sequester two orthophosphates along with a proton and then disgorge the pyrophosphate into the cytoplasm.[209] Green rust has been called upon as the precursor here too. However, though experiments to date have demonstrated some condensation, they have failed to show the generation of a strong pyrophosphate-to-orthophosphate disequilibrium.[62]

An even more challenging expectation is a demonstration of a prebiotic mechanism for redox bifurcation involving the separate transfer of two electrons from entities that are most stable in their fully oxidized or fully reduced forms. Life commonly uses this gambit to drive otherwise endergonic reductions with even larger exergonic ones.[250,251] Although organic enzymes are commonly used to expedite such bifurcations, molybdenum is (still) used for the most recalcitrant.[237] Thus, we assume this element, somehow ligated in sulfide and/or oxide clusters, was brought to bear on particularly difficult reactions at the onset of life. For example, carbon dioxide must be activated before it can be reduced to carbon monoxide, a probable added condition to the ambient proton motive force alluded to above.[149] This requires a high-energy electron which could be delivered endergonically if, and only if, another electron is released exergonically at the same time as molybdenum transitions directly from the Mo(IV) to the Mo(VI) state. Nitrate in the early ocean offers itself as the high potential electron acceptor.[262]

Difficult though these experimental tests will be, there are grounds for confidence that a probiotic pathway from CO_2, H_2, CH_4, and NO_3^- to activated acetate, the entry point to the incomplete reverse tricarboxylic acid cycle and thereby autotrophic metabolism, will be demonstrated in chemical-garden walls in the next few years. This endeavor will call upon the careful study of anionic, cationic and proton flow in channels through chemical-garden membranes and their analogs, perhaps involving microfluidics.[255,263−265] At the same time the likely circuits of electron conduction and bifurcation along the semiconducting minerals comprising the membrane will need to be mapped.[255]

8.4. Brinicles: Chemical Gardens in Sea Ice

Brinicles are hollow tubes of ice that grow downward from the bottom of the sea ice floating in the polar oceans (Figure 44). They are formed when a stream of cold and dense brine is ejected from the ice into the sea, freezing seawater around itself. They can be considered as a form of inverse chemical garden, as the density difference in this case is causing the tube to grow downward (Figure 45).

The filtering mechanism in the case of brinicles is the ice pack itself, through the process known as brine rejection. As air temperature drops during the Antarctic winter, heat flows from the water, through the ice, out to the atmosphere. This causes ice platelets to form in the water, which immediately float upward and add to the ice sheet. The aggregation of such platelets forms a porous mass of ice soaked in seawater, known as the skeleton layer. The water trapped within this layer will continue to freeze as heat continues to flow, increasing its salt concentration and density. For this reason the skeleton layer, which behaves as a mushy layer with a typical pore size small enough initially to prevent density driven convection, can be interpreted as an inverse semipermeable membrane which filters out water molecules and increases the concentration of the solution trapped inside, the brine.[266] Eventually, this brine becomes sufficiently dense to convect downward through the ice layer.

DOI: 10.1021/acs.chemrev.5b00014
Chem. Rev. XXXX, XXX, XXX−XXX

Figure 44. Brinicle found under the ice pack in the Antarctic ocean. Typically they are centimeters to meters long. Image courtesy of Rob Robbins.

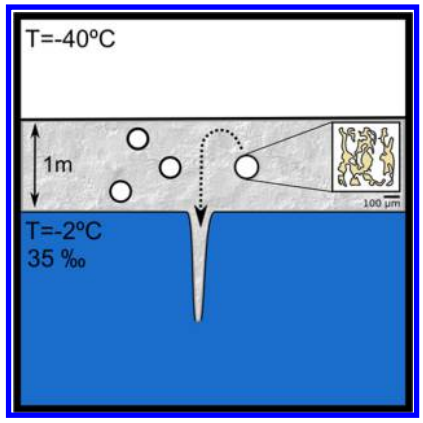

Figure 45. Cross section through sea ice illustrating brinicle formation. The temperature in the ice is defined by a gradient between the temperatures of the air and the sea. The brine inside the ice is siphoned through the channel network and ejected through a single opening, forming a tubular brinicle. Reprinted with permission from ref 268. Copyright 2013 American Chemical Society.

Below the ice, it flows downward freezing the seawater around itself and forming a hollow tube of ice through which brine flows, a brinicle.[267] The appearance of such a structure seems to affect the way brine migrates within the ice pack. It creates a siphon effect which ensures constant flow and can drain hundreds of liters of brine coming from multiple entrapments connected by a network of microscopic brine channels.[268] Without this effect, most of the brine could remain trapped within the ice until temperatures rose again in the summer.

Salt concentration in brine entrapments increases by 10% per °C of cooling. However, this is also true for every other chemical compound found in seawater, and enrichment of compounds is one of the conditions for the emergence of life. The origin of life is commonly placed in a hot environment, such as hydrothermal vents, but there is also a well developed theory placing the origin of life in a cold environment like sea ice.[269,270] Apart from the enrichment of compounds, sea ice also meets all other conditions that are generally considered necessary for the emergence of life on our planet. The inner walls of brine entrapments are coated by lipids that could form a primitive membrane. In the oceans today these lipids are produced by extracellular polymeric substances generated by phytoplankton,[271] but could also be produced by complex prebiotic molecules. As an energy source, there are electric potentials and pH gradients across the interface between ice and brine, as well as UV radiation coming from the Sun. Furthermore, the surface of ice has been proven to have catalytic effects.[270]

The fact that brinicles influence the fluid dynamics of brine within the ice might imply that they also play a role in this scenario of a cold origin of life on "icy worlds",[272−275] just as hydrothermal vents do in the hot environment theories.

9. INTELLECTUAL CHALLENGES AND RESEARCH OPPORTUNITIES

As we have seen, chemical gardens are not a new subject but, on the contrary, one of the oldest in chemistry. Now, at the beginning of the 21st century, chemical gardens may be viewed in their rightful place at the interface of chemistry, fluid dynamics, and materials science as perhaps the best example in chemistry of a self-organizing nonequilibrium process that creates complex structures. With the aim of defining the field at this intersection, we have suggested the term chemobrionics. From the Greek khemia, the "art of transmuting metals", from which we obtain chemistry, we have the prefix chemo-, to which we have added, also from the Greek, bruein "swell", or "grow", which gives us -brionics, the idea of growing structures, swelling under osmotic pressure.

In classical chemical gardens the motive force is endogenous: osmotic and buoyancy forces arise from within the system. But one can break the system down into components: instead supply an exogenous motive force by pumping the system externally, and thence obtain the same pattern formation, tubes, vesicles, and so on, as in the endogenous case. One can also isolate just the wall of the system, by producing a semipermeable membrane within an unglazed porcelain pot or about a dialysis membrane. What then constitutes, precisely, a chemobrionic system? We propose to define a chemobrionic system as the self-organization of a semipermeable membrane of some sort, about which steep concentration gradients may be formed and maintained by osmosis. Self-assembled semipermeable membranes are the common link between all systems we have described, from silicates to polyoxometalates, from corrosion tubes to Portland cement, and from hydrothermal vents to brinicles. Chemobrionics, then, is essentially the study of systems possessing these self-assembled semipermeable membranes.

9.1. How Can We Make Experimental, Computational, and Theoretical Progress in This Field?

Chemobrionic processes are varied and applicable to many disciplines; specific systems and properties are being studied in fields including geology, planetary science, astrobiology, biology, materials science, catalysis, etc. Researchers from these disciplines generally do not communicate with one another and there is not yet the general knowledge that these phenomena are all very interrelated; of course, in part this problem is being addressed with this review. Understanding that chemical-garden phenomena can give rise to such a wide array of systems may help

DOI: 10.1021/acs.chemrev.5b00014
Chem. Rev. XXXX, XXX, XXX−XXX

us to understand the fundamental principles that underly these processes.

One of the questions that hinders computational and theoretical progress in the understanding of chemical-garden complexity is that experiments are still typically performed in 3D reactors and the structures result from a combination of precipitation reactions, buoyancy, osmosis, and mechanical effects. The modeling of each of these processes separately is already not trivial, and analyzing their interplay in 3D is a daunting task from both theoretical modeling and numerical perspectives. From experience with experiments we know that some aspects of chemical-garden growth are reproducible and some seem random, and it is hard to determine what factors control each part. To move forward in this regard we must move from the classical seed growth setup to experimental setups in which one aspect or another is constrained, suppressed, or controlled. For instance, buoyancy and composition of the reactants can be controlled by injecting one solution of the metallic salt into the other solution or vice versa to produce a single tube. This allows the classification of the dynamics in a parameter space spanned by controlled parameters like the injection speed and concentrations of the reactant solutions. Using quasi-2D geometries further reduces the number of spatial degrees of freedom and the numerous tools of analysis of 2D patterns developed in nonlinear science can be used to obtain generic information on the patterns.

9.2. What Are the Most Important Research Questions in Chemobrionics Today?

We suggest the following selection:

Can We Predict Which Reactions Will Produce Chemical Gardens? Many precipitation reactions, or phase-change induced reactions, can potentially form a chemical garden; it is a matter of structural stability plus semipermeability. This is a complex question involving elements of both chemistry and materials science; the chemical reaction must produce a material of the right characteristics to form a membrane that has some degree of semipermeability.

What Is the Nature of the Traveling Reaction Zone? Can we understand this complex phenomenon involving the interaction of fluid advection with mass and heat transport and chemical kinetics?

Can We Make Progress with Mathematical Modeling? We need more theoretical work to be able to predict aspects of chemical-garden formation like tube width, flow velocity, etc., as we have discussed in section 6.

How Small Can We Go? We would guess at least to the biological cellular scale; cell membranes operate under some of the same energetic principles as chemical gardens, and it is possible to grow micrometer-scale osmotic inorganic membrane structures.

Are There Organic Gardens? It is possible to trap organics within a chemical garden. There are also driven reactions of organics inside a chemical-garden wall. Probably there could exist purely organic chemical gardens; they need to be looked for. Of course life itself might be considered an organic chemical garden, in the sense pointed out just above.

How Far Can We Go with the Manipulation of Tube Growth? This manipulation is now well-established; see sections 3.3 and 7.4. But can one arrive at a viable technology based on such control of tube growth?

Were Natural Chemical Gardens the Hatchery of Life? The next few years should provide us with an answer to this question, though it will require a concerted effort by many researchers given to an exhaustive and detailed research into the energetics, mechanisms, and pathways involved, as we have earlier discussed (section 8.3).

9.3. What Are the Possibilities for Technological Applications?

From a technological perspective, chemobrionics can be used to learn about chemical systems that in some ways mimic biological systems and, if these systems are mastered, may lead to the development of new self-assembling technologies that could operate from nanometer to meter scales. The richness and complexity of these chemical motors and chemical batteries, and the fact that they emerge from simple, mostly two-component chemical systems, indicates that their formation is an intrinsic property of the specific chemical systems.

By simply changing concentrations or reactants or other experimental parameters we may arrive at a collection or library of these chemical "engines". By expanding on the self-assembling nature of these out-of-equilibrium chemical systems, we may eventually be able to form larger functioning structures. One of the main challenges is to control the morphology, size, and thickness of these structures. Related to this, another important challenge and a great technological development opportunity is the application of micro- or nanoprobes to analyze chemical compositions of internal and external fluids, microelectrical potentials, fluid dynamics, and thickness of layers.

In overcoming these challenges, a great research opportunity can be opened to produce homogeneous and tailored microtubes for industrial applications. However, for these last opportunities to become possible, it will be necessary to overcome another challenge, that is to modify these structures in order to improve their plasticity and mechanical strength.

Here are some possible technological applications:

Organic and Biomaterials. It is a challenge to extend chemical gardens to organic and mixed inorganic−organic chemobrionic systems. This can open a great opportunity to create nanostructures for biomaterials with high biocompatibility with living cells and tissues. Chemical gardens may also be worth considering with regard to selective adsorption−desorption processes with interest, for example, for the slow release of drugs.

Electrochemistry. The electrochemical properties of self-assembling chemobrionic membranes are poorly understood and further studies of these phenomena in laboratory experiments will help us understand the larger-scale energy generation that occurs in natural chemical-garden systems. There may be technological applications to fuel cells.

Catalysis. Chemical gardens are controlled crystal growth at an interface, not unlike electroplating material onto a surface or growing thin solid films. Taking into account that chemical-garden micro- or nanotubes can have reactive internal surfaces with chemical and adsorption properties, these structures can have interesting applications as nanocatalysts or nanosupport for catalysts.

Gas Exchange. The porosity and the large surface area of these tubes could be considered advantageous for selective absorption−desorption of gaseous pollutants and gas exchange processes. For these potential applications, other challenges should be overcome, such as the necessary mechanical properties, plasticity, and morphology control.

Microfluidics, Controlled Branching, and Tubular Networks. If we can control branching in chemical-garden tubes, we can construct tubular microfluidic networks for fluid

DOI: 10.1021/acs.chemrev.5b00014
Chem. Rev. XXXX, XXX, XXX−XXX

processing, mixing, and so on. Already we are progressing toward this goal, as we have discussed in section 7.4.

Sensors and Filtration. Semipermeable membrane materials are of great interest for many applications and chemical gardens have already been shown to exhibit size exclusion properties. Choice of starting components, or incorporation of functional molecules, in these soft materials could open new avenues in hybrid membrane research for small-molecule sensing or filtration.

Chemical Motors. Chemical motors may be defined as structures that move using chemical reactions to produce the required energy. In chemical gardens the motors first self-construct spontaneously, and then they may move in many different modes. Examples of the motion include linear translation, rotation, periodic rupturing, periodic buoyancy oscillations, periodic waving or stretching of the entire structure, and periodic ejection of complex tubes.

Back to Cement. The application of chemical-garden ideas to cement has lain mostly dormant since a burst of activity from the 1970s to the 1990s. With fresh insights and new analytical techniques available today, determined researchers could make a large contribution to this subfield.

Complex Materials. A possible outcome of experiments where one reactant solution is injected into the other one at given concentrations is to be able to control the composition and structures of the precipitates and crystals formed. For instance, layered or complex materials could be synthesized upon successive injection of solutions of different composition. This provides a route to the formation of complex materials.

9.4. Coda

Despite nearly four hundred years of research on chemical gardens, major aspects of the underlying chemistry and physics are still not understood. Since the turn of the millennium, research activity in this field has steadily increased, and is returning to questions that were considered in much earlier work. For these reasons, we consider that now is an ideal time to review this progress comprehensively, as we aim to have done here. We hope that this review will act as a catalyst for further research in this area that is likely to branch out quickly covering sophisticated modeling efforts, novel materials including organic and polymeric compounds, research into life's origins, as well as technological applications of chemical gardens. For this reason we have suggested the new, broader term for the field of chemobrionics. Lastly, we hope that our review will also be a valuable resource for chemical educators and advanced students who want to learn about this widely known yet imperfectly understood system from a contemporary and scientifically rigorous point of view.

AUTHOR INFORMATION

Corresponding Authors

*E-mail: julyan.cartwright@csic.es.
*E-mail: steinbck@chem.fsu.edu.

Notes

The authors declare no competing financial interest.

Biographies

Laura Marie (Laurie) Barge (Laura.M.Barge@jpl.nasa.gov) studied astronomy and astrophysics at Villanova University and then received her Ph.D. in geological sciences from the University of Southern California. For several years she was a Caltech Postdoctoral Scholar and currently she is a NASA Astrobiology Institute postdoctoral fellow at the NASA Jet Propulsion Laboratory in Pasadena, California. Her research focuses on understanding how self-organization in chemical and geological systems can lead to the emergence of pattern formation, organic chemistry, and energetic processes. Previously she studied Liesegang banding and the influence of organics on inorganic crystal growth, including simulating the formation of self-nucleating concretions in geological systems. Now, as an astrobiologist, she works on understanding how the first biological processes are related to and could have emerged from inorganic self-organizing systems, and how this can help us understand whether life could have emerged on other worlds.

Silvana S. S. Cardoso (sssc1@cam.ac.uk) is a Reader in the Department of Chemical Engineering and Biotechnology, University of Cambridge, U.K. With a background in chemical engineering and applied mathematics, her expertise is in experimental and theoretical fluid mechanics, focusing on the interaction of natural convection and chemical kinetics. Her current research interests include the effects of buoyancy and chemical changes in turbulent plumes and thermals and in flows in porous media. Important applications include the flow of methane and carbon dioxide in the Earth's subsurface and in the oceans.

DOI: 10.1021/acs.chemrev.5b00014
Chem. Rev. XXXX, XXX, XXX−XXX

Julyan H. E. Cartwright (julyan.cartwright@csic.es) is a physicist interested in understanding the emergence of structure and pattern in nature. He has been studying mechanisms and processes of pattern formation, self-organization, and self-assembly in numbers of different natural systems. He first played with chemical gardens as a boy and is still playing with them today.

Geoff J. T. Cooper (Geoff.Cooper@glasgow.ac.uk) studied at the University of Birmingham and then moved to the University of Glasgow for a Ph.D. position in 2002. He worked as a postdoctoral researcher at the Leiden Institute of Chemistry, The Netherlands, before returning to Glasgow and is currently a senior postdoctoral research associate in the Cronin group at the University of Glasgow. His research interests include complex systems chemistry and inorganic biology, specifically the study and manipulation self-organizing or self-growing materials towards their possible uses in microdevices.

Leroy (Lee) Cronin FRSE. (Lee.Cronin@glasgow.ac.uk) Professional Career: 2013, Regius Professor of Chemistry. Alexander von Humboldt research fellow (Uni. of Bielefeld); 1997−1999, Research fellow (Uni. of Edinburgh); 1997, Ph.D. Bio-Inorganic Chemistry, Uni. of York; 1994, BSc. Chemistry, First Class, Uni. of York. Prizes include 2013 BP/RSE Hutton Prize, 2012 RSC Corday Morgan, 2011 RSC Bob Hay Lectureship, a Wolfson-Royal Society Merit Award in 2009, Election to the Royal Society of Edinburgh in 2009. The focus of his work is understanding and controlling self-assembly and self-organization in Chemistry to develop functional molecular and nanomolecular chemical systems, linking architectural design with function, and recently engineering system-level functions (e.g., coupled catalytic self-assembly, emergence of inorganic materials and fabrication of inorganic cells that allow complex cooperative behaviors). Much of this work is converging on exploring the assembly and engineering of emergent chemical systems aiming towards "inorganic biology". This work has been presented in over 250 papers and 220 lectures worldwide. It is also worth pointing out that the expertise in the Cronin group is unique bringing together inorganic chemists, chemical engineers, complex system modeling, evolutionary theory, robotics, and AI.

Anne De Wit (adewit@ulb.ac.be) is Professor in the Chemistry Department of the Université libre de Bruxelles. Her Ph.D. has focused on modelling reaction-diffusion patterns in particular 3D Turing structures and Turing-Hopf dynamics. She went next as a postdoc to Stanford University to perform research on simulations of transport and fingering instabilities in porous media. Back in Brussels, she now heads the Nonlinear Physical Chemistry Research Unit, in which both experimental and theoretical work is performed in the field of chemo-hydro-dynamics. Her research focuses on analysing which spatiotem-poral dynamics and patterns can develop when chemical reactions and hydrodynamic instabilities interplay. Her objective is to achieve a chemical control of convective flows with applications in carbon dioxide sequestration and mineralization or oil recovery to name a few. Recently, she has focused on analysing the complex precipitate patterns obtained when chemical gardens are grown in confined quasi-two-dimensional geometries.

DOI: 10.1021/acs.chemrev.5b00014
Chem. Rev. XXXX, XXX, XXX−XXX

Ivria J. Doloboff (ijdoloboff@gmail.com) is a graduate of California State University, Long Beach. She has spent the first four years of her scientific career at NASA Jet Propulsion Laboratory in Pasadena, CA. Her research in the Planetary Science and Astrobiology section focuses on developing experimental methods to understand how self-organizing systems, in chemical gardens and electrochemical fuel cells, can help facilitate an understanding of the emergence of life in inorganic systems on wet rocky worlds.

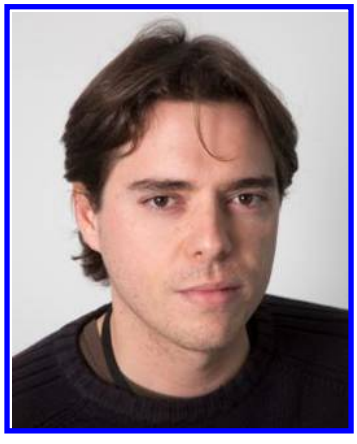

Bruno Escribano (bescribano@bcamath.org) studied physics at the Universidad Autonoma of Madrid and later moved to Granada where he obtained his Ph.D. at the Andalusian Institute of Earth Sciences. He is currently working at the Basque Center for Applied Mathematics in Bilbao. His research is focused on pattern formation and self-organization in geophysics. He is interested in chemical gardens as a useful model to simulate many other systems which are difficult to study in practice and in particular for their role played in the emergence of life on our planet.

Raymond E. Goldstein FRS (reg53@damtp.cam.ac.uk) is the Schlumberger Professor of Complex Physical Systems at the University of Cambridge. With a background in chemistry, physics, and applied mathematics his primary research areas involve theoretical and experimental studies of biological physics, with occasional forays into problems of natural pattern formation. Before moving to Cambridge he worked closely with then Ph.D. student David Stone on problems of precipitative pattern formation ranging from the growth of tubular electrochemical structures and Liesegang patterns to the shapes of stalactites and icicles.

Florence Haudin (florence.haudin@univ-paris-diderot.fr) is a physicist specializing in nonlinear dynamics. She has performed an experimental Ph.D. thesis on the dynamics of localized states and fronts in nonlinear optics of liquid crystals at the University of Nice. She currently works in the field of hydrodynamics. She is interested in interfacial phenomena like the formation of bubbles in complex fluids or the development of instabilities in miscible displacements (buoyancy-driven or viscous fingering instabilities). She has also been analyzing experimentally at the Université libre de Bruxelles spatiotemporal patterns and dynamics obtained when growing chemical gardens by injection in a Hele-Shaw set up. She is now working on surface waves at the University Paris Diderot.

David E. H. Jones (davidjones9@googlemail.com) obtained his chemical Ph.D. at Imperial College, the University of London. He is perhaps best known for the weekly "Daedalus" column, which was seldom serious but always scientifically well-informed. He wrote it from 1964 to 2002, first in *New Scientist* and after 1988 in *Nature* and the British newspaper *The Guardian*. (Thus Daedalus proposed the hollow carbon molecule before buckminsterfullerene was made, and long before its synthesizers won a Nobel prize.) From 1969 to 1972 he worked at the

DOI: 10.1021/acs.chemrev.5b00014
Chem. Rev. XXXX, XXX, XXX−XXX

chemical Corporate Laboratory of ICI Ltd, where he developed the modern theory of the bicycle. Later he researched as a guest staff member of the Chemistry Department of the University of Newcastle upon Tyne. His most interesting study there was perhaps the determination of arsenic in Napoleon's wallpaper. It was at this University that he constructed the chemical-garden apparatus which Dr. Walter operated in the Space Shuttle. His publications include both formal scientific papers, and popular items such as his recent book *The Aha! Moment*.

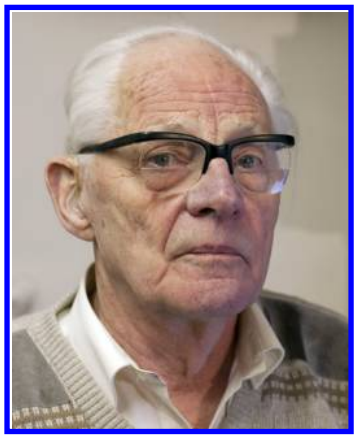

Alan L. Mackay FRS (alanlmackay@gmail.com) is a crystallographer. He spent his scientific career at Birkbeck College, where he was immersed in a liberal scientific atmosphere under the leadership of John Desmond Bernal. In 1962 he published a manuscript that showed how to pack atoms in an icosahedral fashion; a first step towards five-fold symmetry in materials science. These arrangements are now called Mackay icosahedra. In 1981 he predicted quasicrystals in a paper entitled "De Nive Quinquangula" in which he used a Penrose tiling in two and three dimensions to predict a new kind of ordered structure not allowed by traditional crystallography. In a later work, in 1982, he took the optical Fourier transform of a 2-D Penrose tiling decorated with atoms, obtaining a pattern with sharp spots and five-fold symmetry. This brought the possibility of identifying quasiperiodic order in a material through diffraction. Quasicrystals with icosahedral symmetry were found shortly thereafter. Mackay has been interested in a generalized crystallography, which can describe not only crystals but also more complex structures and nanomaterials.

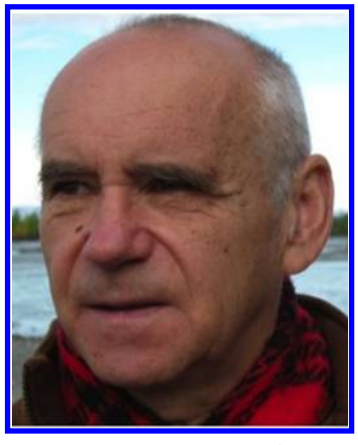

Jerzy Maselko (jmaselko2@uaa.alaska.edu) is a professor of Chemistry at the University of Alaska, Anchorage (UAA). He obtained his Ph.D. in Inorganic Chemistry from the Technical University, Wroclaw, Poland. Starting from 1982 he worked with the groups of Irving Epstein, at Brandeis University U.S.A., Harry Swinney, at the University of Texas, Austin, and Ken Showalter at the University of West Virginia, Morgantown. His scientific interests are complex chemical systems, the origin of life, artificial life, and chemobrionics.

Jason J. Pagano (jpagano@svsu.edu) obtained his B.S. degree in Biochemistry at the State University of New York at Oswego in 1997. He received his M.S. degree in Chemistry from the same institution in 1999. His Masters Research Project was entitled "The Mobility of Heavy Metals on a Synthetic Soil Liquid Chromatograph Support" under the supervision of Professor Jeffery A. Schneider. Following this he worked as a Chemistry Laboratory Coordinator at Daytona Beach Community College during 2000−2002. He completed his Ph.D. in Chemistry at Florida State University in 2008 under the supervision of Professor Oliver Steinbock. The title of his dissertation was "Growth Dynamics and Composition of Tubular Structures in a Reaction-Precipitation System." Currently he is a faculty member in the Department of Chemistry at Saginaw Valley State University (SVSU) Michigan. His research interests include nonlinear dynamics in chemical systems and chemobrionics.

James (Jim) Pantaleone (jtpantaleone@uaa.alaska.edu) is a Professor of Physics at the University of Alaska, Anchorage (UAA). He received his Ph.D. in Theoretical Physics from Cornell University in 1985 and has held postdoctoral positions at Purdue University, the University of California Riverside, and Indiana University before arriving at UAA in 1994. For many years he worked in the area of particle physics phenomenology, especially the dynamics of neutrino oscillations in matter. His current interests include fluid dynamics and its influence on pattern formation in chemical systems.

DOI: 10.1021/acs.chemrev.5b00014
Chem. Rev. XXXX, XXX, XXX−XXX

Michael J. Russell (michael.j.russell@jpl.nasa.gov) began work in an East London chemical factory, improving nickel catalysts for hydrogenating phenols to cyclohexanols. A degree in geology, with organic chemistry and ancillary physics, led to prospecting for the same metal, along with copper and gold, in the Solomon Islands. While there he also investigated volcanic solfataras, acidic hydrothermal vents, sedimentary iron formations, and gauged eruptive hazard; thence to British Columbia searching for molybdenum, the Yukon for silver, and then to Ph.D. research into the genesis of zinc−lead ore deposits in Ireland. Here, in the mines, he and his students found 350 million year old hydrothermal chimneys, accompanying fossil worms and associated natural chemical gardens comprising metal sulfides. These experiences and discoveries, augmented by research into magnesite deposits and their alkaline hydrothermal feed sourced from serpentinized ophiolites in the Alps, formed the foundations to the submarine alkaline theory for the emergence of life.

C. Ignacio Sainz-Díaz (ignacio.sainz@iact.ugr-csic.es) obtained his Ph.D. in organic chemistry from the University of Alcalá de Henares (Madrid, Spain). After several years in research centres of the chemical industry and European centres, he moved to a CSIC (Spanish Research Council) institute in Granada, Spain. Since 2004 he is a member of the Instituto Andaluz de Ciencias de la Tierra (IACT, CSIC-UGR) as a senior researcher. His research interests include organic−inorganic interatomic interactions in crystals and on the surface of solids, crystal growth, biomineralization, crystal polymorphism, and infrared and Raman spectroscopy of organic molecules, crystal structures and minerals. His multidisciplinary research includes experimental work and atomistic calculations at a quantum-mechanical level of organic molecules and crystal structures.

Oliver Steinbock (steinbck@chem.fsu.edu) studied at the Georg August University, Göttingen and the Max Planck Institute for molecular Physiology, Dortmund. He received his doctoral degree in 1993, was a postdoctoral fellow at the West Virginia University, and a research scientist at the Otto von Guericke University, Magdeburg. Since 1998 he has been a faculty member at the Florida State University (FSU) and since 2012 Cottrell Professor of Chemistry. Recently he was a guest scientist at the Max Planck Institute for Dynamics and Self-Organization. He held a scholarship of the German National Merit Foundation (Studienstiftung des deutschen Volkes), a Liebig Fellowship of the Fund of German Chemical Industry (FCI), and received several awards and honors including the Friedrich Wilhelm Bessel Research Award of the Alexander von Humboldt Foundation and FSU's University Teaching Award. He is also a Fellow of the American Association for the Advancement of Science (AAAS). Dr. Steinbock's research focuses on the self-organization of reaction systems far from the thermodynamic equilibrium. He investigated problems as diverse as chemotactic cell motion, complex reaction mechanisms, nonlinear waves in autocatalytic systems, three-dimensional vortices in reaction-diffusion media, and applications of chemical self-organization to materials science.

David A. Stone (dajstone@gmail.com) received his Ph.D. in environmental chemistry from the University of Arizona under Joan Curry. There he also worked extensively in Ray Goldstein's physics lab on chemobrionics, specifically on novel tubular precipitation and Liesegang bands in iron-based systems. He did postdoctoral study on the incorporation of arsenic into iron carbonate. His subsequent research has focused on iron corrosion processes and the controlled precipitation of iron minerals within multicomponent pastes. This led to a discovery of a novel iron carbonate binder for which a U.S. patent was

DOI: 10.1021/acs.chemrev.5b00014
Chem. Rev. XXXX, XXX, XXX−XXX

awarded. Currently he is the research director of an effort to commercialize this binder as a substitute for Portland cement in some applications. This material technology recycles solid wastes such as steel dust while capturing CO_2 and generating hydrogen during the curing stage.

Yoshifumi Tanimoto (yt1112@hiroshima-u.ac.jp) studied at Hiroshima University, Hiroshima, and the University of Tokyo, Tokyo, and received his Ph.D. degree from the University of Tokyo in 1974. He worked at Kanazawa University, Hiroshima University, the Institute for Molecular Science, and Osaka Ohtani University before his retirement in 2012. He is Professor Emeritus of Hiroshima University and Honorary Professor at Orenburg State University, Orenburg, Russia. Currently he is a visiting scientist at the Institute for Amphibian Biology, Hiroshima University. His main interest is in magnetic field effects in chemical reactions and physical processes of dia- and para-magnetic materials and the biological effects of magnetic fields.

Noreen L. Thomas (N.L.Thomas@Lboro.ac.uk) is a Reader in polymer science and technology at the Department of Materials, Loughborough University, U.K. Her research is currently focussed on biodegradable and bioderived polymers, nanotechnology, and nanofibers. She started work on chemical gardens during the period 1979−1982 when, as a junior research fellow at Oxford University, she had the privilege of working with David Double on cement hydration mechanisms.

ACKNOWLEDGMENTS

We thank Shawn McGlynn, Paul Davies, and Fabian Brau for useful discussions. We acknowledge the U.S. National Science Foundation, Grants CHE-0608631 and DMR-1005861, the Spanish Ministerio de Ciencia e Innovación Grant FIS2013-48444-C2-2-P, and the Andalusian PAIDI group Grant RNM363. L.M.B., I.J.D., and M.J.R.'s research was carried out at the Jet Propulsion Laboratory, California Institute of Technology, under a contract with the National Aeronautics and Space Administration with support by the NASA Astrobiology Institute (Icy Worlds). We acknowledge useful discussions within the NAI-sponsored Thermodynamics Disequilibrium and Evolution Focus Group. This review has emerged from the discussions held at the Lorentz Center workshop on Chemical Gardens, 7−11 May 2012, Leiden organized by Julyan Cartwright, Michael Russell, and Oliver Steinbock; we thank the Lorentz Center staff for their wonderful support.

REFERENCES

(1) Glauber, J. R. *Furni Novi Philosophici*; Amsterdam, 1646; English translation by Christopher Packe, London, 1689.
(2) Newman, W. R.; Principe, L. M. *Alchemy Tried in the Fire: Starkey, Boyle, and the Fate of Helmontian Chymistry*; University of Chicago Press: Chicago, IL, 2005.
(3) Boyle, R. *Works*; vol. *13* c. 1650.
(4) Newton, I. *Of natures obvious laws & processes in vegetation*; c. 1675.
(5) Traube, M. Experimente zur Theorie der Zellenbildung und Endosmose. *Arch. Anat. Physiol.* **1867**, 87−165.
(6) Marx, K. *Letter to Pyotr Lavrov*, 1875.
(7) Engels, F. *Dialectics of Nature*, 1883.
(8) Pfeffer, W. *Osmotische Untersuchungen*; 1877; English translation *Osmotic Investigations*; Van Nostrand Reinhold: New York, 1985.
(9) Morse, H. N. *The Osmotic Pressure of Aqueous Solutions*; Carnegie Institute of Washington: Washington, 1914.
(10) Wald, G. How the theory of solutions arose. *J. Chem. Educ.* **1986**, *63*, 658−659.
(11) van't Hoff, J. H. Die Rolle des osmotischen Druckes in der Analogie zwischen Lösungen und Gasen (The role of osmotic pressure in the analogy between solutions and gases). *Z. Phys. Chem.* **1887**, *1*, 481.
(12) Leduc, S. *The Mechanism of Life*; Rebman: London, 1911.
(13) Herrera, A. L. *Nociones de Biología*; Imprenta de la Secretaria de Fomento: Mexico, 1903; facsimile ed., Universidad Autónoma de Puebla: Mexico, 1992.
(14) Zeleny, M.; Klir, J.; Hufford, K. D. Precipitation membranes, osmotic growths and synthetic biology. *Artificial Life, SFI Studies in the Sciences of Complexity* **1988**, 125−139.
(15) Thompson, D. W. *On Growth and Form*, 2nd ed.; Cambridge University Press: Cambridge, U.K., 1942.
(16) Mann, T. *Doktor Faustus*; Bermann-Fischer: Stockholm, 1947.
(17) Sacks, O. *Uncle Tungsten*; Vintage Books: New York, 2001.
(18) Loeb, J. *The mechanistic conception of life: biological essays*; The University of Chicago Press: Chicago, 1912.
(19) Copisarow, M. The Liesegang phenomenon and stratification. *J. Chem. Soc.* **1927**, 222−234.
(20) Eastes, R. E.; Darrigan, C. Jardins chimiques. *La Recherche* **2006**, *400*, 90−97.
(21) Bernal, J. D. *The Origin of Life*; World: Cleveland, OH, 1967.
(22) Clunies Ross, W. J. Experiments with silicate of soda and observations thereon. *J. R. Soc. N. S. Wales* **1910**, *44*, 583−592.
(23) Hazlehurst, T. H. Structural precipitates: the silicate garden type. *J. Chem. Educ.* **1941**, *18*, 286−289.
(24) Damerell, V. R.; Brock, H. Colloidal gardens from sodium silicate. *J. Chem. Educ.* **1949**, *26*, 148.
(25) Eastes, R. E.; Darrigan, C.; Bataille, X. Recréer la vie? *Actual. Chim.* **2010**, *344*, 28−35.
(26) Coatman, R. D.; Thomas, N. L.; Double, D. D. Studies of the growth of "silicate gardens" and related phenomena. *J. Mater. Sci.* **1980**, *15*, 2017−2026.
(27) Cartwright, J. H. E.; García-Ruiz, J. M.; Novella, M. L.; Otálora, F. Formation of chemical gardens. *J. Colloid Interface Sci.* **2002**, *256*, 351−359.

DOI: 10.1021/acs.chemrev.5b00014
Chem. Rev. XXXX, XXX, XXX−XXX

(28) Dent Glasser, L. S. Sodium silicates. *Chem. Britain* **1982**, *18*, 33−39.
(29) Malusis, M. A.; Shackelford, C. D.; Olsen, H. W. Flow and transport through clay membrane barriers. *Eng. Geol.* **2003**, *70*, 235−248.
(30) Jones, D. E. H.; Walter, U. The silicate garden reaction in microgravity: A fluid interfacial instability. *J. Colloid Interface Sci.* **1998**, *203*, 286−293.
(31) Cartwright, J. H. E.; Escribano, B.; Khokhlov, S.; Sainz-Díaz, C. I. Chemical gardens from silicates and cations of group 2: a comparative study of composition, morphology and microstructure. *Phys. Chem. Chem. Phys.* **2011**, *13*, 1030−1036.
(32) Cartwright, J. H. E.; Escribano, B.; Sainz-Díaz, C. I. Chemical-garden formation, morphology, and composition. I. Effect of the nature of the cations. *Langmuir* **2011**, *27*, 3286−3293.
(33) Cartwright, J. H. E.; Escribano, B.; Sainz-Díaz, C. I.; Stodieck, L. S. Chemical-garden formation, morphology, and composition. II. Chemical gardens in microgravity. *Langmuir* **2011**, *27*, 3294−3300.
(34) Makki, R.; Al-Humiari, M.; Dutta, S.; Steinbock, O. Hollow microtubes and shells from reactant loaded polymer beads. *Angew. Chem., Int. Ed.* **2009**, *48*, 8752−8756.
(35) Ibsen, C. J. S.; Mikladal, B. F.; Jensen, U. B.; Birkedal, H. Hierarchical tubular structures grown from the gel/liquid interface. *Chem.—Eur. J.* **2014**, *20*, 16112−16120.
(36) Lüppo-Cramer, H. Kolloidchemie und Photographie. *Kolloid Z.* **1911**, *9*, 116−118.
(37) Barge, L. M.; Doloboff, I. J.; White, L. M.; Russell, M. J.; Stucky, G. D.; Kanik, I. Characterization of iron-phosphate-silicate chemical garden structures. *Langmuir* **2012**, *28*, 3714−3721.
(38) Haudin, F.; Cartwright, J. H. E.; Brau, F.; De Wit, A. Spiral precipitation patterns in confined chemical gardens. *Proc. Natl. Acad. Sci. U.S.A.* **2014**, *111*, 17363−17367.
(39) Satoh, H.; Tsukamoto, K.; Garcia-Ruiz, J. M. Formation of chemical gardens on granitic rock: a new type of alteration for alkaline systems. *Eur. J. Mineral.* **2014**, *26*, 415−426.
(40) Bormashenko, E.; Bormashenko, Y.; Stanevsky, O.; Pogreb, R. Evolution of chemical gardens in aqueous solutions of polymers. *Chem. Phys. Lett.* **2006**, *417*, 341−344.
(41) Thouvenel-Romans, S.; van Saarloos, W.; Steinbock, O. Silica tubes in chemical gardens: Radius selection and its hydrodynamic origin. *Europhys. Lett.* **2004**, *67*, 42−48.
(42) Thouvenel-Romans, S.; Steinbock, O. Oscillatory growth of silica tubes in chemical gardens. *J. Am. Chem. Soc.* **2003**, *125*, 4338−4341.
(43) Stone, D. A.; Lewellyn, B.; Baygents, J. C.; Goldstein, R. E. Precipitative growth templated by a fluid jet. *Langmuir* **2005**, *21*, 10916−10919.
(44) Stone, D. A.; Goldstein, R. E. Tubular precipitation and redox gradients on a bubbling template. *Proc. Natl. Acad. Sci. U.S.A.* **2004**, *101*, 11537−11541.
(45) Batista, B. C.; Cruz, P.; Steinbock, O. From hydrodynamic plumes to chemical gardens: The concentration-dependent onset of tube formation. *Langmuir* **2014**, *30*, 9123−9129.
(46) Clément, R.; Douady, S. Ocean-ridge-like growth in silica tubes. *Europhys. Lett.* **2010**, *89*, 44004.
(47) Pagano, J. J.; Bánsági, T., Jr Steinbock, O. Tube formation in reverse silica gardens. *J. Phys. Chem. C* **2007**, *111*, 9324−9329.
(48) Makki, R.; Roszol, L.; Pagano, J. J.; Steinbock, O. Tubular precipitation structures: materials synthesis under nonequilibrium conditions. *Philos. Trans. R. Soc. A* **2012**, *370*, 2848−2865.
(49) Mielke, R. E.; Russell, M. J.; Wilson, P. R.; McGlynn, S.; Coleman, M.; Kidd, R.; Kanik, I. Design, fabrication and test of a hydrothermal reactor for origin-of-life experiments. *Astrobiology* **2010**, *10*, 799−810.
(50) Mielke, R. E.; Robinson, K. J.; White, L. M.; McGlynn, S. E.; McEachern, K.; Bhartia, R.; Kanik, I.; Russell, M. J. Iron-sulfide-bearing chimneys as potential catalytic energy traps at life's emergence. *Astrobiology* **2011**, *11*, 933−950.
(51) Kaminker, V.; Maselko, J.; Pantaleone, J. Chemical precipitation structures formed by drops impacting on a deep pool. *J. Chem. Phys.* **2012**, *137*, 184701.
(52) Thouvenel-Romans, S.; Pagano, J. J.; Steinbock, O. Bubble guidance of tubular growth in reaction-precipitation systems. *Phys. Chem. Chem. Phys.* **2005**, *7*, 2610−2615.
(53) Roszol, L.; Makki, R.; Steinbock, O. Postsynthetic processing of copper hydroxide-silica tubes. *Chem. Commun.* **2013**, *49*, 5736−5738.
(54) Roszol, L.; Steinbock, O. Controlling the wall thickness and composition of hollow precipitation tubes. *Phys. Chem. Chem. Phys.* **2011**, *13*, 20100.
(55) Galfi, L.; Racz, Z. Properties of the reaction front in an A + B → C type reaction-diffusion process. *Phys. Rev. A* **1988**, *38*, 3151−3154.
(56) Makki, R.; Steinbock, O. Synthesis of inorganic tubes under actively controlled growth velocities and injection rates. *J. Phys. Chem. C* **2011**, *115*, 17046−17053.
(57) Makki, R.; Steinbock, O. Nonequilibrium synthesis of silica-supported magnetite tubes and mechanical control of their magnetic properties. *J. Am. Chem. Soc.* **2012**, *134*, 15519−15527.
(58) Makki, R.; Ji, X.; Mattoussi, H.; Steinbock, O. Self-organized tubular structures as platforms for quantum dots. *J. Am. Chem. Soc.* **2014**, *136*, 6463−6469.
(59) Ayalon, A. Precipitation membranes − A review. *J. Membr. Sci.* **1984**, *20*, 93−102.
(60) Takiguchi, M.; Igarashi, K.; Azuma, N.; Ooshima, H. Tubular structure agglomerates of calcium carbonate crystals formed on a cation-exchange membrane. *Cryst. Growth Des.* **2006**, *6*, 1611−1614.
(61) Igarashi, K.; Takiguchi, M.; Ooshima, H. Growth mechanism of the calcium carbonate tubes on a cation-exchange membrane. *J. Ceramic Soc. Jpn.* **2008**, *116*, 111−114.
(62) Barge, L. M.; Doloboff, I. J.; Russell, M. J.; VanderVelde, D.; White, L. M.; Stucky, G. D.; Baum, M. M.; Zeytounian, J.; Kidd, R.; Kanik, I. Pyrophosphate synthesis in iron mineral films and membranes simulating prebiotic submarine hydrothermal systems. *Geochim. Cosmochim. Acta* **2014**, *128*, 1−12.
(63) Barge, L. M.; Kee, T. P.; Doloboff, I. J.; Hampton, J. M. P.; Ismail, M.; Pourkashanian, M.; Zeytounian, J.; Baum, M. M.; Moss, J. A.; Lin, C.-K.; et al. The fuel cell model of abiogenesis: A new approach to origin-of-life simulations. *Astrobiology* **2014**, *14*, 254−270.
(64) Tinker, F. The microscopic mtructure of semipermeable membranes and the part played by surface forces in osmosis. *Proc. R. Soc. London A* **1916**, *92*, 357−372.
(65) Fordham, S.; Tyson, J. T. The structure of semipermeable membranes of inorganic salts. *J. Chem. Soc.* **1937**, 483−487.
(66) Sakashita, M.; Fujita, S.; Sato, N. Current-voltage characteristics and oxide formation of bipolar $PbSO_4$ precipitate membranes. *J. Electroanal. Chem.* **1983**, *154*, 273−280.
(67) Beg, M. N.; Siddiqi, F. A.; Shyam, R. Studies with inorganic precipitate membranes: Part XIV. Evaluation of effective fixed charge densities. *Can. J. Chem.* **1977**, *55*, 1680−1686.
(68) Beg, M. N.; Matin, M. A. Studies with nickel phosphate membranes: evaluation of charge density and test of recently developed theory of membrane potential. *J. Membr. Sci.* **2002**, *196*, 95−102.
(69) Siddiqi, F. A.; Alvi, N. I.; Khan, S. A. Transport studies with model membranes. *Colloids Surf.* **1988**, *32*, 57−73.
(70) Beg, M. N.; Siddiqi, F. A.; Shyam, R.; Altaf, I. Studies with inorganic precipitative membranes XI. Membrane potential response, characterization and evaluation of effective fixed charge density. *J. Electroanalytic Chem.* **1978**, *89*, 141−147.
(71) Malik, W. U.; Srivastava, S. K.; Bhandari, V. M.; Kumar, S. Electrochemical properties of zirconyl tungstate membrane. *J. Electroanal. Chem.* **1980**, *110*, 181−203.
(72) Malik, W. U.; Siddiqi, F. A. Studies in the membrane permeability of chromic ferro and ferricyanides. *J. Colloid Sci.* **1963**, *18*, 161−173.
(73) Siddiqi, F. A.; Lakshminarayanaiah, N.; Beg, M. N. Studies with inorganic precipitate membranes. III. Consideration of energetics of electrolyte permeation through membranes. *J. Polymer Sci. A* **1971**, *9*, 2853−2867.
(74) Siddiqi, F. A.; Alvi, N. I. Transport studies with parchment supported model membranes. *J. Membr. Sci.* **1989**, *46*, 185−202.
(75) Kushwaha, R. S.; Ansari, M. A.; Tiwari, R. Transport studies of parchment supported model membrane: Test of bi-ionic potential

DOI: 10.1021/acs.chemrev.5b00014
Chem. Rev. XXXX, XXX, XXX−XXX

theories and evaluation of membrane selectivity for metal ions. *Indian J. Chem.* **2001**, *40A*, 270−274.
(76) Sakashita, M.; Sato, N. The effect of molybdate anion on the ion-selectivity of hydrous ferric oxide films in chloride solutions. *Corros. Sci.* **1977**, *17*, 473−486.
(77) van Oss, C. J. Specifically impermeable precipitate membranes. *Surf. Colloid Sci.* **1984**, *13*, 115−144.
(78) Hantz, P. Pattern formation in the NaOH + $CuCl_2$ reaction. *J. Phys. Chem. B* **2000**, *104*, 4266−4272.
(79) Hantz, P. Regular microscopic patterns produced by simple reaction-diffusion systems. *Phys. Chem. Chem. Phys.* **2002**, *4*, 1262−1267.
(80) Hantz, P. Germing surfaces in reaction-diffusion systems? Experiments and a hypothesis. *J. Chem. Phys.* **2002**, *117*, 6646−6654.
(81) de Lacy Costello, B. P. J.; Hantz, P.; Ratcliffe, N. M. Voronoi diagrams generated by regressing edges of precipitation fronts. *J. Chem. Phys.* **2004**, *120*, 2413−2416.
(82) Volford, A.; Izsák, F.; Ripszám, M.; Lagzi, I. Pattern formation and self-organization in a simple precipitation system. *Langmuir* **2007**, *23*, 961−964.
(83) Dúzs, B.; Lagzi, I.; Szalai, I. Propagating fronts and morphological instabilities in a precipitation reaction. *Langmuir* **2014**, *30*, 5460−5465.
(84) Hantz, P.; Partridge, J.; Láng, G.; Horvát, S.; Ujvári, M. Ion-Selective membranes involved in pattern-forming processes. *J. Phys. Chem. B* **2004**, *108*, 18135−18139.
(85) Horvát, S.; Hantz, P. Pattern formation induced by ion-selective surfaces: Models and simulations. *J. Chem. Phys.* **2005**, *123*, 034707.
(86) Tinsley, M. R.; Collison, D.; Showalter, K. Propagating precipitation waves: experiments and modeling. *J. Phys. Chem. A* **2013**, *117*, 12719−12725.
(87) Henisch, H. K. *Crystals in Gels and Liesegang Rings*; Cambridge University Press: Cambridge, U.K., 1988.
(88) Jones, D. E. H. Gardening in space. *Am. Sci.* **2002**, *90*, 454−461.
(89) Jones, D. E. H. *The Aha! Moment: A Scientist's Take on Creativity*; Johns Hopkins University Press: Baltimore, MD, 2012.
(90) Stockwell, B.; Williams, A. Experiment in space. *School Sci. Rev.* **1994**, *76*, 7−14.
(91) Homsy, G. M. Viscous fingering in porous media. *Annu. Rev. Fluid Mech.* **1987**, *19*, 271−311.
(92) Podgorski, T.; Sostarecz, M.; Zorman, S.; Belmonte, A. Fingering instabilities of a reactive micellar interface. *Phys. Rev. E* **2007**, *76*, 016202.
(93) Nagatsu, Y.; Hayashi, A.; Ban, M.; Kato, Y.; Tada, Y. Spiral pattern in a radial displacement involving a reaction-producing gel. *Phys. Rev. E* **2008**, *78*, 026307.
(94) Riolfo, L. A.; Nagatsu, Y.; Iwata, S.; Maes, R.; Trevelyan, P. M. J.; De Wit, A. Experimental evidence of reaction-driven miscible viscous fingering. *Phys. Rev. E* **2012**, *85*, 015304(R).
(95) Haudin, F.; Brasiliense, V.; Cartwright, J. H. E.; Brau, F.; De Wit, A. Genericity of confined chemical garden patterns with regard to changes in the reactants. *Phys. Chem. Chem. Phys.* **2015**, *17*, 12804−12811.
(96) Haudin, F.; Cartwright, J. H. E.; De Wit, A. Direct and reverse chemical garden patterns grown upon injection in confined geometries. *J. Phys. Chem. C* **2015**, *119*, 15067−15076.
(97) Baker, A.; Tóth, A.; Horváth, D.; Walkush, J.; Ali, A.; Morgan, W.; Kukovecz, A.; Pantaleone, J.; Maselko, J. Precipitation pattern formation in the copper(II) oxalate system with gravity flow and axial symmetry. *J. Phys. Chem. A* **2009**, *113*, 8243−8248.
(98) Maselko, J.; Miller, J.; Geldenhuys, A.; Atwood, D. Self-construction of complex forms in a simple chemical system. *Chem. Phys. Lett.* **2003**, *373*, 563.
(99) Smith, R.; McMahan, J. R.; Braden, J.; Mathews, E.; Tóth, A.; Horváth, D.; Maselko, J. Phase diagram of precipitation morphologies in the $Cu^{2+} - PO_4^{3-}$ system. *J. Phys. Chem. C* **2007**, *111*, 14762−14767.
(100) Nagatsu, Y.; Ishii, Y.; Tada, Y.; De Wit, A. Hydrodynamic fingering instability induced by a precipitation reaction. *Phys. Rev. Lett.* **2014**, *113*, 024502.
(101) De Wit, A.; Eckert, K.; Kalliadasis, S. Introduction to the focus issue "Chemo-hydrodynamic patterns and instabilities". *Chaos* **2012**, *22*, 037101.
(102) Udovichenko, V. V.; Strizhak, P. E.; Tóth, A.; Horváth, D.; Ning, S.; Maselko, J. Temporal and spatial organization of chemical and hydrodynamic processes. The system Pb^{2+}−chlorite−thiourea. *J. Phys. Chem. A* **2008**, *112*, 4584−4592.
(103) Maselko, J.; Tóth, A.; Horváth, D.; Pantaleone, J.; Strizhak, P. In *Precipitation patterns in reaction-diffusion systems*; Lagzi, I., Ed.; Research Signpost: Kerala, India, 2010; pp 93−115.
(104) Tóth, A.; Horváth, D.; Kukovecz, A.; Bake, A.; Ali, S.; Maselko, J. Control of precipitation patterns formation in system copper - oxalate. *J. Systems Chem.* **2012**.
(105) Copisarow, M. Mineralische Baumformationen: ihre Bildung und Bedeutung. *Kolloid Z.* **1929**, *47*, 60−65.
(106) Harting, P. *Recherches de morphologie synthétique sur la production artificielle de quelques formations calcaires organiques*; C. G. Van der Post: Amsterdam, 1872.
(107) Maselko, J.; Strizhak, P. Spontaneous formation of cellular chemical system that sustains itself far from thermodynamic equilibrium. *J. Phys. Chem. B* **2004**, *108*, 4937−4939.
(108) Maselko, J.; Borisova, P.; Carnahan, M.; Dreyer, E.; Devon, R.; Schmoll, M.; Douthat, D. Spontaneous formation of chemical motors in simple inorganic systems. *J. Mater. Sci.* **2005**, *40*, 4671−4673.
(109) Maselko, J.; Kiehl, M.; Couture, J.; Dyonizy, A.; Kaminker, V.; Nowak, P.; Pantaleone, J. Emergence of complex behavior in chemical cells: The system $AlCl_3$-NaOH. *Langmuir* **2014**, *30*, 5726−5731.
(110) Beutner, R. New electric properties of a semipermeable membrane of copper ferrocyanide. *J. Phys. Chem.* **1913**, *17*, 344−360.
(111) Lillie, R. S.; Johnston, E. N. Precipitation-structures simulating organic growth. II. *Biol. Bull.* **1919**, *36*, 225−272.
(112) Iverson, W. P. Formation of "hollow whiskers" from metals by reaction with ferricyanide and ferrocyanide. *Nature* **1967**, *213*, 486−487.
(113) Ritchie, C.; Cooper, G. J. T.; Song, Y.-F.; Streb, C.; Yin, H.; Parenty, A. D. C.; MacLaren, D. A.; Cronin, L. Spontaneous assembly and real-time growth of micrometre-scale tubular structures from polyoxometalate-based inorganic solids. *Nat. Chem.* **2009**, *1*, 47−52.
(114) Cooper, G. J. T.; Cronin, L. Real-time direction control of self fabricating polyoxometalate-based microtubes. *J. Am. Chem. Soc.* **2009**, *131*, 8368−8369.
(115) Boulay, A. G.; Cooper, G. J. T.; Cronin, L. Morphogenesis of amorphous polyoxometalate cluster-based materials to microtubular network architectures. *Chem. Commun.* **2012**, *48*, 5088−5090.
(116) Cooper, G. J. T.; Boulay, A. G.; Kitson, P. J.; Ritchie, C.; Richmond, C. J.; Thiel, J.; Gabb, D.; Eadie, R.; Long, D.-L.; Cronin, L. Osmotically driven crystal morphogenesis: A general approach to the fabrication of micrometer-scale tubular architectures based on polyoxometalates. *J. Am. Chem. Soc.* **2011**, *133*, 5947−5954.
(117) Cooper, G. J. T.; Kitson, P. J.; Winter, R.; Zagnoni, M.; Long, D.-L.; Cronin, L. Modular redox-active inorganic chemical cells: iCHELLs. *Angew. Chem., Int. Ed.* **2011**, *50*, 10373−10376.
(118) Cooper, G. J. T.; Bowman, R. W.; Magennis, E. P.; Fernandez-Trillo, F.; Alexander, C.; Padgett, M. J.; Cronin, L. Directed assembly of inorganic polyoxometalate-based micron-scale tubular architectures using optical control. *Angew. Chem., Int. Ed.* **2012**, *51*, 12754−12758.
(119) Collins, C.; Zhou, W.; Mackay, A. L.; Klinowski, J. The 'silica garden': A hierarchical nanostructure. *Chem. Phys. Lett.* **1998**, *286*, 88−92.
(120) Collins, C.; Mann, G.; Hoppe, E.; Duggal, T.; Barr, T. L.; Klinowski, J. NMR and ESCA studies of the "silica garden" Brønsted acid catalyst. *Phys. Chem. Chem. Phys.* **1999**, *1*, 3685−3687.
(121) Kaminker, V.; Maselko, J.; Pantaleone, J. The dynamics of open precipitation tubes. *J. Chem. Phys.* **2014**, *140*, 244901.
(122) Balköse, D.; Özkan, F.; Köktürk, U.; Ulutan, S.; Ülkü, S.; NiSli, G. Characterization of hollow chemical garden fibers from metal salts and water glass. *J. Sol-Gel Sci. Technol.* **2002**, *23*, 253−263.
(123) Pantaleone, J.; Tóth, A.; Horvath, D.; McMahan, J. R.; Smith, R.; Butki, D.; Braden, J.; Mathews, E.; Geri, H.; Maselko, J. Oscillations of a chemical garden. *Phys. Rev. E* **2008**, *77*, 046207.

DOI: 10.1021/acs.chemrev.5b00014
Chem. Rev. XXXX, XXX, XXX−XXX

(124) Pantaleone, J.; Tóth, A.; Horvath, D.; RoseFigura, L.; Maselko, J. Pressure oscillations in chemical gardens. *Phys. Rev. E* **2009**, *79*, 056221.
(125) Pratama, F. S.; Robinson, H. F.; Pagano, J. J. Spatially resolved analysis of calcium-silica tubes in reverse chemical gardens. *Colloids Surf. A* **2011**, *389*, 127−133.
(126) Parmar, K.; Bandyopadhya, N. R.; Chongder, D.; Bhattacharjee, S. Detailed characterization of calcium silicate precipitation tube (CaSPT) as a multi-cation adsorbent in aqueous medium. *Mater. Res. Bull.* **2012**, *47*, 677−682.
(127) Yokoi, H.; Kuroda, N.; Kakadate, Y. Magnetic field induced helical structure in freestanding metal silicate tubes. *J. Appl. Phys.* **2005**, *97*, 10R513.
(128) Parmar, K.; Chaturvedi, H. T.; Akhtar, M. W.; Bandyopadhya, N.; Bhattacharjee, S. Characterization of cobalt precipitation tube synthesized through "silica garden" route. *Mater. Charact.* **2009**, *60*, 863−868.
(129) Parmar, K.; Chongder, D.; Bandyopadhya, N.; Bhattacharjee, S. Investigation on Cu(II) adsorption on cobalt silicate precipitation tube (CSPT) in aqueous medium. *J. Hazardous Mater.* **2011**, *185*, 1326−1331.
(130) Glaab, F.; Kellermeier, M.; Kunz, W.; Morallon, E.; Garca-Ruiz, J. M. Formation and evolution of chemical gradients and potential differences across self-assembling inorganic membranes. *Angew. Chem., Int. Ed.* **2012**, *51*, 4317−4321.
(131) Collins, C.; Zhou, W.; Klinowski, J. A unique structure of $Cu_2(OH)_3{\cdot}NH_3$ crystals in the 'silica garden' and their degradation under electron beam irradiation. *Chem. Phys. Lett.* **1999**, *312*, 346; **1999**, *312*, 346.
(132) Duan, W.; Kitamura, S.; Uechi, I.; Katsuki, A.; Tanimoto, Y. Three-dimensional morphological chirality induction using high magnetic fields in membrane tubes prepared by a silicate garden reaction. *J. Phys. Chem. B* **2005**, *109*, 13445−13450.
(133) Pagano, J. J.; Thouvenel-Romans, S.; Steinbock, O. Compositional analysis of copper-silica precipitation tubes. *Phys. Chem. Chem. Phys.* **2007**, *9*, 110−116.
(134) Parmar, K.; Pramanik, A. K.; Bandopadhyay, N. R.; S, B. Synthesis and characterization of Fe(III)-silicate precipitation tubes. *Mater. Res. Bull.* **2010**, *45*, 1283−1287.
(135) Tanimoto, Y., Duan, W. In *Materials Processing In Magnetic Fields*; Schneider-Muntau, H. J., Wada, H., Eds.; World Scientific: Singapore, 2005; pp 141−146.
(136) Uechi, I.; Katsuki, A.; Dunin-Barkovskiy, L.; Tanimoto, Y. 3D-morphological chirality induction in since silicate membrane tube using a high magnetic field. *J. Phys. Chem. B* **2004**, *108*, 2527−2530.
(137) Pagano, J. J.; Bánsági, T., Jr; Steinbock, O. Bubble-templated and flow-controlled synthesis of macroscopic silica tubes supporting zinc oxide nanostructures. *Angew. Chem., Int. Ed.* **2008**, *47*, 9900−9903.
(138) McGlynn, S. E.; Kanik, I.; Russell, M. J. Modification of simulated hydrothermal iron sulfide chimneys by RNA and peptides. *Philos. Trans. R. Soc. London A* **2012**, *370*, 3007−3022.
(139) Russell, M. J.; Hall, A. J.; Turner, D. In vitro growth of iron sulphide chimneys: possible culture chambers for origin-of-life experiments. *Terra Nova* **1989**, *1*, 238−241.
(140) Russell, M. J.; Hall, A. J. The emergence of life from iron monosulphide bubbles at a submarine hydrothermal redox and pH front. *J. Geol. Soc. London* **1997**, *154*, 377−402.
(141) Russell, M. J., Hall, A. J. In *Evolution of Early Earth's Atmosphere, Hydrosphere, and Biosphere−Constraints from Ore Deposits*; Kesler, S. E., Ohmoto, H., Eds.; Geological Society of America: Boulder, CO, 2006; Vol. *198*; pp 1−32.
(142) Noorduin, W. L.; Grinthal, A.; Mahadevan, L.; Aizenberg, J. Rationally designed complex, hierarchical microarchitectures. *Science* **2013**, *340*, 832−837.
(143) Kellermeier, M.; Glaab, F.; Melero-García, E.; García-Ruiz, J. M. Experimental Techniques for the Growth and Characterization of Silica Biomorphs and Silica Gardens. *Methods Enzymol.* **2013**, *532*, 225−256.
(144) Collins, C.; Mokaya, R.; Klinowski, J. The "silica garden" as a Brønsted acid catalyst. *Phys. Chem. Chem. Phys.* **1999**, *1*, 4669−4672.
(145) Schultz, S. G. *Basic Principles of Membrane Transport*; Cambridge University Press: New York, 1980.
(146) Donnan, F. G. Theorie der Membrangleichgewichte und Membranpotentiale bei Vorhandensein von nicht dialysierenden Elektrolyten. Ein Beitrag zur physikalisch-chemischen Physiologie. *Z. Elektrochem. Angew. Phys. Chem.* **1911**, *17*, 572−581.
(147) Julian, K. New ideas on the lead-acid battery. *J. Power Sources* **1984**, *11*, 47−61.
(148) Filtness, M. J.; Butler, I. B.; Rickard, D. The origin of life: The properties of iron sulphide membranes. *Trans. Inst. Mining Metallurgy, Appl.Earth Sci.* **2003**, 171−172.
(149) Nitschke, W.; Russell, M. J. Hydrothermal focusing of chemical and chemiosmotic energy, supported by delivery of catalytic Fe, Ni, Mo/W, Co, S and Se, forced life to emerge. *J. Mol. Evol.* **2009**, *69*, 481−496.
(150) Nitschke, W.; Russell, M. J. Beating the acetyl coenzyme-A pathway to the origin of life. Phil. *Trans. R. Soc. London B* **2013**, *368*, 20120258.
(151) Barge, L. M.; Abedian, Y.; Russell, M. J.; Doloboff, I. J.; Cartwright, J. H. E.; Kidd, R. D.; Kanik, I. From chemical gardens to fuel cells: Generation of electrical potential and current across self-assembling iron mineral membranes. *Angew. Chem., Int. Ed.* **2015**, *44*, 8184−8187.
(152) Tanimoto, Y. In *Magneto-Science*; Yamaguchi, M., Tanimoto, Y., Eds.; Kodansha/Springer: Tokyo, 2006; pp 130−135.
(153) Tanimoto, Y. Magnetic field effect in silicate garden reaction − Morphological chirality induction using a magnetic field. *Kagaku-to-Kyoiku (Chem. Educ.)* **2006**, *54*, 4−7.
(154) Hill, B. S.; Findlay, G. P. The power of movement in plants: the role of osmotic machines. *Q. Rev. Biophys.* **1981**, *14*, 173−222.
(155) Addicott, F. T. *Abscission*; University of California Press: CA, 1982.
(156) Vogel, S. *Glimpses of Creatures in Their Physical Worlds*; Princeton University Press, 2009.
(157) Dumais, J.; Forterre, Y. "Vegetable Dynamicks": The role of water in plant movements. *Annu. Rev. Fluid Mech.* **2012**, *44*, 453−478.
(158) Forterre, Y. Slow and fast and furious: understanding the physics of plant movements. *J. Exp. Bot.* **2013**, *64*, 4745−4760.
(159) Lord Rayleigh. The theory of solution. *Nature* **1897**, *55*, 253−254.
(160) Gibbs, J. W. Semi-permeable films and osmotic pressure. *Nature* **1897**, *55*, 461.
(161) Lachish, U. Osmosis and thermodynamics. *Am. J. Phys.* **2007**, *75*, 997.
(162) Kedem, O.; Katchalsky, A. Thermodynamic analysis of the permeability of biological membranes to non-electrolytes. *Biochim. Biophys. Acta* **1958**, *27*, 229.
(163) Staverman, A. J. The theory of measurement of osmotic pressure. *Rec. Trav. Chim. Pays-Bas* **1951**, *70*, 344.
(164) Medved, I.; Cerny, R. Osmosis in porous media: A review of recent studies. *Microporous Mesoporous Mater.* **2013**, *170*, 299.
(165) Cardoso, S. S. S.; Cartwright, J. H. E. Dynamics of osmosis in a porous medium. *R. Soc. Open Sci.* **2014**, *1*, 140352.
(166) Sørensen, T. S. A theory of osmotic instabilities of a moving semipermeable membrane: preliminary model for the initial stages of silicate garden formation and of Portland cement hydration. *J. Colloid Interface Sci.* **1981**, *79*, 192−208.
(167) Merritt, D. R.; Weinhaus, F. The pressure curve for a rubber balloon. *Am. J. Phys.* **1978**, *46*, 976.
(168) Ackermann, A. Die mikroskopischen Formen des Eisenrostes. *Kolloid Z.* **1921**, *28*, 270−281.
(169) Ackermann, A. Die mikroskopischen Formen des Eisenrostes. *Kolloid Z.* **1932**, *59*, 49−55.
(170) Ackermann, A. Die mikroskopischen Formen des Eisenrostes. *Kolloid Z.* **1940**, *90*, 26−28.
(171) Ackermann, A. Die mikroskopischen Formen des Eisenrostes IV. *Kolloid Z.* **1954**, *137*, 20−24.
(172) Butler, G.; Ison, H. C. K. An unusual form of corrosion product. *Nature* **1958**, *182*, 1229−1230.

DOI: 10.1021/acs.chemrev.5b00014
Chem. Rev. XXXX, XXX, XXX−XXX

(173) Riggs, O. L.; Sudbury, J. D.; Hutchinson, M. Effect of pH on oxygen corrosion at elevated pressures. *Corrosion* **1960**, *16*, 94−98.
(174) Sudbury, J. D.; Riggs, O. L.; Radd, F. J. Oxygen Corrosion in the Petroleum Industry. *Mater. Protect.* **1962**, *1*, 8−25.
(175) Fontana, M. G. *Corrosion Engineering*, 3rd ed.; McGraw-Hill: New York, 1986.
(176) Smith, D. C.; McEnaney, B. The influence of dissolved oxygen concentration on the corrosion of grey cast iron in water at 50°C. *Corros. Sci.* **1979**, *19*, 379−394.
(177) Bernal, J. D.; Dasgupta, D. R.; Mackay, A. L. The oxides and hydroxides of iron and their structural inter-relationships. *Clay Miner. Bull.* **1959**, *4*, 15−30.
(178) Gerke, T. L.; Scheckel, K. G.; Ray, R. I.; Little, B. J. Can dynamic bubble templating play a role in corrosion product morphology? *Corrosion* **2012**, *68*, 025004.
(179) Double, D. D.; Hellawell, A. The hydration of Portland cement. *Nature* **1976**, *261*, 486.
(180) Double, D. D.; Hellawell, A. The solidification of cement. *Sci. Am.* **1977**, *237*, 82.
(181) Double, D. D.; Hellawell, A.; Perry, S. J. The hydration of Portland cement. *Proc. R. Soc. A* **1978**, *359*, 435−451.
(182) Double, D. D. An examination of the hydration of Portland cement by electron microscopy. *Silicates Ind.* **1978**, *11*, 233−246.
(183) Birchall, J. D.; Howard, A. J.; Bailey, J. E. On the hydration of Portland cement. *Proc. R. Soc. A* **1978**, *360*, 445−453.
(184) Jennings, H. M.; Pratt, P. L. An experimental argument for the existence of a protective membrane surrounding Portland cement during the induction period. *Cem. Concr. Res.* **1979**, *9*, 501−506.
(185) Barnes, P.; Ghose, A.; Mackay, A. L. Cement tubules − another look. *Cem. Concr. Res.* **1980**, *10*, 639−645.
(186) Lasic, D. D.; Pintar, M. M.; Blinc, R. Are proton NMR observations supportive of the osmotic model of cement hydration? *Philos. Mag. Lett.* **1988**, *58*, 227−232.
(187) Mitchell, L. D.; Prica, M.; Birchall, J. D. Aspects of Portland cement hydration studied using atomic force microscopy. *J. Mater. Sci.* **1996**, *31*, 4207−4212.
(188) Clark, S. M.; Morrison, G. R.; Shib, W. D. The use of scanning transmission X-ray microscopy for the real-time study of cement hydration. *Cem. Concr. Res.* **1999**, *29*, 1099−1102.
(189) Bullard, J. W.; Jennings, H. M.; Livingston, R. A.; Nonat, A.; Scherer, G. W.; Schweitzer, J. S.; Scrivener, K. L.; Thomas, J. J. Mechanisms of cement hydration. *Cem. Concr. Res.* **2011**, *41*, 1208−1223.
(190) Thomas, N. L.; Jameson, D. A.; Double, D. D. The effect of lead nitrate on the early hydration of Portland cement. *Cem. Concr. Res.* **1981**, *11*, 143−153.
(191) Thomas, N. L.; Double, D. D. Calcium and silicon concentrations in solution during the early hydration of Portland cement and tricalcium silicate. *Cem. Concr. Res.* **1981**, *11*, 675−687.
(192) Thomas, N. L.; Double, D. D. The hydration of Portland cement, C_3S and C_2S in the presence of a calcium complexing admixture (EDTA). *Cem. Concr. Res.* **1983**, *13*, 391−400.
(193) Double, D. D. New developments in understanding the chemistry of cement. *Philos. Trans. R. Soc. A* **1983**, *310*, 53−66.
(194) Thomas, N. L. Corrosion problems in reinforced concrete: why accelerators of cement hydration usually promote corrosion of steel. *J. Mater. Sci.* **1987**, *22*, 3328−3334.
(195) Shi, J. J.; Sun, W. Effects of phosphate on the chloride-induced corrosion behaviour of reinforcing steel in mortars. *Cement Concrete Comp.* **2014**, *45*, 166−175.
(196) Aleva, G. J. J., Ed.; *Laterites. Concepts, geology, morphology and chemistry*; ISRIC: Wageningen, 1994.
(197) Karol, R. H. *Chemical grouting and soil stabilization*, 3rd ed.; CRC Press: Boca Raton, FL, 2003.
(198) Joosten, H. J. *The Joosten process for chemical soil solidification and sealing and its development from 1925 to date*; Amsterdamsche Ballast Maatschappij, 1954.
(199) Long, D.-L.; Tsunashima, R.; Cronin, L. Polyoxometalates: building blocks for functional nanoscale systems. *Angew. Chem., Int. Ed.* **2010**, *49*, 1736−1758.
(200) Long, D.-L.; Burkholder, E.; Cronin, L. Polyoxometalate clusters, nanostructures and materials: From self assembly to designer materials and devices. *Chem. Soc. Rev.* **2007**, *36*, 105−121.
(201) Müller, A.; Shah, S. Q. N.; Bögge, H.; Schmidtmann, M. Molecular growth from a Mo_{176} to a Mo_{248} cluster. *Nature* **1999**, *397*, 48−50.
(202) Long, D.-L.; Abbas, H.; Kögerler, P.; Cronin, L. Confined electron-transfer reactions within a molecular metal oxide "Trojan horse. *Angew. Chem., Int. Ed.* **2005**, *44*, 3415−3419.
(203) Rhule, J.; Neiwert, W. A.; Hardcastle, K. I.; Do, B. T.; Hill, C. L. $Ag_5PV_2Mo_{10}O_{40}$, a heterogeneous catalyst for air-based selective oxidation at ambient temperature. *J. Am. Chem. Soc.* **2001**, *123*, 12101−12102.
(204) Bowman, R. W.; Gibson, G.; Carberry, D.; Picco, L.; Miles, M.; Padgett, M. J. iTweezers: optical micromanipulation controlled by an Apple iPad. *J. Opt.* **2011**, *13*, 044002.
(205) Short, M. B.; Baygents, J. C.; Beck, J. W.; Stone, D. A.; Toomey, R. S.; Goldstein, R. E. Stalactite growth as a free-boundary problem: a geometric law and its Platonic ideal. *Phys. Rev. Lett.* **2005**, *94*, 018501.
(206) Short, M. B.; Baygents, J. C.; Goldstein, R. E. Stalactite growth as a free-boundary problem. *Phys. Fluids* **2005**, *17*, 083101.
(207) Anderson, I. K.; Ashton, J. H.; Boyce, A. J.; Fallick, A. E.; Russell, M. J. Ore depositional process in the Navan Zn-Pb deposit, Ireland. *Econ. Geol.* **1998**, *93*, 535−563.
(208) Boyce, A. J.; Coleman, M. L.; Russell, M. J. Formation of fossil hydrothermal chimneys and mounds from Silvermines, Ireland. *Nature* **1983**, *306*, 545−550.
(209) Russell, M. J.; Nitschke, W.; Branscomb, E. The inevitable journey to being. Phil. *Trans. R. Soc. London B* **2013**, *368*, 20120254.
(210) Ludwig, K. A.; Shen, C. C.; Kelley, D. S.; Cheng, H.; Edwards, R. L. U-Th systematics and 230Th ages of carbonate chimneys at the Lost City hydrothermal field. *Geochim. Cosmochim. Acta* **2011**, *75*, 1869−1888.
(211) Janecky, D. R.; Seyfried, W. E. The solubility of magnesium-hydroxide-sulfate-hydrate in seawater at elevated temperatures and pressures. *Am. J. Sci.* **1983**, *283*, 831−860.
(212) Neal, C.; Stanger, G. Calcium and magnesium hydroxide precipitation from alkaline groundwater in Oman, and their significance to the process of serpentinization. *Mineral. Mag.* **1984**, *48*, 237−241.
(213) Etiope, G.; Sherwood, L. B. Abiotic methane on Earth. *Rev. Geophys.* **2013**.
(214) Etiope, G.; Tsikouras, B.; Kordella, S.; Ifandi, E.; Christodoulou, D.; Papatheodorou, G. Methane flux and origin in the Othrys ophiolite hyperalkaline springs, Greece. *Chem. Geol.* **2013**, *347*, 161−174.
(215) Macleod, G.; Mckeown, C.; Hall, A. J.; Russell, M. J. Hydrothermal and oceanic pH conditions at 4Ga relevant to the origin of life. *Orig. Life Evol. Biosph.* **1994**, *24*, 19−41.
(216) Ludwig, K. A.; Kelley, D. S.; Butterfield, D. A.; Nelson, B. K.; Früh-Green, G. L. Formation and evolution of carbonate chimneys at the Lost City hydrothermal field. *Geochim. Cosmochim. Acta* **2006**, *70*, 3625−3645.
(217) Mloszewska, A. M.; Pecoits, E.; Cates, N. L.; Mojzsis, S. J.; O'Neil, J.; Robbins, L. J.; Konhauser, K. O. The composition of Earth's oldest iron formations: The Nuvvuagittuq Supracrustal Belt (Québec, Canada). *Earth Planet. Sci. Lett.* **2012**, *317−318*, 331−342.
(218) Schrenk, M. O.; Brazelton, W. J.; Lang, S. Q. Serpentinization, carbon, and deep life. *Rev. Mineral. Geochem.* **2013**, *75*, 575−606.
(219) Mitchell, P. Coupling of phosphorylation to electron and hydrogen transfer by a chemiosmotic mechanism. *Nature* **1961**, *191*, 144−148.
(220) Russell, M. J.; Hall, A. J. From geochemistry to biochemistry: Chemiosmotic coupling and transition element clusters in the onset of life and photosynthesis. *Geochem. News* **2002**, *113*, 6−12.
(221) Lane, N. Why are cells powered by proton gradients? *Nature Educ.* **2010**, *3*, 18.

DOI: 10.1021/acs.chemrev.5b00014
Chem. Rev. XXXX, XXX, XXX−XXX

(222) Yamaguchi, A.; Yamamoto, M.; Takai, K.; Ishii, T.; Hashimoto, K.; Nakamura, R. Electrochemical CO_2 reduction by Ni-containing iron sulfides: How is CO_2 electrochemically reduced at bisulfide-bearing deep-sea hydrothermal precipitates? *Electrochim. Acta* **2014**, *141*, 311−318.
(223) Herschy, B.; Whicher, A.; Camprubi, E.; Watson, C.; Dartnell, L.; Ward, J.; Evans, J. R. G.; Lane, N. An origin-of-life reactor to simulate alkaline hydrothermal vents. *J. Mol. Evol.* **2014**, *79*, 213−227.
(224) Roldan, A.; Hollingsworth, N.; Roffrey, A.; Islam, H. U.; Goodall, J.; Catlow, C. R. A.; Darr, J. A.; Bras, W.; Sankar, G.; Holt, K.; et al. Bio-inspired CO_2 conversion by iron sulfide catalysts under sustainable conditions. *Chem. Commun.* **2015**.
(225) Allmann, R. Die Doppelschichtstruktur der plättchenförmigen Calcium-Aluminium-Hydroxidsalze am Beispiel des $3CaO \cdot Al_2O_3 \cdot CaSO_4 \cdot H_2O$. *N. Jb. Miner.* **1968**, 140−144.
(226) Arrhenius, G. O. Crystals and life. *Helv. Chim. Acta* **2003**, *86*, 1569−1586.
(227) Trolard, F.; Bourrié, G. In *Clay minerals in nature − their characterization, modification and application*; Valaskova, M., Martynkova, G. S., Eds.; 2012; pp 171−188.
(228) Yamanaka, J.; Inomata, K.; Yamagata, Y. Condensation of oligoglycines with trimeta- and tetrametaphosphate in aqueous solutions. *Orig. Life Evol. Biosph.* **1988**, *18*, 165−178.
(229) Yamagata, Y.; Inomata, K. Condensation of glycylglycine to oligoglycines with trimetaphosphate in aqueous solution. *Orig. Life Evol. Biosph.* **1997**, *27*, 339−344.
(230) Lowell, R. P.; Rona, P. A. Seafloor hydrothermal systems driven by the serpentinization of peridotite. *Geophys. Res. Lett.* **2002**, *29*, 26−1.
(231) Kelley, D. S.; Karson, J. A.; Blackman, D. K.; Früh-Green, G. L.; Butterfield, D. A.; Lilley, M. D.; Olson, E. J.; Schrenk, M. O.; Roe, K. K.; Lebon, G.; et al. An off-axis hydrothermal vent field near the Mid-Atlantic Ridge at 30°N. *Nature* **2001**, *412*, 145−149.
(232) Proskurowski, G.; Lilley, M. D.; Kelley, D. S.; Olson, E. J. Low temperature volatile production at the Lost City hydrothermal field, evidence from a hydrogen stable isotope geothermometer. *Chem. Geol.* **2006**, *229*, 331−343.
(233) Proskurowski, G.; Lilley, M. D.; Seewald, J. S.; Früh-Green, G. L.; Olson, E. J.; Lupton, J. E.; Sylva, S. P.; Kelley, D. S. Abiogenic hydrocarbon production at Lost City hydrothermal field. *Science* **2008**, *319*, 604−607.
(234) Branscomb, E.; Russell, M. J. Turnstiles and bifurcators: the disequilibrium converting engines that put metabolism on the road. *Biochim. Biophys. Acta, Bioenergetics* **2013**, *1827*, 62−78.
(235) McCollom, T. M.; Seewald, J. S. Experimental constraints on the hydrothermal reactivity of organic acids and acid anions: I. Formic acid and formate. *Geochim. Cosmochim. Acta* **2003**, *67*, 3625.
(236) Nitschke, W.; McGlynn, S. E.; Milner-White, E. J.; Russell, M. J. On the antiquity of metalloenzymes and their substrates in bioenergetics. *Biochim. Biophys. Acta, Bioenergetics* **2013**, *1827*, 871−881.
(237) Nitschke, W.; Russell, M. J. Redox bifurcations; how they work and what they mean to extant life and (potentially) to its inorganic roots. *BioEssays* **2011**, *34*, 106−109.
(238) Helz, G. R.; Erickson, B. E.; Vorlicek, T. P. Stabilities of thiomolybdate complexes of iron: implications for retention of essential trace elements (Fe, Cu, Mo) in sulfidic waters. *Metallomics* **2014**, *6*, 1131−1140.
(239) Fuchs, G. Alternative pathways of carbon dioxide fixation: insights into the early evolution of life? *Annu. Rev. Microbiol.* **2011**, *65*, 631−658.
(240) Nakamura, R.; Takashima, T.; Kato, S.; Takai, K.; Yamamoto, M.; Hashimoto, K. Electrical current generation across a black smoker chimney. *Angew. Chem., Int. Ed.* **2010**, *49*, 7692−7694.
(241) Baaske, P.; Weinert, F.; Duhr, S.; Lemke, K.; Russell, M. J.; Braun, D. Extreme accumulation of nucleotides in simulated hydrothermal pore systems. *Proc. Natl. Acad. Sci. U.S.A.* **2007**, *104*, 9346−9351.
(242) Starokon, E. V.; Parfenov, M. V.; Pirutko, L. V.; Abornev, S. I.; Panov, G. I. Room-temperature oxidation of methane by α-oxygen and extraction of products from the FeZSM-5 Surface. *J. Phys. Chem. C* **2011**, *115*, 2155−2161.
(243) Huber, C.; Wächtershäuser, G. Activated acetic acid by carbon fixation on (Fe,Ni)S under primordial conditions. *Science* **1997**, *276*, 245−247.
(244) Huber, C.; Wächtershäuser, G. Primordial reductive amination revisited. *Tetrahedron Lett.* **2003**, *44*, 1695−1697.
(245) Huber, C.; Wächtershäuser, G. Peptides by activation of amino acids on (Fe, Ni)S surfaces: implications for the origin of life. *Science* **1998**, *281*, 670−672.
(246) Huber, C.; Eisenreich, W.; Hecht, S.; Wächtershäuser, G. A possible primordial peptide cycle. *Science* **2003**, *301*, 938−940.
(247) Efremov, R. G.; Sazanov, L. A. Respiratory complex I: "steam engine" of the cell? *Curr. Opin. Struct. Biol.* **2011**, *21*, 532−540.
(248) Thauer, R. K.; Shima, S. Methane as fuel for anaerobic microorganisms. *Ann. N.Y. Acad. Sci.* **2008**, *1125*, 158−170.
(249) Yoshida, M.; Muneyuki, E.; Hisabori, T. ATP synthase − a marvellous rotary engine of the cell. *Nat. Rev. Mol. Cell Biol.* **2001**, *2*, 669−677.
(250) Buckel, W.; Thauer, R. K. Energy conservation via electron bifurcating ferredoxin reduction and proton/Na^+ translocating ferredoxin oxidation. *Biochim. Biophys. Acta* **2013**, *1827*, 94−113.
(251) Poehlein, A.; Schmidt, S.; Kaster, A.-K.; Goenrich, M.; Vollmers, J.; Thürmer, A.; Bertsch, J.; Schuchmann, K.; Voigt, B.; Hecker, M.; et al. An ancient pathway combining carbon dioxide fixation with the generation and utilization of a sodium ion gradient for ATP synthesis. *PLoS one* **2012**, *7*, e33439.
(252) Kletzin, A.; Adams, M. W. Tungsten in biological systems. *FEMS Microbiol. Rev.* **2006**, *18*, 5−63.
(253) Brazelton, W. J., Mehta, M. P., Kelley, D. S., Baross, J. A. Physiological differentiation within a single-species biofilm fueled by serpentinization *Biology*. **2011**2.
(254) Haroon, M. F.; Hu, S.; Shi, Y.; Imelfort, M.; Keller, J.; Hugenholtz, P.; Tyson, G. W. Anaerobic oxidation of methane coupled to nitrate reduction in a novel archaeal lineage. *Nature* **2013**, *500*, 567−570.
(255) Russell, M. J.; Barge, L. M.; Bhartia, R.; Bocanegra, D.; Bracher, P. J.; Branscomb, E.; Kidd, R.; McGlynn, S. E.; Meier, D. H.; Nitschke, W.; et al. The drive to life on wet and icy worlds. *Astrobiology* **2014**, *14*, 308−343.
(256) Génin, J. M.; Mills, S. J.; Christy, A. G.; Guérin, O.; Herbillon, A. J.; Kuzmann, E.; Ona-Nguema, G.; Ruby, C.; Upadhyay, C. Mössbauerite, $Fe^{3+}{}_6O_4(OH)_8[CO_3] \cdot 3H_2O$, the fully oxidized 'green rust' mineral from Mont Saint-Michel Bay, France. *Mineralog. Mag.* **2014**, *78*, 447−465.
(257) Shimizu, M.; Zhou, J.; Schröder, C.; Obst, M.; Kappler, A.; Borch, T. Dissimilatory reduction and transformation of ferrihydrite-humic acid coprecipitates. *Environ. Sci. Technol.* **2013**, *47*, 13375−13384.
(258) Hansen, H. C. B.; Gulberg, S.; Erbs, M.; Koch, C. B. Kinetics of nitrate reduction by green rusts: effects of interlayer anion and Fe(II): Fe(III) ratio. *Appl. Clay Sci.* **2001**, *18*, 81−91.
(259) Baltscheffsky, H.; Persson, B. On an early gene for membrane-integral inorganic pyrophosphatase in the genome of an apparently pre-LUCA extremophile, the archaeon Candidatus Korarchaeum cryptofilum. *J. Mol. Evol.* **2014**, *78*, 140−147.
(260) Lin, S. M.; Tsai, J. Y.; Hsiao, C. D.; Huang, Y. T.; Chiu, C. L.; Liu, M. H.; Tung, J. Y.; Liu, T. H.; Pan, R. L.; Sun, Y. J. Crystal structure of a membrane-embedded H^+-translocating pyrophosphatase. *Nature* **2012**, *484*, 399−403.
(261) Tsai, J. Y.; Kellosalo, J.; Sun, Y. J.; Goldman, A. Proton/sodium pumping pyrophosphatases: the last of the primary ion pumps. *Current Opin. Struct. Biol.* **2014**, *27*, 38−47.
(262) Ducluzeau, A.-L.; van Lis, R.; Duval, S.; Schoepp-Cothenet, B.; Russell, M. J.; Nitschke, W. Was nitric oxide the first strongly oxidizing terminal electron sink. *Trends Biochem. Sci.* **2009**, *34*, 9−15.
(263) Duhr, S.; Arduini, S.; Braun, D. Thermophoresis of DNA determined by microfluidic fluorescence. *Eur. Phys. J. E* **2004**, *15*, 277−286.

DOI: 10.1021/acs.chemrev.5b00014
Chem. Rev. XXXX, XXX, XXX−XXX

(264) Whitesides, G. M. The origins and the future of microfluidics. *Nature* **2006**, *442*, 368−373.
(265) Siria, A.; Poncharal, P.; Biance, A. L.; Fulcrand, R.; Blase, X.; Purcell, S. T.; Bocquet, L. Giant osmotic energy conversion measured in a single transmembrane boron nitride nanotube. *Nature* **2013**, *494*, 455−458.
(266) Miller, R. D. Ice sandwich: functional semipermeable membrane. *Science* **1970**, *169*, 584−585.
(267) Martin, S. Ice stalactites: comparison of a laminar flow theory with experiment. *J. Fluid Mech.* **1974**, *63*, 51−79.
(268) Cartwright, J. H. E.; Escribano, B.; González, D. L.; Sainz-Díaz, C. I.; Tuval, I. Brinicles as a case of inverse chemical gardens. *Langmuir* **2013**, *29*, 7655−7660.
(269) Bartels-Rausch, T.; Bergeron, V.; Cartwright, J. H. E.; Escribano, R.; Finney, J. L.; Grothe, H.; Gutiérrez, P. J.; Haapala, J.; Kuhs, W. F.; Pettersson, J. B. C.; et al. Ice structures, patterns, and processes: A view across the icefields. *Rev. Mod. Phys.* **2012**, *84*, 885−944.
(270) Trinks, H.; Schröder, W.; Bierbricher, C. K. Sea ice as a promoter of the emergence of first life. *Origins Life Evol. Biospheres* **2005**, *35*, 429−445.
(271) Krembs, C.; Eicken, H.; Deming, J. W. Exopolymer alteration of physical properties of sea ice and implications for ice habitability and biogeochemistry in a warmer Arctic. *Proc. Natl. Acad. Sci. U.S.A.* **2011**, *108*, 3653−3658.
(272) Pappalardo, R. T.; Vance, S.; Bagenal, F.; Bills, B. G.; Blaney, D. L.; Blankenship, D. D.; Brinckerhoff, W. B.; Connerney, J. E. P.; Hand, K. P.; Hoehler, T. M.; et al. Science potential from a Europa lander. *Astrobiology* **2013**, *13*, 740−773.
(273) Vance, S.; Bouffard, M.; Choukroun, M.; Sotin, C. Ganymede's internal structure including thermodynamics of magnesium sulfate oceans in contact with ice. *Planet. Space Sci.* **2014**, *96*, 62−70.
(274) Hsu, H.-W.; Postberg, F.; Sekine, Y.; Shibuya, T.; Kempf, S.; Horányi, M.; Juhász, A.; Altobelli, N.; Suzuki, K.; Masaki, Y.; et al. Ongoing hydrothermal activities within Enceladus. *Nature* **2015**, *519*, 207−210.
(275) Romero-Wolf, A.; Vance, S.; Maiwald, F.; Heggy, E.; Ries, P.; Liewer, K. A passive probe for subsurface oceans and liquid water in Jupiter's icy moons. *Icarus* **2015**, *248*, 463−477.

DOI: 10.1021/acs.chemrev.5b00014
Chem. Rev. XXXX, XXX, XXX−XXX